Contribution of Heart-Brain Interactions to Conscious Visual Perception

Dissertation

for the award of the degree

"Doctor rerum naturalium" (Dr. rer. nat.)

of the Georg-August-Universität Göttingen

within the doctoral program Behavior and Cognition

of the Georg-August University School of Science (GAUSS)

submitted by

Aishwarya Bhonsle

from Mumbai, India

Göttingen, 2024

Thesis Committee

Prof. Dr. Melanie Wilke
Department of Cognitive Neurology, University Medical Center Göttingen

PD Dr. Roberto Goya-Maldonado
Department of Psychiatry and Psychotherapy, University Medical Center Göttingen

apl. Prof. Dr. Ulrich Parlitz
Department of Biomedical Physics, Max Planck Institute for Dynamics and Self-Organization

Members of the Examination Board

Reviewer: **Prof. Dr. Melanie Wilke**
Department of Cognitive Neurology, University Medical Center Göttingen

Second reviewer: **PD Dr. Roberto Goya-Maldonado**
Department of Psychiatry and Psychotherapy, University Medical Center Göttingen

Further members of the Examination Board:

PD Dr. rer. nat. Peter Dechent
Department of Cognitive Neurology, University Medical Center Göttingen

Prof. Dr. med. Niels Focke
Department of Clinical Neurophysiology, University Medical Center Göttingen

Prof. Dr. Nivedita Mani
Department of Psychology of Language, Georg-Elias-Müller-Institute of Psychology

Prof. Dr. Caspar Schwiedrzik
Department of Cognitive Biology, Ruhr-Universität Bochum;
Neural Circuits and Cognition, European Neuroscience Institute

Date of oral examination: 12.02.2025

Declaration on the use of ChatGPT and comparable tools in the context of examinations

In this thesis, I have used ChatGPT or another AI as follows:

[] not at all
[] during brainstorming
[] when creating the outline
[] to write individual passages, altogether to the extent of …% of the entire text
[] for the development of software source texts
[] for optimizing or restructuring software sources texts
[X] for proofreading or optimizing
[X] further, namely: for preparing the German version of the Summary section of the thesis (Zussamenfassung)

I hereby declare that I have stated all uses completely.

Missing or incorrect information will be considered as an attempt to cheat.

Table of Contents

Summary

The objective of this thesis is to investigate the interplay between afferent cardiac signals and neural processing of exteroceptive inputs and how this dynamic contributes to conscious visual perception. This investigation is grounded in two EEG-ECG studies that explore how exercise-induced modulation of cardiac activity influences perceptual suppression, a phenomenon where a salient visual stimulus becomes subjectively invisible despite unchanged sensory input.

Chapter 1 introduces the anatomical, physiological, and theoretical foundations of heart-brain interactions in conscious perception, framing the aims of the experimental studies.

Chapter 2 presents the first experimental study, which investigates how light-intensity cycling exercise affects perceptual suppression, pre-stimulus alpha activity, and heartbeat-evoked potentials (HEPs) using the Generalized Flash Suppression (GFS) paradigm. Exercise reduced the likelihood of perceptual suppression and decreased alpha amplitudes, indicating increased cortical excitability. These results challenge the baroreceptor hypothesis, which predicts that increased heart rate should reduce cortical excitability and suppress sensory processing. Additionally, exercise-induced decreases in HEP amplitudes provide novel evidence of the influence of cardiac physiology on the neural processing of cardiac signals. However, HEPs did not predict perceptual suppression. Nonetheless, the concurrent observation of low alpha activity, reflecting increased cortical excitability, and low HEP amplitudes, suggesting decreased interoceptive processing, indirectly hints at a potential attentional trade-off between exteroceptive and interoceptive processing during exercise.

Chapter 3 reports the second experimental study, which examines the impact of exercise-induced heart rate changes on perceptual suppression dynamics in the Motion-Induced Blindness (MIB) paradigm. Unlike the GFS findings, no significant effect of exercise was observed on perceptual suppression rate or duration, and no correlations were found between heart rate changes and suppression metrics. Stimulus-locked analyses of HEPs in a Replay condition revealed significantly lower amplitudes during

physical target removal compared to target presence. However, response-locked analyses of HEPs in both MIB and Replay conditions showed no significant differences, indicating no difference in interoceptive processing concurrent with subjective perceptual changes.

Taken together, these findings suggest that cardiac influences on perceptual suppression may depend on the cognitive and neural demands of the specific paradigm. While subtle indications of attentional trade-offs between interoceptive and exteroceptive processing were observed, these effects appear to operate independently of cortical excitability. The absence of a clear link between interoceptive signals and perceptual outcomes points to a modulatory, rather than deterministic, role for interoception. Furthermore, the results reinforce the idea that neural variability plays a more prominent role in shaping perceptual processes than cardiac influences.

Chapter 4 discusses the broader implications of these findings on the role of heart-brain interactions in conscious perception, highlights the limitations of the present studies, and outlines potential directions for future research.

Zusammenfassung

Das Ziel dieser Dissertation ist es, die Wechselwirkung zwischen afferenten Herzsignalen und der neuronalen Verarbeitung exterozeptiver Eingaben zu untersuchen und herauszufinden, wie diese Dynamik zur bewussten visuellen Wahrnehmung beiträgt. Diese Untersuchung basiert auf zwei EEG-ECG-Studien, die erforschen, wie die durch Bewegung induzierte Modulation der Herzaktivität die Wahrnehmungssuppression beeinflusst – ein Phänomen, bei dem ein auffälliger visueller Reiz trotz unveränderter sensorischer Eingabe subjektiv unsichtbar wird.

Kapitel 1 führt in die anatomischen, physiologischen und theoretischen Grundlagen von Herz-Hirn-Interaktionen bei bewusster Wahrnehmung ein und umreißt die Zielsetzungen der experimentellen Studien.

Kapitel 2 präsentiert die erste experimentelle Studie, die untersucht, wie sich leichtes Fahrradfahren auf die Wahrnehmungssuppression, die prästimulus Alpha-Aktivität und die Heartbeat-Evoked Potentials (HEPs) im Generlized Flash Suppression (GFS)-Paradigma auswirkt. Die Bewegung reduzierte die Wahrscheinlichkeit einer Wahrnehmungssuppression und verringerte die Alpha-Amplituden, was auf eine erhöhte kortikale Erregbarkeit hindeutet. Diese Ergebnisse stellen die Baroreceptor Hypothesis infrage, die vorhersagt, dass eine erhöhte Herzfrequenz die kortikale Erregbarkeit reduzieren und die sensorische Verarbeitung unterdrücken sollte. Darüber hinaus liefern die durch Bewegung induzierten Abnahmen der HEP-Amplituden neuartige Beweise für den Einfluss der Herzphysiologie auf die neuronale Verarbeitung kardialer Signale. HEPs sagten die Wahrnehmungssuppression jedoch nicht voraus. Dennoch deutet die gleichzeitige Beobachtung von niedriger Alpha-Aktivität, die auf erhöhte kortikale Erregbarkeit hinweist, und niedrigen HEP-Amplituden, die auf eine verringerte interozeptive Verarbeitung hinweisen, indirekt auf ein potenzielles Aufmerksamkeits-Ungleichgewicht zwischen exterozeptiver und interozeptiver Verarbeitung während der Bewegung hin.

Kapitel 3 berichtet über die zweite experimentelle Studie, die den Einfluss durch Bewegung induzierter Veränderungen der Herzfrequenz auf die Dynamik der Wahrnehmungssuppression im Motion-Induced Blindness (MIB)-Paradigma untersucht. Im Gegensatz zu den Ergebnissen des GFS zeigte sich kein signifikanter Effekt der Bewegung auf die Rate oder Dauer der Wahrnehmungssuppression, und es wurden keine Korrelationen zwischen Herzfrequenzänderungen und Suppressionsmetriken gefunden. Stimulus-gebundene Analysen der HEPs in einer Replay-Bedingung ergaben signifikant niedrigere Amplituden während der physischen Entfernung des Zielreizes im Vergleich zu dessen Anwesenheit. Antwort-gebundene Analysen der HEPs sowohl in den MIB- als auch in den Replay-Bedingungen zeigten jedoch keine signifikanten Unterschiede, was darauf hindeutet, dass es keine Unterschiede in der interozeptiven Verarbeitung gibt, die mit subjektiven Wahrnehmungsänderungen einhergehen.

Zusammenfassend deuten diese Ergebnisse darauf hin, dass die kardialen Einflüsse auf die Wahrnehmungssuppression von den kognitiven und neuronalen Anforderungen des jeweiligen Paradigmas abhängen können. Während subtile Hinweise auf ein Aufmerksamkeitsungleichgewicht zwischen interozeptiver und exterozeptiver Verarbeitung beobachtet wurden, scheinen diese Effekte unabhängig von der kortikalen Erregbarkeit zu wirken. Das Fehlen eines klaren Zusammenhangs zwischen interozeptiven Signalen und Wahrnehmungsergebnissen deutet auf eine modulatorische und nicht deterministische Rolle der Interozeption hin. Darüber hinaus untermauern die Ergebnisse die Idee, dass neuronale Variabilität eine wichtigere Rolle bei der Gestaltung von Wahrnehmungsprozessen spielt als kardiale Einflüsse.

Kapitel 4 diskutiert die breiteren Implikationen dieser Ergebnisse für die Rolle von Herz-Hirn-Interaktionen bei bewusster Wahrnehmung, hebt die Einschränkungen der vorliegenden Studien hervor und skizziert potenzielle Richtungen für zukünftige Forschung.

Disclaimer:

This translation was generated using ChatGPT and may contain inaccuracies or errors.

Chapter 1 General Introduction

Conscious perception of the same sensory input can spontaneously shift between distinct interpretations. These perceptual variations arise from fluctuations in ongoing neural activity, which set the stage for the processing of sensory information from the external environment, i.e. exteroceptive signals, and influence perceptual outcomes (Dijk et al., 2008; Gelbard-Sagiv et al., 2018; Palva et al., 2013; Sadaghiani et al., 2009; Linkenkaer-Hansen et al., 2004). These fluctuations in neural activity are shaped by multiple factors, including anatomical connectivity, intrinsic neural dynamics and states, and concurrent mental processes (Fox & Raichle, 2007; Deco et al., 2011). Recently, internal bodily signals have also been proposed as a source of these fluctuations, further modulating neural dynamics and shaping our perceptual experience of the external world (Park & Tallon-Baudry, 2014; Critchley & Garfinkel, 2015; Tallon-Baudry et al., 2018; Park et al., 2014).

Interoception – the continuous neural monitoring and processing of bodily signals (Sherrington, 1906) such as cardiac, respiratory, and gastric activity, to generate a sense of the body's physiological state (Craig, 2002) – is a core function of the central nervous system (CNS). Interoceptive processing underpins two regulatory mechanisms crucial for the survival of an organism: homeostasis (Bernard, 1974; Cannon, 1963) and allostasis (Sterling & Eyer, 1988). Homeostasis regulates physiological variables within biologically optimal ranges (Bernard, 1974; Cannon, 1963), whereas allostasis anticipates future bodily needs, for instance, when an organism prepares for physical effort, and adjusts these variables accordingly (Sterling & Eyer, 1988). A balance between these two processes maintains optimal functioning and physiological stability, enabling an organism to adapt to its environment (Smith et al., 2017).

Therefore, interoceptive perception and interoceptive control form a continuous loop: regulating the efferent homeostatic-allostatic balance relies on afferent interoceptive signals to inform and influence brain dynamics. Over the course of evolution, these afferent interoceptive signals are thought to have further adapted to interact with higher-level cognitive functions such as conscious perception of the external world (Smith et al.,

2017), shaping how an organism perceives and responds to its environment. Thus, interoceptive processing is inherently linked to exteroception, or processing of the external environment, both contributing to the overarching function of keeping an organism alive (Engelen et al., 2023).

Building on the role of interoception in shaping exteroceptive brain dynamics and subsequent conscious perception, one specific organ stands out for its potential influence: the heart. It generates rhythmic patterns of electrical activity that are continuously monitored and regulated by the brain on timescales compatible with perceptual processes (Azzalini et al., 2019). These cardiac signals are conveyed beyond the brainstem to a widespread network of subcortical and cortical regions (Azzalini et al., 2019). The brain registers each heartbeat, the cortical processing of which can be studied by measuring heartbeat-evoked potentials (HEPs) (Schandry et al., 1986; Park & Tallon-Baudry, 2014). Furthermore, cardiac activity (Corcoran et al., 2021; Salomon et al., 2016; Veillette et al., 2024) and cardiac interoceptive processing (Park et al., 2014) have been linked to the processing of external stimuli and conscious visual perception. However, it remains unclear, at both the neural and perceptual level, how and to what extent cardiac signals can modulate the conscious access to exteroceptive visual input.

Most theories of cardiac interoception in the context of exteroception and conscious perception focus on baroreceptor activity—the mechanosensory signals generated by the arterial walls in response to cardiac contraction (Bishop et al., 1983). However, theoretical and experimental accounts of heart–brain–perception interactions are divided. Some suggest an attentional trade-off, in which baroreceptor signals compete with visual processing for neural resources (Salomon et al., 2016; Corcoran et al., 2021; J. I. Lacey, 1967; B. C. Lacey & Lacey, 1974; Skora et al., 2022; Allen et al., 2022), while others propose that cardiac activity facilitates visual processing (Park et al., 2014; Veillette et al., 2024; Tallon-Baudry et al., 2018).

Guided by these insights, this thesis investigates how cardiac afferent signals interact with the neural processing of exteroceptive visual inputs and contribute to subsequent conscious perception. The first section of this introduction delves into the anatomy and

physiology underlying heart-brain interactions, starting with the generation of cardiac signals, followed by the afferent pathways of cardiac interoception, and concluding with their neural targets. The next section reviews experimental evidence on the influence of cardiac activity on neural dynamics and perception, focusing on the various aspects of cardiac signals and their processing in the brain. The next section discusses various theoretical perspectives and proposed mechanisms underlying the integration of cardiac signals with ongoing brain activity and the processing of external inputs. Finally, the introduction concludes with the aims of this thesis, outlining the direction of the empirical investigations presented in the subsequent chapters.

1.1 Anatomy and Physiology Underlying Heart-Brain Interactions

1.1.1 Cardiac Anatomy and Physiology

The heart is a vital organ that functions as a pump, sustaining blood circulation throughout the body. It contains four chambers: two **atria** and two **ventricles** (Betts et al., 2022) (**Figure 1-1A**). The atria act as receiving chambers, with the right atrium filling with deoxygenated blood from the venous system and contracting to push it into the right ventricle, while the left atrium fills with oxygenated blood from the pulmonary veins and ejects it into the left ventricle (Betts et al., 2022). The ventricles serve as the primary pumping chambers: the right ventricle propels deoxygenated blood into the pulmonary arteries, and the left ventricle pumps oxygenated blood into the aorta for systemic circulation (Betts et al., 2022) (**Figure 1-1A**). The heart has its own intrinsic nervous system (Armour et al., 1997) and generates its own electrical rhythm. This activity originates in the **sinoatrial** (**SA**) **node**, often referred to as the heart's primary pacemaker, which initiates electrical impulses that are then transmitted by the **cardiac conduction system** to trigger heart muscle contractions (Betts et al., 2022) (**Figure 1-1A**). This pacemaker activity generates the **cardiac cycle**, a coordinated sequence beginning with atrial contraction as the ventricles relax to fill with blood, followed by ventricular contraction to eject blood into circulation as the atria relax to receive the next inflow (Betts et al., 2022). The cardiac cycle is broadly categorised into two phases (**Figure 1-1B**). The period of ventricular contraction, known as **systole**, corresponds to the heart pumping

blood into circulation and has a relatively fixed duration (Engelen et al., 2023). In contrast, the period of ventricular relaxation, called **diastole**, involves the heart filling with blood and has a more variable duration (Engelen et al., 2023). This rhythmic alternation between contraction and relaxation ensures efficient blood circulation.

The electrical activity of the heart, the **electrocardiogram** (**ECG**), can be measured by placing surface electrodes on the body. The ECG, which captures electrical signals on the order of millivolts, reflects key phases of the cardiac cycle (Betts et al., 2022) (**Figure 1-1B**). The **P-wave** corresponds to the electrical activation of the atria, leading to their contraction and causing the ventricles to fill. The **QRS complex** marks the electrical activation of the ventricles, triggering their contraction. The atria relax during this phase but is this event is masked within the QRS complex. Finally, the **T-wave** signifies ventricular relaxation, the recovery phase that prepares the ventricles for the next cycle. In other words, systole corresponds to the interval from the R-peak to the end of the T-wave, while diastole spans from the end of the T-wave to the onset of the next R-peak (Betts et al., 2022) (**Figure 1-1B**).

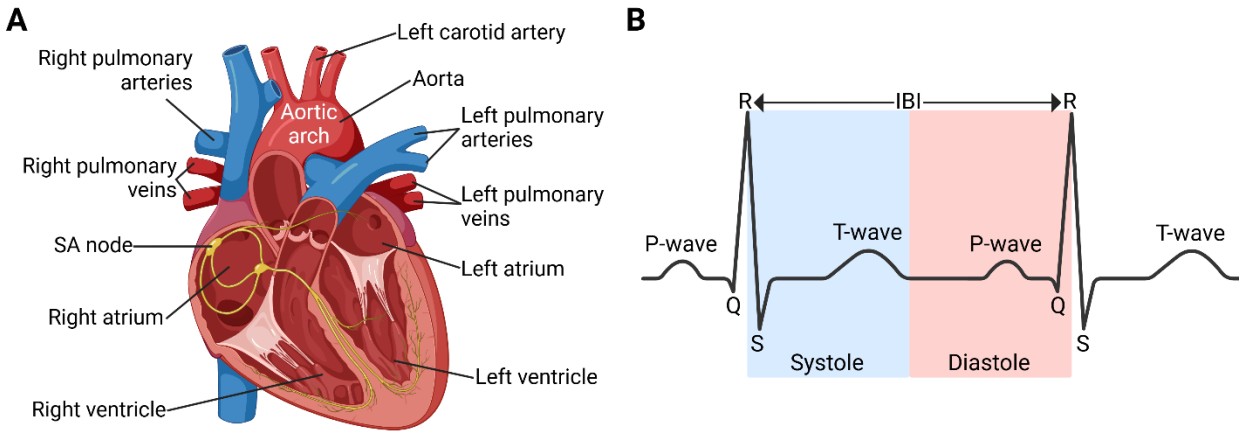

Figure 1-1 – Anatomy of the heart and ECG waveform

(**A**) Cross-sectional view of the heart highlighting key anatomical structures, including the right and left atria, right and left ventricles, SA node and cardiac conduction system (shown in yellow). Additionally, the right pulmonary arteries and veins, aortic arch, aorta, left carotid artery, and left pulmonary arteries and veins are shown, as these represent some of the key sites where mechanoreceptors are located (the right carotid and the coronary arteries are not depicted as they are not visible from this perspective). (**B**) Example of an electrocardiogram (ECG) waveform showing two PQRST complexes, with intervals

corresponding to the two phases of the cardiac cycle, systole and diastole, labelled in blue and red respectively. The inter-beat interval (IBI), measured as the time interval between successive R-peaks, is also illustrated. Figures adapted from Betts et al., 2022. Created in BioRender.com.

The interval between successive R-peaks of the QRS complex, known as the inter-beat interval (IBI) (**Figure 1-1B**), is used to compute **heart rate** (60/IBI gives the instantaneous heart rate in beats per minute (bpm)). Shorter IBIs indicate a faster heart rate, while longer IBIs correspond to a slower heart rate. The resting heart rate of healthy adult humans is typically in the range of 60–100 bpm, while during exercise, heart rate may increase to 150 bpm in healthy young individuals (Betts et al., 2022). Maximum heart rates are generally within the range of 200–220 bpm (Betts et al., 2022).

Although the heart intrinsically generates a regular pattern of electrical activity (approximately 100 bpm, set by the SA node (M. Wang et al., 2020)), its output is shaped by a combination of local influences from the intrinsic cardiac nervous system and descending influences from the CNS (Beissner et al., 2013; K. Kim et al., 2019). This interplay results in the heart rate of healthy individuals being highly irregular, and a reduction in this natural variability—resulting in a highly regular heart rhythm—can serve as a clinically significant indicator of impaired neurological function (Bahari et al., 2018; Fujiwara et al., 2016), particularly in assessing consciousness in non-communicating patients (Raimondo et al., 2017; Riganello et al., 2018).

This natural irregularity in heart rate is quantified as **heart rate variability** (**HRV**), which measures the variability in the intervals between successive heartbeats (Shaffer & Ginsberg, 2017). HRV provides valuable insight into the dynamic interplay between the branches of the autonomic nervous system (ANS) that regulate heart function, reflecting the balance between **parasympathetic** and **sympathetic** activity (Shaffer & Ginsberg, 2017). Parasympathetic activity, primarily mediated by the vagus nerve, decreases heart rate by slowing pacemaker activity, acting like a brake to counteract sympathetic drive. Sympathetic activity, transmitted via sympathetic cardiac nerves, increases heart rate by accelerating pacemaker discharge when the inhibitory parasympathetic ‘brake’ is removed (Jose & Collison, 1970; Opthof, 2000; Salo et al., 2006). The balance between

these autonomic influences is regulated by the central autonomic network (CAN), a complex system of interconnected brain regions that modulates autonomic outflow to the heart (Benarroch, 1993). Changes in heart rate and HRV are thus largely driven by descending influences from the brain to the heart[1].

1.1.2 Pathways of Cardiac Interoception

Heartbeats are transduced into neural signals by **mechanoreceptors**, which are located within the atria and ventricles of the heart as well as in various blood vessels, including the aorta, carotid artery, pulmonary vessels, and coronary vessels (Bishop et al., 1983; Jänig, 1996; Zeng et al., 2018) (**Figure 1-1A**). **Baroreceptors**, a type of stretch receptor located in the carotid artery and aortic arch among other locations, are particularly well-studied for their role in the baroreflex, which regulates heart rate and blood pressure (G. G. Berntson et al., 2007; Dampney et al., 2003). Most cardiac receptors, including baroreceptors, discharge at each cardiac cycle (Bronk & Stella, 1932), signalling transient changes in blood pressure and the strength of cardiac contraction (systole) (Bishop et al., 1983). Thus, baroreceptor firing increases during systole and also during increases in heart rate due to more frequent cardiac cycles.

The latencies of signalling can vary depending on receptor type and location (Bishop et al., 1983; Paintal, 1973). Other cardiac mechanoreceptors signal the occurrence of a contraction, independent of contraction parameters and pressure changes (Bishop et al., 1983). These mechanoreceptors collectively form the starting point of interoceptive pathways that communicate cardiac signals to the brain, providing critical information about the occurrence and characteristics of each heartbeat (**Figure 1-2**).

The mechanoreceptors relay signals to the central nervous system (CNS) through two main pathways: **cranial nerves** and **spinal nerves** (**Figure 1-2**) (Azzalini et al., 2019; Engelen et al., 2023). The cranial nerves involved in cardiac signalling include the vagus

[1] While the primary emphasis of this thesis is on the ascending influences of cardiac interoception, briefly addressing the descending influences is relevant for understanding the bidirectional communication that forms the foundation of heart-brain interactions, and because this research examines heart rate changes and employs exercise as an intervention.

and glossopharyngeal nerves (Azzalini et al., 2019; Engelen et al., 2023). The **vagus nerve** plays a dual role in cardiac function, both sensing the heart by transmitting sensory information from baroreceptors, including those in the aortic arch (with 80% of its fibres being ascending (Agostoni et al., 1957)), and controlling the heart through descending parasympathetic pathways (Betts et al., 2022). The **glossopharyngeal nerve** conveys sensory information specifically from the baroreceptors of the carotid sinus (Azzalini et al., 2019). These cranial nerves directly enter the brainstem, while cardiac spinal nerves ascend via the spinal cord (Engelen et al., 2023). It must be noted that many interoceptive signals beyond cardiac activity, such as those arising from gastric and respiratory systems, share overlapping pathways with cardiac interoceptive signals, converging at similar relay points in the brainstem (**Figure 1-2**) and higher centres (Engelen et al., 2023).

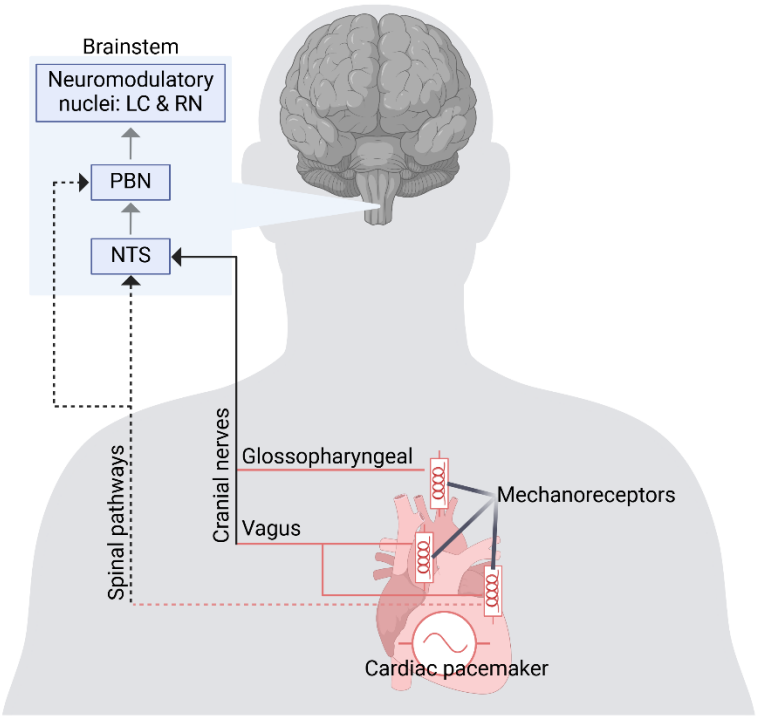

Figure 1-2 – Primary cardiac interoception pathways to brainstem

The heart contains its own autonomous electrical pacemaker, which generates rhythmic electrical impulses to coordinate cardiac contractions. Cardiac activity is sensed by mechanoreceptors located within the heart and large blood vessels, which detect pressure changes and contraction strength. Cardiac signals are transmitted to the CNS via two primary afferent pathways: cranial nerves (vagus and

glossopharyngeal) which directly enter the brainstem, and spinal pathways while travel through the spinal cord. These pathways converge on key relay centres in the brainstem, including the nucleus tractus solitarius (NTS) and parabrachial nucleus (PBN), which in turn project to neuromodulatory nuclei such as the locus coeruleus (LC) and raphe nuclei (RN). Figure adapted from Engelen et al., 2023. Created in BioRender.com.

In addition to these primary pathways, cardiac activity is also signalled to the CNS through alternative mechanisms. Tactile and proprioceptive receptors in the periphery detect vessel pulsatility and changes in thoracic volume, indicating that cardiac activity is already represented even at the most peripheral levels of the somatosensory system (Azzalini et al., 2019; Birznieks et al., 2012; Ford & Kirkwood, 2018; Macefield, 2003).

Emerging evidence in rodents suggests that astrocytes in the CNS can function as intracranial baroreceptors, modulating brainstem neurons and cortical firing (K. J. Kim et al., 2016; Marina et al., 2020). Furthermore, pyramidal neurons (K. J. Kim et al., 2016; J. Wang & Hamill, 2021) and mitral cells in the olfactory bulb (Jammal Salameh et al., 2024) expressing PIEZO2 channels, mechanosensitive ion channels that transduce mechanical stimuli, such as membrane tension into electrical and biochemical signals (Kefauver et al., 2020), may directly detect intracranial pressure pulses, highlighting the potential for vasculoneuronal coupling as another route for cardiac signal transduction.

These diverse pathways convey cardiac signals to the CNS, forming the foundation for interoceptive monitoring and processing.

1.1.3 Subcortical and Cortical Targets of Cardiac Interoceptive Signals

Both vagal and spinal interoceptive pathways mentioned in the previous section converge on interoceptive relay centres in the brainstem (**Figure 1-3**), primarily the **nucleus tractus solitarius** (NTS) (Rinaman & Schwartz, 2004) and the **parabrachial nucleus** (PBN) (Saper & Loewy, 1980).

These brainstem nuclei project to subcortical structures such as the **hypothalamus**, **amygdala**, **cerebellum**, **striatum**, and **hippocampus** (Castle et al., 2005), as well as

neuromodulatory nuclei within the brainstem, including the **locus coeruleus** and **raphe nuclei** (Chen et al., 2021; Kleckner et al., 2017), and several **thalamic nuclei**, including the ventroposterior medial and lateral nuclei (Cechetto & Saper, 1987), as well as the paraventricular nucleus (Penzo & Gao, 2021) (**Figure 1-3**).

Interoceptive information is then relayed to the cortex either via thalamic relays or direct projections from the PBN (Grady et al., 2020). Cortical targets of cardiac interoceptive signals include the **primary** and **secondary somatosensory cortices** (Amassian, 1951)**,** the **ventromedial prefrontal cortex** (**vmPFC**) (Vogt & Derbyshire, 2009), and the **cingulate motor areas** (Dum et al., 2009). The **insula**, both anterior (Craig, 2002) and particularly its posterior granular region, which is viscerotopically organised (Cechetto & Saper, 1987), play a central role in processing these inputs. Furthermore, **heartbeat-evoked potentials** (**HEPs**), which are cortical responses to cardiac activity (elaborated on below in **Section 1.2.3**), have been observed in a variety of cortical regions, including in some primary sensory cortices. These include areas that receive cardiac interoceptive signals, such as the somatosensory cortex, vmPFC, insula and **frontal operculum**, as well as other regions such as **posterior cingulate cortex** (**PCC**) / **ventral precuneus**, and **parietal** and **occipital cortices** (Engelen et al., 2023) (**Figure 1-3**).

Thus, cardiac signals are conveyed to and processed by an extensive network, highlighting the distributed nature of interoceptive representation in the human brain. This broad network underscores the importance of interoceptive signals in shaping brain function and calls for refined anatomical and functional characterisations of the pathways from cardiac transduction sites to their cortical and subcortical targets (Engelen et al., 2023).

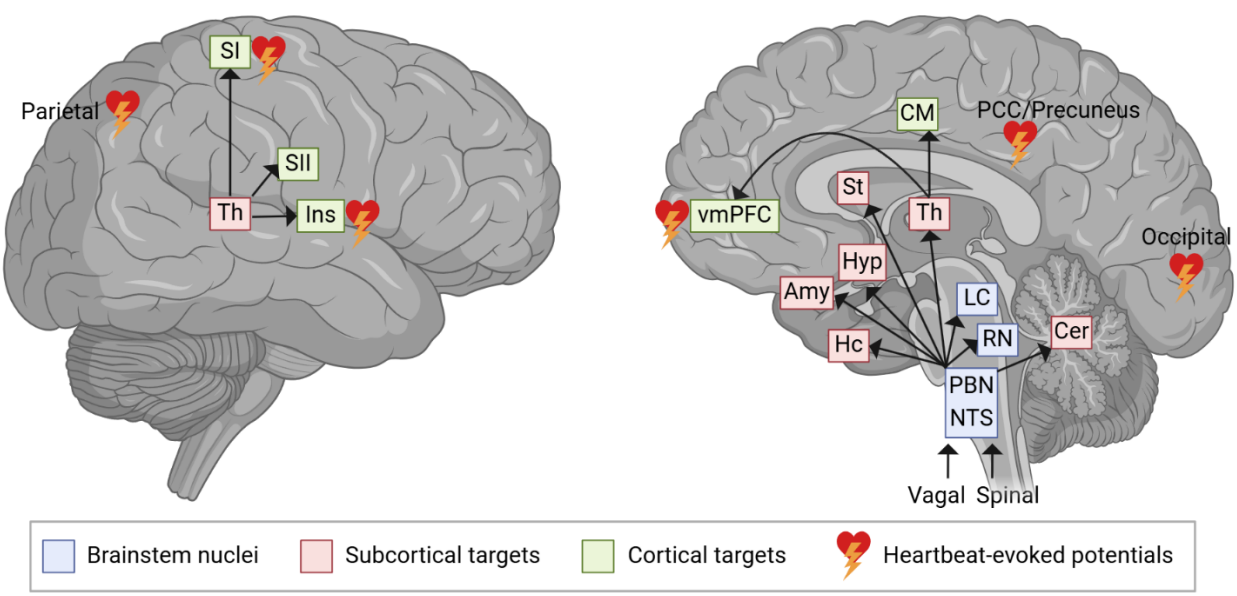

Figure 1-3 – Subcortical and cortical targets of cardiac interoceptive signals and regions where Heartbeat-evoked potentials (HEPs) have been observed

Cardiac interoceptive signals reach the nucleus tractus solitarius (NTS) and parabrachial nucleus (PBN) relay nuclei in the brainstem (blue) via vagal and spinal pathways. These, in turn, project to the locus coeruleus (LC) and raphe (RN) neuromodulator nuclei in the brainstem, and to subcortical (red) and cortical (green) regions. HEPs have been observed in the parietal, somatosensory, insular, ventromedial prefrontal, posterior cingulate, and occipital cortices (markers indicate the contribution of a general region and not an exact location).

Abbreviations: Amy, amygdala; Cer, cerebellum; CM, cingulate motor regions; Hc, hippocampus; Hyp, hypothalamus; Ins, insula; LC, locus coeruleus; NTS, nucleus of the solitary tract; PBN, parabrachial nucleus; RN, raphe nucleus; SI, primary somatosensory cortex; SII, secondary somatosensory cortex; St, striatum; Th, thalamus; vmPFC, ventromedial prefrontal cortex. PCC, posterior cingulate cortex. Adapted from Azzalini et al., 2019 and Engelen et al., 2023. Created in BioRender.com.

1.2 Influence of Cardiac Activity on Neural Dynamics and Perception: Experimental Insights

The intrinsic oscillatory activity of the heart is continuously monitored by the brain, with signals reaching even cortical regions. This ongoing interaction between cardiac activity and the brain allows for the interplay of interoceptive information with external sensory signals, potentially influencing conscious perception. Experimental findings on the cardiac contribution to perception can be grouped into three categories, each associated with different aspects of cardiac activity and its neural processing, which will be reviewed in this section: cardiac phase (specifically, the synchrony between external stimuli and phases of the cardiac cycle), heart rate, and neural responses to heartbeats, also known as heartbeat-evoked potentials (HEPs).

1.2.1 Cardiac Phase

There is evidence to suggest that behavioural performance can be influenced by the timing of stimulus presentation within the cardiac cycle. This effect is thought to be mediated by baroreceptors firing, which may inhibit cortical excitability and consequently, sensory processing (B. C. Lacey & Lacey, 1974; J. I. Lacey, 1967) (elaborated on below in **Section 1.3**).

First, let us consider evidence from experiments in which stimuli were delivered randomly, and their timing along the cardiac cycle was determined *a posteriori*. Findings from the visual domain is mixed: some studies have reported no change in visual detection of near-threshold stimuli as a function of the cardiac cycle (Elliott & Graf, 1972; Park et al., 2014; Sandman et al., 1977). However, visual discrimination (Pramme et al., 2014) and visual search (Pramme et al., 2016) are facilitated during systole compared to diastole. Additionally, increased reaction times during systole have been consistently observed in simple reaction-time tasks involving suprathreshold visual stimuli (Callaway & Layne, 1964; McIntyre et al., 2007; Saari & Pappas, 1976; Stewart et al., 2006).

In a continuous flash suppression paradigm, where stimulus timing was controlled to align with specific moments in the cardiac cycle, reduced visual awareness and decreased accuracy were observed for stimuli presented during systole (Salomon et al., 2016). In contrast, in a controlled stimulus-timing binocular rivalry paradigm, visual awareness, as measured by dominance durations, was enhanced for stimuli presented during systole (Veillette et al., 2024).

If the timing of a stimulus within the cardiac cycle can influence behavioural performance, it follows that neural responses to external stimuli could also depend on the cardiac phase. Indeed, larger visual evoked potential amplitudes have been observed during diastole; however, the relationship between these neural fluctuations and behavioural outcomes was not examined in this context (Walker & Sandman, 1982).

Comparing these findings across different modalities also gives further insights on how cardiac signals may interact with perceptual processing. The perception of emotional (visual) stimuli, particularly those associated with fear, threat, and disgust is enhanced during systole (Azevedo et al., 2017; Garfinkel et al., 2014; Garfinkel & Critchley, 2016; Gray et al., 2012). It has been proposed that processing emotional stimuli differently during systole and diastole may not confer a specific functional advantage, but that in states of high sympathetic arousal, such as during systole, emotional stimuli may be prioritised (Azzalini et al., 2019).

Findings in the somatosensory domain more consistently show attenuation of sensation during systole (Al et al., 2020, 2021; Grund et al., 2022; Motyka et al., 2019), particularly pain sensation (Dworkin et al., 1994; Edwards et al., 2001, 2002; Wilkinson et al., 2013). However, some evidence suggests lower somatosensory sensitivity during diastole (Edwards et al., 2009; Martins et al., 2009). This may reflect the anatomical overlap between interoceptive and somatosensory pathways (as described above in **Section 1.1.2**), leading to differences in how somatosensation and vision are processed (Engelen et al., 2023).

Several additional factors may account for the mixed findings in studies investigating cardiac cycle effects on perception. Variations in the measures used to define cardiac phases (e.g., electrocardiogram vs. pulse at different locations) and in the temporal definitions of systole and diastole across studies likely contribute to inconsistencies, as does whether stimuli are presented at or above perceptual thresholds (Engelen et al., 2023). Additionally, the timing of stimuli relative to the cardiac cycle plays a critical role. As described above, some studies determine stimulus timing retrospectively, while others present stimuli at controlled, predefined moments in the cardiac cycle. The latter approach can lead to expectancy effects (Gray et al., 2010), as participants may learn to anticipate stimuli occurring at predictable intervals following heartbeats, potentially influencing visceral rhythms (Engelen et al., 2023). Furthermore, conscious perception of external stimuli has been shown to slow heart rate (Park et al., 2014; Skora et al., 2022). Such entrainment of cardiac activity by experimental variables might explain observed differences in cardiac phase-related effects (Engelen et al., 2023).

Cardiac phase-related effects have yet to be tested outside the highly controlled conditions of laboratory experiments. An additional caveat is that these effects may reflect a coincidental alignment between cardiac activity and perceptual outcomes, rather than a direct causal relationship between the two. A mechanistic understanding of these cardiac phase-related effects is crucial for understanding heart-brain interactions in conscious perception.

1.2.2 Heart Rate

Individuals with lower average heart rates demonstrate increased visual stimulus detection accuracy for stimuli presented near threshold (Sandman et al., 1977). However, preliminary evidence from a somatosensory detection task suggests that the instantaneous heart rate before a stimulus does not influence perceptual performance (Motyka et al., 2019).

Preliminary findings also suggest that activation and functional connectivity in resting-state and default-mode networks are positively correlated with both heart rate (Wong et

al., 2007; Ziegler et al., 2009) and HRV (Chang et al., 2013; Nikolaou et al., 2016). Additionally, heart rate shows a positive correlation with individual alpha frequency (Lechinger et al., 2015). However, these results may not necessarily reflect ascending interoceptive influences on neural dynamics, as heart rate and HRV are largely driven by descending brain-to-heart processes, suggesting top-down modulation rather than direct interoceptive effects on brain activity (Azzalini et al., 2019).

While HRV may not reflect ascending interoceptive influences on neural dynamics, transient heart rate changes might still provide insights into the interplay between interoceptive and exteroceptive processing. In perceptual tasks, heart rate often responds dynamically to environmental demands, adjusting in anticipation of stimuli and in relation to subsequent responses. For example, in forewarned perceptual reaction-time tasks (Jennings & Wood, 1977; B. C. Lacey & Lacey, 1974, 1978, 1980; J. I. Lacey, 1967; Somsen et al., 2004), or threshold detection tasks (Park et al., 2014; Grund et al., 2022; Motyka et al., 2019; Cobos et al., 2019), heart rate typically slows before stimulus presentation in response to a warning cue, then accelerates following stimulus detection or the participant's response. Some studies reporting this deceleration-acceleration pattern have shown that heart rate deceleration is more prominent *before* stimulus detection (hit) than when no detection occurs (miss) (Cobos et al., 2019; Motyka et al., 2019), while others observe a less pronounced heart rate acceleration *following* a miss than a hit (Grund et al., 2022; Park et al., 2014). This pattern reflects the central regulation of heart rate through the interplay of parasympathetic and sympathetic activity, which is thought to modulate the interaction between internal bodily signals and sensory processing, reflecting shifting attentional and preparatory processes (Skora et al., 2022), even if the magnitude of deceleration or acceleration does not always reflect perceptual outcomes. Supporting this idea, cardiac deceleration has been found to correlate with active attention during binocular rivalry, linking heart rate dynamics to visual sensitivity (Corcoran et al., 2021).

The theoretical implications of this regulation of heart rate for interoceptive-exteroceptive interplay will be explored further in **Section 1.3** below. The influence of heart rate on

conscious visual perception, particularly the neural mechanisms linking cardiac activity to perceptual outcomes, remains understudied and warrants further investigation.

1.2.3 Heartbeat-Evoked Potentials

Heartbeat-evoked potentials (HEPs) are transient neural responses time-locked to heartbeats, obtained from electrophysiological data (e.g. M/EEG and intracranial recordings) (Schandry et al., 1986; Montoya et al., 1993). HEPs are computed in a manner similar to standard evoked potentials: by aligning and averaging brain activity to the occurrence of an event, but in this case, the event is a heartbeat rather than an external stimulus (Schandry et al., 1986; Montoya et al., 1993). HEPs were initially thought to be primarily linked to the activity of baroreceptors responding to cardiac contractions (Schandry & Montoya, 1996; Gray et al., 2007). However, current thinking has evolved to suggest that they may arise from any of the pathways involved in cardiac interoception mentioned above (Engelen et al., 2023). The exact contributions of the different receptors and pathways involved remain unclear (Azzalini et al., 2019). The effects of HEPs have been observed in a variety of brain regions (**Figure 1-3**) and latencies (usually 200-400 ms after the R-peak), likely due to multiple mechanisms of cardiac-related information transduction and the previously described varying latencies of cardiac mechanoreceptors activation (Azzalini et al., 2019; Park & Blanke, 2019b).

HEPs are regarded as responses evoked by the preceding heartbeat, rather than anticipatory signals for the next heartbeat, as an anticipatory response would be time-locked to the upcoming heartbeat rather than the previous one (Azzalini et al., 2019). Thus far, the influence of cardiac parameters, such as heart rate or stroke volume, on HEPs seems to be limited (Buot et al., 2021; Coll et al., 2021; Engelen et al., 2023; Park & Blanke, 2019b). Explicitly attending to one's own heartbeats consistently modulates HEPs (Montoya et al., 1993; Petzschner et al., 2019; Pollatos et al., 2005; Pollatos & Schandry, 2004; Schandry et al., 1986; Villena-González et al., 2017). Taken together, HEPs have been proposed as a neurophysiological marker of cardiac interoceptive processing, encompassing both implicit (unconscious) and explicit (conscious) forms of interoception (Coll et al., 2021; Park & Blanke, 2019b).

HEPs have been extensively studied and linked to emotions, mood, arousal, as well as bodily self-awareness and self-related cognition, and have been shown to reliably index residual consciousness in post-comatose individuals (Coll et al., 2021; Engelen et al., 2023; Park & Blanke, 2019b). More importantly for this thesis, HEPs have been found to predict the conscious perception of visual (Park et al., 2014) and somatosensory (Al et al., 2020, 2021) stimuli at threshold, further linking interoceptive and perceptual processing. Interestingly, the study involving visual stimuli found higher HEP amplitudes for hits compared to misses (Park et al., 2014), while the opposite was observed for somatosensory stimuli (Al et al., 2020, 2021), with lower HEP amplitudes for hits than misses. This suggests a difference in the role of interoceptive processing across modalities, similar to the variability in previously described cardiac phase-linked effects.

In conclusion, HEPs seem to play a role in conscious perception, providing a valuable tool for examining the interplay between interoceptive and exteroceptive processing. By investigating HEPs in studies of heart-brain interactions in conscious perception, we can compare neural markers of interoception with those of exteroception, offering insights into how their relative contributions to our conscious experience.

1.3 Role of Heart-Brain Interactions in Conscious Perception: Theoretical Perspectives and Proposed Mechanisms

Building on the understanding of interoception as a core regulatory function of the central nervous system, theoretical frameworks originally developed for exteroception have been extended to include the interplay between interoception, ongoing brain dynamics, and subsequent conscious perception (Engelen et al., 2023).

One such framework, the scaffolding hypothesis (Fries, 2005; Singer, 1993), has been extended to suggest that bodily rhythms synchronize neural activity across brain regions, acting as "carrier waves" that modulate brain dynamics (Engelen et al., 2023). This mechanism is analogous to intrinsically generated oscillatory synchrony in the brain, where rhythmic patterns regulate sensory sampling, such as visual attention (Busch & VanRullen, 2010), by creating temporal windows of excitability for different neural

systems (Engelen et al., 2023). In the cardiac context, the baroreceptor hypothesis posits that afferent signals from baroreceptors, firing during systole, attenuate cortical excitability, which can impair the processing of external stimuli (B. C. Lacey & Lacey, 1974; J. I. Lacey, 1967). Experimental support for this hypothesis has demonstrated that stimulating baroreceptors via neck-cuff manipulation leads to global reductions in cortical excitability and inhibition of concurrent brain processing (Duschek et al., 2015; Makovac et al., 2015; Rau et al., 1993).

Under the scaffolding / baroreceptor hypotheses, cardiac phase-related effects would be a natural consequence of the cyclical nature of cardiovascular activity and synchronised cortical excitability (Engelen et al., 2023; Skora et al., 2022). During systole, when baroreceptor firing is maximal, sensory processing might be dampened. Conversely, during diastole, when baroreceptor input is minimal, cortical excitability increases, potentially enhancing sensory perception. By extension, any increase in heart rate, corresponding to a rise in baroreceptor firing, would therefore be associated with an attenuation in cortical excitability, while a decrease in heart rate, reducing baroreceptor noise, would allow for greater neural responsiveness (Skora et al., 2022). Whether and how this oscillatory pattern and its consequences impact conscious visual perception remains an open area of investigation, especially given the inconsistent cardiac phase-related findings.

A related framework, adapting a predictive coding approach to the role of cardiac activity in influencing neural dynamics and perception, proposes that the brain adjusts the precision of sensory evidence by modulating the impact of interoceptive (cardiac) and exteroceptive (sensory) information (Skora et al., 2022). When heightened perceptual sensitivity is required, such as in visual detection tasks, the brain reduces the influence of interoceptive signals by decreasing the impact of baroreceptor firing during parasympathetically driven cardiac deceleration, thereby enhancing cortical excitability and allowing exteroceptive inputs to dominate (Skora et al., 2022). Conversely, when the brain shifts toward action, such as in a state of arousal or fight-or-flight, the sympathetic nervous system withdraws the parasympathetic brake, increasing heart rate and

facilitating the prioritisation of internal signals (such as those related to action preparation) (Skora et al., 2022). In a manner akin to active noise cancellation (Parviainen et al., 2022), the brain modulates the precision of sensory signals by adjusting the relative influence of interoceptive and exteroceptive inputs (Allen et al., 2022; Skora et al., 2022). The proposed balance between parasympathetic and sympathetic systems is consistent with the classical view that parasympathetic activity supports information processing and gathering, while sympathetic activation prepares the body for action (Bradley, 2009; Sara, 2009).

Such predictive coding models propose that bodily rhythms help optimise perception by aligning sensory windows with expected timing of stimuli, or vice versa – a process that can be seen in cycle-based effects, like the inhibition of stimuli during systole, based on predicted cardiac rhythms (Engelen et al., 2023). These frameworks also contextualise the previously mentioned empirical evidence on the pattern of anticipatory cardiac deceleration followed by post-decisional cardiac acceleration, shedding light on how such cardiac dynamics might reflect the optimisation of attentional processes for perceptual sensitivity (Skora et al., 2022).

Each of the theoretical perspectives discussed so far suggests, in one way or another, an attentional trade-off between interoceptive and exteroceptive processing. Attentional resources are thought to be shared and competed for between these two domains, with shifts in attention influencing the prioritisation of bodily signals versus environmental inputs, ultimately shaping perceptual outcomes.

Lastly, an extension of the multisensory integration framework proposes that exteroceptive and interoceptive information converge onto the same neurons, leading to either additive or subtractive interactions between these signals, resulting in either a larger or smaller response, respectively, compared to the sum of the individual responses to each input presented separately (Park & Blanke, 2019a; Engelen et al., 2023). While most frameworks covered so far have emphasised intero-exteroceptive competition, this framework introduces the idea of facilitation, where combined inputs may enhance perception in certain contexts. This could help explain the inconsistent cardiac phase-

linked effects and the differences in the processing of various modalities, as the key factor in multisensory integration theory is the temporal coincidence between inputs (Azzalini et al., 2019). As a result, the dynamics of competition and facilitation may vary depending on how these inputs are synchronised across modalities.

There is also a notion of indirect facilitation in the literature, arising from the frameworks mentioned above, in which interoceptive signals can enhance aspects of exteroceptive perception by contributing to the generation of a sense of experiential (Tallon-Baudry et al., 2018), emotional (Damasio, 2010), or bodily (Park & Blanke, 2019a; Seth, 2013) self, providing a frame of reference for integrating and interpreting external signals. However, this thesis does not focus on self-related aspects. The main point here is to highlight that there is an implicit divide in the literature regarding whether interoceptive signals facilitate or compete with exteroceptive signals in shaping conscious perception.

These often overlapping theoretical frameworks not only inform the design of experimental paradigms but also shape the interpretation of findings (Engelen et al., 2023). While they provide valuable insights into the potential roles of interoception and its interactions with exteroception in shaping conscious perception, the neural mechanisms linking heart rate dynamics to perceptual outcomes remain largely understudied and warrant further exploration.

Specifically, oscillatory activity in the alpha frequency range (8–12 Hz), often used as an index of cortical excitability (Klimesch et al., 2007; Romei, Rihs, et al., 2008; Romei, Brodbeck, et al., 2008; Jensen & Mazaheri, 2010; Iemi et al., 2017) and exteroceptive attention (Kelly et al., 2006; Sauseng et al., 2005; Thut et al., 2006), offers a promising avenue for investigating how cardiac-related neural modulation influences sensory processing and perception (Skora et al., 2022). Alpha activity might reflect the proposed baroreceptor-driven cortical inhibition and its subsequent influences on exteroceptive processing (B. C. Lacey & Lacey, 1978; Koriath et al., 1987).

Alpha-driven inhibition may play a role in optimising the system’s response to irrelevant or periodic inputs, such as the oscillatory baroreceptor signal, although this hypothesis

has yet to be directly tested (Skora et al., 2022). The balance of alpha and HEP activity associated with perceptual awareness also provides a foundation for studying attentional trade-offs between interoceptive (HEPs) and exteroceptive (alpha) inputs. The following section outlines the aims of this thesis, which seeks to address these gaps by examining the influence of interoceptive processing on neural dynamics and subsequent visual conscious perception.

1.4 Aims of this Thesis

The overarching aim of this thesis is to explore the interplay between interoception, the brain's processing of internal bodily signals, specifically cardiac signals, and exteroception, the perception of external stimuli, and to investigate how these processes influence conscious visual perception. While previous research has examined the role of interoceptive signals at perceptual threshold, their contribution to multistable perception, particularly in perceptual suppression paradigms, where salient stimuli subjectively disappear and reappear, remains unexplored. Furthermore, heart rate-related effects on perception remain underexplored.

The studies presented in this thesis use exercise as an intervention to modulate the interoceptive signalling loop and to investigate the dynamic balance between interoceptive and exteroceptive processing under conditions of sympathetic dominance. These studies, employing simultaneous EEG and ECG recordings, examine how exercise-induced changes in heart rate and physiological state impact visual perception in two perceptual suppression paradigms: Generalized Flash Suppression (GFS) and Motion-Induced Blindness (MIB).

The Generalized Flash Suppression (GFS) study, presented in **Chapter 2**, explores how pre-stimulus neural and physiological states influence the likelihood of stimulus suppression during physical exercise. This study tests the baroreceptor hypothesis by examining whether exercise-induced changes in heart rate and cortical excitability, indexed by alpha activity, modulate the likelihood of target suppression. Additionally, it investigates whether heartbeat-evoked potentials (HEPs), a marker of cortical

interoceptive processing, can predict perceptual suppression. Lastly, it examines how exercise-induced changes in cardiac physiology affect HEPs. By exploring these mechanisms under physiological conditions altered by exercise, the study provides insights into how internal bodily signals might shape perceptual outcomes.

The Motion-Induced Blindness (MIB) study, presented in **Chapter 3**, investigates how exercise-induced physiological changes, specifically heart rate, impact perceptual suppression dynamics, post-perceptual changes (both subjective and physical), and post-response registration dynamics. Specifically, this study examines whether changes in interoceptive processing influence the rate and duration of target disappearance in MIB. Additionally, it explores how alterations in physiological states during exercise might affect HEP dynamics after the perceptual-change related response has been registered. By testing these mechanisms in a multistable perception paradigm under varying physiological conditions, the study aims to assess the dynamic balance between interoceptive and exteroceptive processing, investigating whether they compete for attentional resources or facilitate one another in shaping conscious perception.

Together, these paradigms provide complementary perspectives on how internal bodily signals shape conscious visual perception under varying physiological conditions.

1.5 References

Agostoni, E., Chinnock, J. E., Daly, M. D. B., & Murray, J. G. (1957). Functional and Histological Studies of the Vagus Nerve and Its Branches to the Heart, Lungs and Abdominal Viscera in the Cat. *The Journal of Physiology*, *135*(1), 182–205. https://doi.org/10.1113/jphysiol.1957.sp005703

Al, E., Iliopoulos, F., Forschack, N., Nierhaus, T., Grund, M., Motyka, P., Gaebler, M., Nikulin, V. V., & Villringer, A. (2020). Heart–Brain Interactions Shape Somatosensory Perception and Evoked Potentials. *Proceedings of the National Academy of Sciences*, *117*(19), 10575–10584. https://doi.org/10.1073/pnas.1915629117

Al, E., Iliopoulos, F., Nikulin, V. V., & Villringer, A. (2021). Heartbeat and Somatosensory Perception. *NeuroImage*, *238*, 118247. https://doi.org/10.1016/j.neuroimage.2021.118247

Allen, M., Levy, A., Parr, T., & Friston, K. J. (2022). In the Body's Eye: The Computational Anatomy of Interoceptive Inference. *PLOS Computational Biology*, *18*(9), e1010490. https://doi.org/10.1371/journal.pcbi.1010490

Amassian, V. E. (1951). Cortical Representation of Visceral Afferents. *Journal of Neurophysiology*, *14*(6), 433–444. https://doi.org/10.1152/jn.1951.14.6.433

Armour, J. A., Murphy, D. A., Yuan, B.-X., MacDonald, S., & Hopkins, D. A. (1997). Gross and Microscopic Anatomy of the Human Intrinsic Cardiac Nervous System. *The Anatomical Record*, *247*(2), 289–298. https://doi.org/10.1002/(SICI)1097-0185(199702)247:2<289::AID-AR15>3.0.CO;2-L

Azevedo, R. T., Garfinkel, S. N., Critchley, H. D., & Tsakiris, M. (2017). Cardiac Afferent Activity Modulates the Expression of Racial Stereotypes. *Nature Communications*, *8*(1), 13854. https://doi.org/10.1038/ncomms13854

Azzalini, D., Rebollo, I., & Tallon-Baudry, C. (2019). Visceral Signals Shape Brain Dynamics and Cognition. *Trends in Cognitive Sciences*, *23*(6), 488–509. https://doi.org/10.1016/j.tics.2019.03.007

Bahari, F., Ssentongo, P., Schiff, S. J., & Gluckman, B. J. (2018). A Brain–Heart Biomarker for Epileptogenesis. *The Journal of Neuroscience*, *38*(39), 8473–8483. https://doi.org/10.1523/JNEUROSCI.1130-18.2018

Beissner, F., Meissner, K., Bär, K.-J., & Napadow, V. (2013). The Autonomic Brain: An Activation Likelihood Estimation Meta-Analysis for Central Processing of Autonomic Function. *Journal of Neuroscience*, *33*(25), 10503–10511. https://doi.org/10.1523/JNEUROSCI.1103-13.2013

Benarroch, E. E. (1993). The Central Autonomic Network: Functional Organization, Dysfunction, and Perspective. *Mayo Clinic Proceedings*, *68*(10), 988–1001. https://doi.org/10.1016/s0025-6196(12)62272-1

Bernard, C. (1974). *Lectures on the Phenomena Common to Animals and Plants* (Hebbel Hoff, R. Guillemin, & L. Guillemin, Trans.). Charles C Thomas Pub Ltd.

Berntson, G. G., Quigley, K. S., & Lozano, D. (2007). Cardiovascular Psychophysiology. In G. Berntson, J. T. Cacioppo, & L. G. Tassinary (Eds.), *Handbook of Psychophysiology* (3rd ed., pp. 182–210). Cambridge University Press. https://www.cambridge.org/core/books/handbook-of-psychophysiology/cardiovascular-psychophysiology/CAB9D08704751D5A26A58C442B3F2BB8

Betts, J. G., Young, K. A., Wise, J. A., Johnson, E., Poe, B., Kruse, D. H., Korol, O., Johnson, J. E., Womble, M., & DeSaix, P. (2022, April 20). *Ch. 19 Introduction—Anatomy and Physiology 2e | OpenStax*. OpenStax. https://openstax.org/books/anatomy-and-physiology-2e/pages/19-introduction

Birznieks, I., Boonstra, T. W., & Macefield, V. G. (2012). Modulation of Human Muscle Spindle Discharge by Arterial Pulsations—Functional Effects and Consequences. *PLOS ONE*, *7*(4), e35091. https://doi.org/10.1371/journal.pone.0035091

Bishop, V. S., Malliani, A., & Thorén, P. (1983). Cardiac Mechanoreceptors. In J. T. Shephard & F. M. Abbound (Eds.), *Handbook of Physiology* (pp. 497–555). Waverly Press. https://doi.org/10.1002/cphy.cp020315

Bradley, M. M. (2009). Natural Selective Attention: Orienting and Emotion. *Psychophysiology*, *46*(1), 1–11. https://doi.org/10.1111/j.1469-8986.2008.00702.x

Bronk, D. W., & Stella, G. (1932). Afferent Impulses in the Carotid Sinus Nerve I. the Relation of the Discharge from Single End Organs to Arterial Blood Pressure. *Journal of Cellular and Comparative Physiology*, *1*(1), 113–130. https://doi.org/10.1002/jcp.1030010110

Buot, A., Azzalini, D., Chaumon, M., & Tallon-Baudry, C. (2021). Does Stroke Volume Influence Heartbeat Evoked Responses? *Biological Psychology*, *165*, 108165. https://doi.org/10.1016/j.biopsycho.2021.108165

Busch, N. A., & VanRullen, R. (2010). Spontaneous EEG Oscillations Reveal Periodic Sampling of Visual Attention. *Proceedings of the National Academy of Sciences*, *107*(37), 16048–16053. https://doi.org/10.1073/pnas.1004801107

Callaway, E., & Layne, R. S. (1964). Interaction Between the Visual Evoked Response and Two Spontaneous Biological Rhythms: The EEG Alpha Cycle and the Cardiac Arousal Cycle. *Annals of the New York Academy of Sciences*, *112*(1), 421–431. https://doi.org/10.1111/j.1749-6632.1964.tb26762.x

Cannon, W. B. (1963). *The Wisdom of the Body* (Rev. and Enl. Ed). W.W. Norton and Company, Inc.

Castle, M., Comoli, E., & Loewy, A. D. (2005). Autonomic Brainstem Nuclei Are Linked to the Hippocampus. *Neuroscience*, *134*(2), 657–669. https://doi.org/10.1016/j.neuroscience.2005.04.031

Cechetto, D. F., & Saper, C. B. (1987). Evidence for a Viscerotopic Sensory Representation in the Cortex and Thalamus in the Rat. *The Journal of Comparative Neurology*, *262*(1), 27–45. https://doi.org/10.1002/cne.902620104

Chang, C., Metzger, C. D., Glover, G. H., Duyn, J. H., Heinze, H.-J., & Walter, M. (2013). Association Between Heart Rate Variability and Fluctuations in Resting-State Functional Connectivity. *NeuroImage*, *68*, 93–104. https://doi.org/10.1016/j.neuroimage.2012.11.038

Chen, W. G., Schloesser, D., Arensdorf, A. M., Simmons, J. M., Cui, C., Valentino, R., Gnadt, J. W., Nielsen, L., Hillaire-Clarke, C. S., Spruance, V., Horowitz, T. S., Vallejo, Y. F., & Langevin, H. M. (2021). The Emerging Science of Interoception: Sensing, Integrating, Interpreting, and Regulating Signals Within the Self. *Trends in Neurosciences*, *44*(1), 3–16. https://doi.org/10.1016/j.tins.2020.10.007

Cobos, M. I., Guerra, P. M., Vila, J., & Chica, A. B. (2019). Heart-Rate Modulations Reveal Attention and Consciousness Interactions. *Psychophysiology*, *56*(3), e13295. https://doi.org/10.1111/psyp.13295

Coll, M.-P., Hobson, H., Bird, G., & Murphy, J. (2021). Systematic Review and Meta-Analysis of the Relationship Between the Heartbeat-Evoked Potential and

Interoception. *Neuroscience & Biobehavioral Reviews*, *122*, 190–200. https://doi.org/10.1016/j.neubiorev.2020.12.012

Corcoran, A. W., Macefield, V. G., & Hohwy, J. (2021). Be Still My Heart: Cardiac Regulation as a Mode of Uncertainty Reduction. *Psychonomic Bulletin & Review*, *28*(4), 1211–1223. https://doi.org/10.3758/s13423-021-01888-y

Craig, A. D. (2002). How Do You Feel? Interoception: The Sense of the Physiological Condition of the Body. *Nature Reviews Neuroscience*, *3*(8), 655–666. https://doi.org/10.1038/nrn894

Critchley, H. D., & Garfinkel, S. N. (2015). Interactions Between Visceral Afferent Signaling and Stimulus Processing. *Frontiers in Neuroscience*, *9*, 286. https://doi.org/10.3389/fnins.2015.00286

Damasio, A. (2010). *Self Comes to Mind: Constructing the Conscious Brain*. Knopf Doubleday Publishing Group.

Dampney, R. A. L., Polson, J. W., Potts, P. D., Hirooka, Y., & Horiuchi, J. (2003). Functional Organization of Brain Pathways Subserving the Baroreceptor Reflex: Studies in Conscious Animals Using Immediate Early Gene Expression. *Cellular and Molecular Neurobiology*, *23*(4), 597–616. https://doi.org/10.1023/A:1025080314925

Deco, G., Jirsa, V. K., & McIntosh, A. R. (2011). Emerging Concepts for the Dynamical Organization of Resting-State Activity in the Brain. *Nature Reviews Neuroscience*, *12*(1), 43–56. https://doi.org/10.1038/nrn2961

Dijk, H. van, Schoffelen, J.-M., Oostenveld, R., & Jensen, O. (2008). Prestimulus Oscillatory Activity in the Alpha Band Predicts Visual Discrimination Ability. *Journal of Neuroscience*, *28*(8), 1816–1823. https://doi.org/10.1523/JNEUROSCI.1853-07.2008

Dum, R. P., Levinthal, D. J., & Strick, P. L. (2009). The Spinothalamic System Targets Motor and Sensory Areas in the Cerebral Cortex of Monkeys. *The Journal of Neuroscience: The Official Journal of the Society for Neuroscience*, *29*(45), 14223–14235. https://doi.org/10.1523/JNEUROSCI.3398-09.2009

Duschek, S., Wörsching, J., & Reyes del Paso, G. A. (2015). Autonomic Cardiovascular Regulation and Cortical Tone. *Clinical Physiology and Functional Imaging*, *35*(5), 383–392. https://doi.org/10.1111/cpf.12174

Dworkin, B. R., Elbert, T., Rau, H., Birbaumer, N., Pauli, P., Droste, C., & Brunia, C. H. (1994). Central Effects of Baroreceptor Activation in Humans: Attenuation of Skeletal Reflexes and Pain Perception. *Proceedings of the National Academy of Sciences of the United States of America*, *91*(14), 6329–6333.

Edwards, L., McIntyre, D., Carroll, D., Ring, C., & Martin, U. (2002). The Human Nociceptive Flexion Reflex Threshold Is Higher During Systole Than Diastole. *Psychophysiology*, *39*(5), 678–681.

Edwards, L., Ring, C., McIntyre, D., & Carroll, D. (2001). Modulation of the Human Nociceptive Flexion Reflex Across the Cardiac Cycle. *Psychophysiology*, *38*(4), 712–718.

Edwards, L., Ring, C., McIntyre, D., Winer, J. B., & Martin, U. (2009). Sensory Detection Thresholds Are Modulated Across the Cardiac Cycle: Evidence That Cutaneous Sensibility Is Greatest for Systolic Stimulation. *Psychophysiology*, *46*(2), 252–256. https://doi.org/10.1111/j.1469-8986.2008.00769.x

Elliott, R., & Graf, V. (1972). Visual Sensitivity as a Function of Phase of Cardiac Cycle. *Psychophysiology*, *9*(3), 357–361. https://doi.org/10.1111/j.1469-8986.1972.tb03219.x

Engelen, T., Solcà, M., & Tallon-Baudry, C. (2023). Interoceptive Rhythms in the Brain. *Nature Neuroscience*, *26*(10), 1670–1684. https://doi.org/10.1038/s41593-023-01425-1

Ford, T. W., & Kirkwood, P. A. (2018). Cardiac Modulation of Alpha Motoneuron Discharges. *Journal of Neurophysiology*, *119*(5), 1723–1730. https://doi.org/10.1152/jn.00025.2018

Fox, M. D., & Raichle, M. E. (2007). Spontaneous Fluctuations in Brain Activity Observed with Functional Magnetic Resonance Imaging. *Nature Reviews Neuroscience*, *8*(9), 700–711. https://doi.org/10.1038/nrn2201

Fries, P. (2005). A Mechanism for Cognitive Dynamics: Neuronal Communication Through Neuronal Coherence. *Trends in Cognitive Sciences*, *9*(10), 474–480. https://doi.org/10.1016/j.tics.2005.08.011

Fujiwara, K., Miyajima, M., Yamakawa, T., Abe, E., Suzuki, Y., Sawada, Y., Kano, M., Maehara, T., Ohta, K., Sasai-Sakuma, T., Sasano, T., Matsuura, M., & Matsushima, E. (2016). Epileptic Seizure Prediction Based on Multivariate Statistical Process Control of Heart Rate Variability Features. *IEEE Transactions on Biomedical Engineering*, *63*(6), 1321–1332. IEEE Transactions on Biomedical Engineering. https://doi.org/10.1109/TBME.2015.2512276

Garfinkel, S. N., & Critchley, H. D. (2016). Threat and the Body: How the Heart Supports Fear Processing. *Trends in Cognitive Sciences*, *20*(1), 34–46. https://doi.org/10.1016/j.tics.2015.10.005

Garfinkel, S. N., Minati, L., Gray, M. A., Seth, A. K., Dolan, R. J., & Critchley, H. D. (2014). Fear from the Heart: Sensitivity to Fear Stimuli Depends on Individual Heartbeats. *Journal of Neuroscience*, *34*(19), 6573–6582. https://doi.org/10.1523/JNEUROSCI.3507-13.2014

Gelbard-Sagiv, H., Mudrik, L., Hill, M. R., Koch, C., & Fried, I. (2018). Human Single Neuron Activity Precedes Emergence of Conscious Perception. *Nature Communications*, *9*(1), 2057. https://doi.org/10.1038/s41467-018-03749-0

Grady, F., Peltekian, L., Iverson, G., & Geerling, J. C. (2020). Direct Parabrachial-Cortical Connectivity. *Cerebral Cortex (New York, N.Y.: 1991)*, *30*(9), 4811–4833. https://doi.org/10.1093/cercor/bhaa072

Gray, M. A., Beacher, F. D., Minati, L., Nagai, Y., Kemp, A. H., Harrison, N. A., & Critchley, H. D. (2012). Emotional Appraisal Is Influenced by Cardiac Afferent Information. *Emotion*, *12*(1), 180–191. https://doi.org/10.1037/a0025083

Gray, M. A., Minati, L., Paoletti, G., & Critchley, H. D. (2010). Baroreceptor Activation Attenuates Attentional Effects on Pain-Evoked Potentials. *Pain*, *151*(3), 853–861. https://doi.org/10.1016/j.pain.2010.09.028

Gray, M. A., Taggart, P., Sutton, P. M., Groves, D., Holdright, D. R., Bradbury, D., Brull, D., & Critchley, H. D. (2007). A Cortical Potential Reflecting Cardiac Function. *Proceedings of the National Academy of Sciences*, *104*(16), 6818–6823. https://doi.org/10.1073/pnas.0609509104

Grund, M., Al, E., Pabst, M., Dabbagh, A., Stephani, T., Nierhaus, T., Gaebler, M., & Villringer, A. (2022). Respiration, Heartbeat, and Conscious Tactile Perception. *Journal of Neuroscience*, *42*(4), 643–656. https://doi.org/10.1523/JNEUROSCI.0592-21.2021

Iemi, L., Chaumon, M., Crouzet, S. M., & Busch, N. A. (2017). Spontaneous Neural Oscillations Bias Perception by Modulating Baseline Excitability. *The Journal of Neuroscience: The Official Journal of the Society for Neuroscience*, *37*(4), 807–819. https://doi.org/10.1523/JNEUROSCI.1432-16.2016

Jammal Salameh, L., Bitzenhofer, S. H., Hanganu-Opatz, I. L., Dutschmann, M., & Egger, V. (2024). Blood Pressure Pulsations Modulate Central Neuronal Activity Via Mechanosensitive Ion Channels. *Science*, *383*(6682), eadk8511. https://doi.org/10.1126/science.adk8511

Jänig, W. (1996). Neurobiology of Visceral Afferent Neurons: Neuroanatomy, Functions, Organ Regulations and Sensations. *Biological Psychology*, *42*(1–2), 29–51. https://doi.org/10.1016/0301-0511(95)05145-7

Jennings, J. R., & Wood, C. C. (1977). Cardiac Cycle Time Effects on Performance, Phasic Cardiac Responses, and Their Intercorrelation in Choice Reaction Time. *Psychophysiology*, *14*(3), 297–307. https://doi.org/10.1111/j.1469-8986.1977.tb01179.x

Jensen, O., & Mazaheri, A. (2010). Shaping Functional Architecture by Oscillatory Alpha Activity: Gating by Inhibition. *Frontiers in Human Neuroscience*, *4*. https://doi.org/10.3389/fnhum.2010.00186

Jose, A. D., & Collison, D. (1970). The Normal Range and Determinants of the Intrinsic Heart Rate in Man. *Cardiovascular Research*, *4*(2), 160–167. https://doi.org/10.1093/cvr/4.2.160

Kefauver, J. M., Ward, A. B., & Patapoutian, A. (2020). Discoveries in Structure and Physiology of Mechanically Activated Ion Channels. *Nature*, *587*(7835), 567–576. https://doi.org/10.1038/s41586-020-2933-1

Kelly, S. P., Lalor, E. C., Reilly, R. B., & Foxe, J. J. (2006). Increases in Alpha Oscillatory Power Reflect an Active Retinotopic Mechanism for Distracter Suppression During Sustained Visuospatial Attention. *Journal of Neurophysiology*, *95*(6), 3844–3851. https://doi.org/10.1152/jn.01234.2005

Kim, K. J., Ramiro Diaz, J., Iddings, J. A., & Filosa, J. A. (2016). Vasculo-Neuronal Coupling: Retrograde Vascular Communication to Brain Neurons. *The Journal of*

Neuroscience, *36*(50), 12624–12639. https://doi.org/10.1523/JNEUROSCI.1300-16.2016

Kim, K., Ladenbauer, J., Babo-Rebelo, M., Buot, A., Lehongre, K., Adam, C., Hasboun, D., Lambrecq, V., Navarro, V., Ostojic, S., & Tallon-Baudry, C. (2019). Resting-State Neural Firing Rate Is Linked to Cardiac-Cycle Duration in the Human Cingulate and Parahippocampal Cortices. *The Journal of Neuroscience: The Official Journal of the Society for Neuroscience*, *39*(19), 3676–3686. https://doi.org/10.1523/JNEUROSCI.2291-18.2019

Kleckner, I. R., Zhang, J., Touroutoglou, A., Chanes, L., Xia, C., Simmons, W. K., Quigley, K. S., Dickerson, B. C., & Barrett, L. F. (2017). Evidence for a Large-Scale Brain System Supporting Allostasis and Interoception in Humans. *Nature Human Behaviour*, *1*, 0069. https://doi.org/10.1038/s41562-017-0069

Klimesch, W., Sauseng, P., & Hanslmayr, S. (2007). EEG Alpha Oscillations: The Inhibition–Timing Hypothesis. *Brain Research Reviews*, *53*(1), 63–88. https://doi.org/10.1016/j.brainresrev.2006.06.003

Koriath, J. J., Lindholm, E., & Landers, D. M. (1987). Cardiac-Related Cortical Activity During Variations in Mean Heart Rate. *International Journal of Psychophysiology*, *5*(4), 289–299. https://doi.org/10.1016/0167-8760(87)90060-2

Lacey, B. C., & Lacey, J. I. (1974). Studies of Heart Rate and Other Bodily Processes in Sensorimotor Behavior. In *Cardiovascular psychophysiology: Current issues in response mechanisms, biofeedback and methodology* (pp. 538–564). AldineTransaction.

Lacey, B. C., & Lacey, J. I. (1978). Two-Way Communication Between the Heart and the Brain: Significance of Time Within the Cardiac Cycle. *American Psychologist*, *33*(2), 99–113. https://doi.org/10.1037/0003-066X.33.2.99

Lacey, B. C., & Lacey, J. I. (1980). Cognitive Modulation of Time-Dependent Primary Bradycardia. *Psychophysiology*, *17*(3), 209–221. https://doi.org/10.1111/j.1469-8986.1980.tb00137.x

Lacey, J. I. (1967). Somatic Response Patterning and Stress: Some Revisions of Activation Theory. In M. H. Appley & R. Trimbull (Eds.), *Pyschological Stress: Issues in Research*. Appleton Century-Crofts.

Lechinger, J., Heib, D. P. J., Gruber, W., Schabus, M., & Klimesch, W. (2015). Heartbeat-Related EEG Amplitude and Phase Modulations from Wakefulness to Deep Sleep: Interactions with Sleep Spindles and Slow Oscillations. *Psychophysiology*, *52*(11), 1441–1450. https://doi.org/10.1111/psyp.12508

Linkenkaer-Hansen, K., Nikulin, V. V., Palva, S., Ilmoniemi, R. J., & Palva, J. M. (2004). Prestimulus Oscillations Enhance Psychophysical Performance in Humans. *Journal of Neuroscience*, *24*(45), 10186–10190. https://doi.org/10.1523/JNEUROSCI.2584-04.2004

Macefield, V. G. (2003). Cardiovascular and Respiratory Modulation of Tactile Afferents in the Human Finger Pad. *Experimental Physiology*, *88*(5), 617–625. https://doi.org/10.1113/eph8802548

Makovac, E., Garfinkel, S. N., Bassi, A., Basile, B., Macaluso, E., Cercignani, M., Calcagnini, G., Mattei, E., Agalliu, D., Cortelli, P., Caltagirone, C., Bozzali, M., & Critchley, H. (2015). Effect of Parasympathetic Stimulation on Brain Activity During Appraisal of Fearful Expressions. *Neuropsychopharmacology*, *40*(7), 1649–1658. https://doi.org/10.1038/npp.2015.10

Marina, N., Christie, I. N., Korsak, A., Doronin, M., Brazhe, A., Hosford, P. S., Wells, J. A., Sheikhbahaei, S., Humoud, I., Paton, J. F. R., Lythgoe, M. F., Semyanov, A., Kasparov, S., & Gourine, A. V. (2020). Astrocytes Monitor Cerebral Perfusion and Control Systemic Circulation to Maintain Brain Blood Flow. *Nature Communications*, *11*(1), 131. https://doi.org/10.1038/s41467-019-13956-y

Martins, A. Q., Ring, C., McIntyre, D., Edwards, L., & Martin, U. (2009). Effects of Unpredictable Stimulation on Pain and Nociception Across the Cardiac Cycle. *PAIN®*, *147*(1), 84–90. https://doi.org/10.1016/j.pain.2009.08.016

McIntyre, D., Ring, C., Hamer, M., & Carroll, D. (2007). Effects of Arterial and Cardiopulmonary Baroreceptor Activation on Simple and Choice Reaction Times. *Psychophysiology*, *44*(6), 874–879. https://doi.org/10.1111/j.1469-8986.2007.00547.x

Montoya, P., Schandry, R., & Müller, A. (1993). Heartbeat Evoked Potentials (HEP): Topography and Influence of Cardiac Awareness and Focus of Attention. *Electroencephalography and Clinical Neurophysiology/Evoked Potentials Section*, *88*(3), 163–172. https://doi.org/10.1016/0168-5597(93)90001-6

Motyka, P., Grund, M., Forschack, N., Al, E., Villringer, A., & Gaebler, M. (2019). Interactions Between Cardiac Activity and Conscious Somatosensory Perception. *Psychophysiology*, *56*(10), e13424. https://doi.org/10.1111/psyp.13424

Nikolaou, F., Orphanidou, C., Papakyriakou, P., Murphy, K., Wise, R. G., & Mitsis, G. D. (2016). Spontaneous Physiological Variability Modulates Dynamic Functional Connectivity in Resting-State Functional Magnetic Resonance Imaging. *Philosophical Transactions of the Royal Society A: Mathematical, Physical and Engineering Sciences*, *374*(2067), 20150183. https://doi.org/10.1098/rsta.2015.0183

Opthof, T. (2000). The normal range and determinants of the intrinsic heart rate in man*. *Cardiovascular Research*, *45*(1), 177–184. https://doi.org/10.1016/S0008-6363(99)00322-3

Paintal, A. S. (1973). Vagal Sensory Receptors and Their Reflex Effects. *Physiological Reviews*, *53*(1), 159–227. https://doi.org/10.1152/physrev.1973.53.1.159

Palva, J. M., Zhigalov, A., Hirvonen, J., Korhonen, O., Linkenkaer-Hansen, K., & Palva, S. (2013). Neuronal Long-Range Temporal Correlations and Avalanche Dynamics Are Correlated with Behavioral Scaling Laws. *Proceedings of the National Academy of Sciences*, *110*(9), 3585–3590. https://doi.org/10.1073/pnas.1216855110

Park, H.-D., & Blanke, O. (2019a). Coupling Inner and Outer Body for Self-Consciousness. *Trends in Cognitive Sciences*, *23*(5), 377–388. https://doi.org/10.1016/j.tics.2019.02.002

Park, H.-D., & Blanke, O. (2019b). Heartbeat-Evoked Cortical Responses: Underlying Mechanisms, Functional Roles, and Methodological Considerations. *NeuroImage*, *197*, 502–511. https://doi.org/10.1016/j.neuroimage.2019.04.081

Park, H.-D., Correia, S., Ducorps, A., & Tallon-Baudry, C. (2014). Spontaneous Fluctuations in Neural Responses to Heartbeats Predict Visual Detection. *Nature Neuroscience*, *17*(4), Article 4. https://doi.org/10.1038/nn.3671

Park, H.-D., & Tallon-Baudry, C. (2014). The Neural Subjective Frame: From Bodily Signals to Perceptual Consciousness. *Philosophical Transactions of the Royal Society of London. Series B, Biological Sciences*, *369*(1641), 20130208. https://doi.org/10.1098/rstb.2013.0208

Parviainen, T., Lyyra, P., & Nokia, M. S. (2022). Cardiorespiratory Rhythms, Brain Oscillatory Activity and Cognition: Review of Evidence and Proposal for Significance. *Neuroscience and Biobehavioral Reviews*, *142*, 104908. https://doi.org/10.1016/j.neubiorev.2022.104908

Penzo, M. A., & Gao, C. (2021). The Paraventricular Nucleus of the Thalamus: An Integrative Node Underlying Homeostatic Behavior. *Trends in Neurosciences*, *44*(7), 538–549. https://doi.org/10.1016/j.tins.2021.03.001

Petzschner, F. H., Weber, L. A., Wellstein, K. V., Paolini, G., Do, C. T., & Stephan, K. E. (2019). Focus of Attention Modulates the Heartbeat Evoked Potential. *NeuroImage*, *186*, 595–606. https://doi.org/10.1016/j.neuroimage.2018.11.037

Pollatos, O., Kirsch, W., & Schandry, R. (2005). Brain Structures Involved in Interoceptive Awareness and Cardioafferent Signal Processing: A Dipole Source Localization Study. *Human Brain Mapping*, *26*(1), 54–64. https://doi.org/10.1002/hbm.20121

Pollatos, O., & Schandry, R. (2004). Accuracy of Heartbeat Perception Is Reflected in the Amplitude of the Heartbeat-Evoked Brain Potential. *Psychophysiology*, *41*(3), 476–482. https://doi.org/10.1111/1469-8986.2004.00170.x

Pramme, L., Larra, M. F., Schächinger, H., & Frings, C. (2014). Cardiac Cycle Time Effects on Mask Inhibition. *Biological Psychology*, *100*, 115–121. https://doi.org/10.1016/j.biopsycho.2014.05.008

Pramme, L., Larra, M. F., Schächinger, H., & Frings, C. (2016). Cardiac Cycle Time Effects on Selection Efficiency in Vision. *Psychophysiology*, *53*(11), 1702–1711. https://doi.org/10.1111/psyp.12728

Raimondo, F., Rohaut, B., Demertzi, A., Valente, M., Engemann, D. A., Salti, M., Fernandez Slezak, D., Naccache, L., & Sitt, J. D. (2017). Brain-Heart Interactions Reveal Consciousness in Noncommunicating Patients. *Annals of Neurology*, *82*(4), 578–591. https://doi.org/10.1002/ana.25045

Rau, H., Pauli, P., Brody, S., Elbert, T., & Birbaumer, N. (1993). Baroreceptor Stimulation Alters Cortical Activity. *Psychophysiology*, *30*(3), 322–325. https://doi.org/10.1111/j.1469-8986.1993.tb03359.x

Riganello, F., Larroque, S. K., Bahri, M. A., Heine, L., Martial, C., Carrière, M., Charland-Verville, V., Aubinet, C., Vanhaudenhuyse, A., Chatelle, C., Laureys, S., & Di Perri,

C. (2018). A Heartbeat Away From Consciousness: Heart Rate Variability Entropy Can Discriminate Disorders of Consciousness and Is Correlated With Resting-State fMRI Brain Connectivity of the Central Autonomic Network. *Frontiers in Neurology*, *9*, 769. https://doi.org/10.3389/fneur.2018.00769

Rinaman, L., & Schwartz, G. (2004). Anterograde Transneuronal Viral Tracing of Central Viscerosensory Pathways in Rats. *The Journal of Neuroscience: The Official Journal of the Society for Neuroscience*, *24*(11), 2782–2786. https://doi.org/10.1523/JNEUROSCI.5329-03.2004

Romei, V., Brodbeck, V., Michel, C., Amedi, A., Pascual-Leone, A., & Thut, G. (2008). Spontaneous Fluctuations in Posterior Alpha-Band EEG Activity Reflect Variability in Excitability of Human Visual Areas. *Cerebral Cortex*, *18*(9), 2010–2018. https://doi.org/10.1093/cercor/bhm229

Romei, V., Rihs, T., Brodbeck, V., & Thut, G. (2008). Resting Electroencephalogram Alpha-Power Over Posterior Sites Indexes Baseline Visual Cortex Excitability. *Neuroreport*, *19*(2), 203–208. https://doi.org/10.1097/WNR.0b013e3282f454c4

Saari, M. J., & Pappas, B. A. (1976). Cardiac Cycle Phase and Movement and Reaction Times. *Perceptual and Motor Skills*, *42*(3), 767–770. https://doi.org/10.2466/pms.1976.42.3.767

Sadaghiani, S., Hesselmann, G., & Kleinschmidt, A. (2009). Distributed and Antagonistic Contributions of Ongoing Activity Fluctuations to Auditory Stimulus Detection. *Journal of Neuroscience*, *29*(42), 13410–13417. https://doi.org/10.1523/JNEUROSCI.2592-09.2009

Salo, L. M., Campos, R. R., & McAllen, R. M. (2006). Differential Control of Cardiac Functions by the Brain. *Clinical and Experimental Pharmacology and Physiology*, *33*(12), 1255–1258. https://doi.org/10.1111/j.1440-1681.2006.04520.x

Salomon, R., Ronchi, R., Dönz, J., Bello-Ruiz, J., Herbelin, B., Martet, R., Faivre, N., Schaller, K., & Blanke, O. (2016). The Insula Mediates Access to Awareness of Visual Stimuli Presented Synchronously to the Heartbeat. *The Journal of Neuroscience: The Official Journal of the Society for Neuroscience*, *36*(18), 5115–5127. https://doi.org/10.1523/JNEUROSCI.4262-15.2016

Sandman, C. A., McCanne, T. R., Kaiser, D. N., & Diamond, B. (1977). Heart Rate and Cardiac Phase Influences on Visual Perception. *Journal of Comparative and Physiological Psychology*, *91*(1), 189–202. https://doi.org/10.1037/h0077302

Saper, C. B., & Loewy, A. D. (1980). Efferent Connections of the Parabrachial Nucleus in the Rat. *Brain Research*, *197*(2), 291–317. https://doi.org/10.1016/0006-8993(80)91117-8

Sara, S. J. (2009). The Locus Coeruleus and Noradrenergic Modulation of Cognition. *Nature Reviews Neuroscience*, *10*(3), 211–223. https://doi.org/10.1038/nrn2573

Sauseng, P., Klimesch, W., Stadler, W., Schabus, M., Doppelmayr, M., Hanslmayr, S., Gruber, W. R., & Birbaumer, N. (2005). A Shift of Visual Spatial Attention Is Selectively Associated with Human EEG Alpha Activity. *The European Journal of Neuroscience*, *22*(11), 2917–2926. https://doi.org/10.1111/j.1460-9568.2005.04482.x

Schandry, R., & Montoya, P. (1996). Event-Related Brain Potentials and the Processing of Cardiac Activity. *Biological Psychology*, *42*(1), 75–85. https://doi.org/10.1016/0301-0511(95)05147-3

Schandry, R., Sparrer, B., & Weitkunat, R. (1986). From the Heart to the Brain: A Study of Heartbeat Contingent Scalp Potentials. *International Journal of Neuroscience*, *30*(4), 261–275. https://doi.org/10.3109/00207458608985677

Seth, A. K. (2013). Interoceptive Inference, Emotion, and the Embodied Self. *Trends in Cognitive Sciences*, *17*(11), 565–573. https://doi.org/10.1016/j.tics.2013.09.007

Shaffer, F., & Ginsberg, J. P. (2017). An Overview of Heart Rate Variability Metrics and Norms. *Frontiers in Public Health*, *5*, 258. https://doi.org/10.3389/fpubh.2017.00258

Sherrington, C. S. (1906). *The Integrative Action of the Nervous System* (pp. xvi, 411). Yale University Press. https://doi.org/10.1037/13798-000

Singer, W. (1993). Synchronization of Cortical Activity and Its Putative Role in Information Processing and Learning. *Annual Review of Physiology*, *55*, 349–374. https://doi.org/10.1146/annurev.ph.55.030193.002025

Skora, L. I., Livermore, J. J. A., & Roelofs, K. (2022). The Functional Role of Cardiac Activity in Perception and Action. *Neuroscience & Biobehavioral Reviews*, *137*, 104655. https://doi.org/10.1016/j.neubiorev.2022.104655

Smith, R., Thayer, J. F., Khalsa, S. S., & Lane, R. D. (2017). The Hierarchical Basis of Neurovisceral Integration. *Neuroscience and Biobehavioral Reviews*, *75*, 274–296. https://doi.org/10.1016/j.neubiorev.2017.02.003

Somsen, R. J. M., Jennings, J. R., & Van der Molen, M. W. (2004). The Cardiac Cycle Time Effect Revisited: Temporal Dynamics of the Central-Vagal Modulation of Heart Rate in Human Reaction Time Tasks. *Psychophysiology*, *41*(6), 941–953. https://doi.org/10.1111/j.1469-8986.2004.00241.x

Sterling, P., & Eyer, J. (1988). Allostasis: A new paradigm to explain arousal pathology. In S. Fischer & J. Reason (Eds.), *Handbook of Life Stress, Cognition and Health*. John Wiley & Sons.

Stewart, J. C., France, C. R., & Suhr, J. A. (2006). The Effect of Cardiac Cycle Phase on Reaction Time Among Individuals at Varying Risk for Hypertension. *Journal of Psychophysiology*, *20*(1), 1–8. https://doi.org/10.1027/0269-8803.20.1.1

Tallon-Baudry, C., Campana, F., Park, H.-D., & Babo-Rebelo, M. (2018). The Neural Monitoring of Visceral Inputs, Rather Than Attention, Accounts for First-Person Perspective in Conscious Vision. *Cortex*, *102*, 139–149. https://doi.org/10.1016/j.cortex.2017.05.019

Thut, G., Nietzel, A., Brandt, S. A., & Pascual-Leone, A. (2006). Alpha-Band Electroencephalographic Activity Over Occipital Cortex Indexes Visuospatial Attention Bias and Predicts Visual Target Detection. *The Journal of Neuroscience: The Official Journal of the Society for Neuroscience*, *26*(37), 9494–9502. https://doi.org/10.1523/JNEUROSCI.0875-06.2006

Veillette, J. P., Gao, F., & Nusbaum, H. C. (2024). Cardiac Afferent Signals Can Facilitate Visual Dominance in Binocular Rivalry. *ELife*, *13*, RP95599. https://doi.org/10.7554/eLife.95599

Villena-González, M., Moënne-Loccoz, C., Lagos, R. A., Alliende, L. M., Billeke, P., Aboitiz, F., López, V., & Cosmelli, D. (2017). Attending to the Heart Is Associated with Posterior Alpha Band Increase and a Reduction in Sensitivity to Concurrent Visual Stimuli. *Psychophysiology*, *54*(10), 1483–1497. https://doi.org/10.1111/psyp.12894

Vogt, B. A., & Derbyshire, S. W. G. (2009). Visceral Circuits and Cingulate-Mediated Autonomic Functions. In B. A. Vogt (Ed.), *Cingulate Neurobiology and Disease* (p. 0). Oxford University Press. https://doi.org/10.1093/oso/9780198566960.003.0010

Walker, B. B., & Sandman, C. A. (1982). Visual Evoked Potentials Change as Heart Rate and Carotid Pressure Change. *Psychophysiology*, *19*(5), 520–527. https://doi.org/10.1111/j.1469-8986.1982.tb02579.x

Wang, J., & Hamill, O. P. (2021). Piezo2-Peripheral Baroreceptor Channel Expressed in Select Neurons of the Mouse Brain: A Putative Mechanism for Synchronizing Neural Networks by Transducing Intracranial Pressure Pulses. *Journal of Integrative Neuroscience*, *20*(4), 825–837. https://doi.org/10.31083/j.jin2004085

Wang, M., Monticone, R. E., & McGraw, K. R. (2020). Aging of the Heart and Cardiovascular System. In S. I. S. Rattan (Ed.), *Encyclopedia of Biomedical Gerontology* (pp. 173–182). Academic Press. https://doi.org/10.1016/B978-0-12-801238-3.11397-2

Wilkinson, M., McIntyre, D., & Edwards, L. (2013). Electrocutaneous Pain Thresholds Are Higher During Systole Than Diastole. *Biological Psychology*, *94*(1), 71–73. https://doi.org/10.1016/j.biopsycho.2013.05.002

Wong, S. W., Massé, N., Kimmerly, D. S., Menon, R. S., & Shoemaker, J. K. (2007). Ventral Medial Prefrontal Cortex and Cardiovagal Control in Conscious Humans. *NeuroImage*, *35*(2), 698–708. https://doi.org/10.1016/j.neuroimage.2006.12.027

Zeng, W.-Z., Marshall, K. L., Min, S., Daou, I., Chapleau, M. W., Abboud, F. M., Liberles, S. D., & Patapoutian, A. (2018). PIEZOs mediate neuronal sensing of blood pressure and the baroreceptor reflex. *Science*, *362*(6413), 464–467. https://doi.org/10.1126/science.aau6324

Ziegler, G., Dahnke, R., Yeragani, V. K., & Bär, K.-J. (2009). The Relation of Ventromedial Prefrontal Cortex Activity and Heart Rate Fluctuations at Rest. *European Journal of Neuroscience*, *30*(11), 2205–2210. https://doi.org/10.1111/j.1460-9568.2009.07008.x

Chapter 2 Neural and Cardiac Contributions to Perceptual Suppression During Cycling

Aishwarya Bhonsle[1,2] and Melanie Wilke[1,2,3*]

[1.] Department of Cognitive Neurology, University Medical Center Göttingen, Göttingen, Germany

[2.] MR-Research in Neurosciences, University Medical Center Göttingen, Göttingen, Germany

[3.] Cognitive Neurology Group, Department of Cognitive Neuroscience, German Primate Center, Leibniz Institute for Primate Research, Göttingen, Germany

DOI: 10.22541/au.173796146.68913752/v1

*Corresponding author:

Prof. Dr. Melanie Wilke, Department of Cognitive Neurology, Heart & Brain Center, University Medicine Göttingen, Robert-Koch-Strasse 42, 37073 Göttingen, Germany

Email: melanie.wilke@med.uni-goettingen.de

Impact statement

Our study explores how light-intensity cycling impacts perceptual suppression and alters pre-stimulus parieto-occipital alpha activity and heartbeat-evoked potentials (HEPs). We are the first to directly investigate the theory that exercise influences neural activity through baroreceptor-driven cortical excitability, and our findings challenge this mechanism. Additionally, we provide novel evidence of exercise-induced changes in HEPs, reflecting shifts in neural processing of cardiac signals and revealing, for the first time, the influence of cardiac physiology on HEPs.

2.1 Abstract

Exercise influences visual processing and is accompanied by neural and physiological changes in the body. Yet, the underlying mechanisms by which neural and physiological responses to exercise impact ensuing perception remain poorly understood. In particular, the effects of exercise-induced cardiac changes on visual perception and electrophysiological activity are unclear. Here, we aimed to investigate the relationship between conscious visual perception, neural activity, and cardiac responses during exercise. Thirty healthy participants performed a perceptual suppression task while engaging in light-intensity stationary cycling, with EEG and ECG activity recorded simultaneously. Our study shows that the probability of perceptual suppression decreased during cycling. Parieto-occipital alpha amplitudes (8–12 Hz) also decreased during cycling, but this reduction did not correlate with the decrease in perceptual suppression. Additionally, cycling decreased heartbeat-evoked potential (HEP) amplitudes, indicating altered neural processing of cardiac signals during exercise. However, these exercise-induced changes in HEP amplitudes did not predict perceptual outcomes. Moreover, changes in heart rate in response to cycling did not correlate with changes in perceptual suppression rates, pre-RDM alpha, or HEP amplitudes. These findings indicate that while exercise modulates conscious visual perception, the associated changes in alpha activity, heart rate, and HEPs do not fully explain this effect. Our results highlight the complex relationship between interoceptive processing and mechanisms underlying the perception of external stimuli during exercise.

Keywords: exercise, perceptual suppression, alpha, heart rate, heartbeat-evoked potentials, perception, heart-brain

2.2 Introduction

A single bout of exercise can produce positive effects on cognitive function (Cantelon & Giles, 2021; Chang et al., 2012; Garrett et al., 2024; Lambourne & Tomporowski, 2010), alongside various neural (Crabbe & Dishman, 2004; Hosang et al., 2022) and bodily physiological responses (Heinonen et al., 2014). Studies of human visual processing during physical activity reveal that exercise-induced neural changes are linked to altered perceptual dynamics, which differ markedly from those observed at rest (Bullock et al., 2015, 2017; Cao & Händel, 2019; De Sanctis et al., 2014). Among these neural changes, cortical oscillatory activity across the entire frequency spectrum and various brain regions shows consistent modulation during acute bouts of physical activity, with findings in the alpha band (8–12 Hz) being the most consistent, though the direction and location of these effects vary (see refs. (Crabbe & Dishman, 2004; Hosang et al., 2022) for reviews). These neural responses are highly context-dependent, as variations in the combinations of perceptual tasks and types of physical activity contribute to differences in the observed outcomes. For example, naturalistic walking has been linked to a decrease in alpha power, which is thought to reflect reduced inhibitory processes that typically suppress peripheral visual input (Cao & Händel, 2019). During an oddball task, moderate-to-high intensity cycling led to a smaller decrease in parieto-occipital alpha power in response to non-target stimuli compared to light exercise, while detection accuracy remained consistent across intensities (Ciria et al., 2019). In contrast, increased parieto-occipital alpha has also been observed during cycling, coinciding with reduced accuracy in an orientation discrimination task (Bullock et al., 2017). Independent of perceptual task demands, broadband decreases in alpha activity have been observed during cycling and walking, with more pronounced reductions during walking (Storzer et al., 2016). Conversely, increases in alpha activity during cycling have also been observed throughout the brain (Hottenrott et al., 2013), though most frequently across anterior regions (Bailey et al., 2008; Enders et al., 2016; Fumoto et al., 2010; Hosang et al., 2022).

In addition to these neural and perceptual responses, exercise elicits a gamut of physiological responses across virtually all tissues and organs in the human body, including an increase in cardiac activity (Heinonen et al., 2014), including an increase in

heart rate and a decrease in heart rate variability (HRV) (Mongin et al., 2022). In addition, mild exercise has been shown to increase cerebral blood flow (Querido & Sheel, 2007), and neurotransmitter levels of dopamine, norepinephrine, and serotonin (Meeusen & De Meirleir, 1995), up to boosting neurotrophic factor (e.g. BDNF) levels (Ferris et al., 2007). While the effects of exercise on oscillatory neural activity and visual perception are the subject of ongoing investigation, the influence of exercise-induced cardiac changes on neural activity and subsequent perception remains largely understudied. Typically, studies investigating the effects of physical activity have used heart rate as a metric of exercise intensity (Garber et al., 2011), while EEG analyses have considered heart activity as a source of non-cerebral artefacts, especially under physical exertion.

Heartbeats are transduced into neural signals by mechanoreceptors, which are located within the atria and ventricles of the heart as well as in various blood vessels (Bishop et al., 1983; Jänig, 1996; Zeng et al., 2018). Of these, baroreceptors are a type of stretch receptor located in the heart and blood vessels. They are particularly well-studied for their role in the baroreflex, which regulates heart rate and blood pressure (Berntson et al., 2007; Dampney et al., 2003). Baroreceptors relay information to the brain about the timing and strength of cardiac contractions and transient changes in blood pressure (Bishop et al., 1983). An increase in heart rate leads to increased baroreceptor activity, although there are important exceptions to this rule, e.g. in the context of respiratory sinus arrhythmia (RSA) (Berntson et al., 1993; Noble & Hochman, 2019).

In addition to baroreceptor inputs, cardiac activity is also signalled to the CNS through alternative pathways. For instance, vessel pulsatility and changes in thoracic volume are detected by tactile and proprioceptive receptors (Birznieks et al., 2012; Ford & Kirkwood, 2018; Macefield, 2003). Recent findings in rodent models indicate that astrocytes in the CNS may act as intracranial baroreceptors, influencing both brainstem activity and cortical excitability (Kim et al., 2016; Marina et al., 2020). In addition, certain neuron types, such as pyramidal neurons (Kim et al., 2016; Wang & Hamill, 2021), and mitral cells in the olfactory bulb (Jammal Salameh et al., 2024), express PIEZO2 channels, which are mechanosensitive ion channels that transduce mechanical stimuli, such as membrane

tension, into electrical and biochemical signals (Kefauver et al., 2020). Thus, they may directly detect intracranial pressure pulses, offering yet another route for cardiac signal transduction.

It has been theorized (Crabbe & Dishman, 2004; Hosang et al., 2022) that exercise-induced increases in alpha activity might arise from cortical inhibition driven by brainstem and subcortical activation linked to cardiovascular regulation (Koriath et al., 1987; B. C. Lacey & Lacey, 1978). This proposal brings together two key concepts: the baroreceptor hypothesis (B. C. Lacey & Lacey, 1974, 1978; J. I. Lacey, 1967; J. I. Lacey & Lacey, 1958, 1970) and alpha activity as an index of cortical excitability (Klimesch et al., 2007; Romei, Rihs, et al., 2008; Romei, Brodbeck, et al., 2008; Jensen & Mazaheri, 2010; Iemi et al., 2017).The baroreceptor hypothesis suggests that changes in cardiovascular activity influence cortical excitability via inhibitory afferent feedback from baroreceptors. According to this hypothesis, higher heart rates, which cause the heart to pump more frequently and increase baroreceptor firing, should lead to an increase in inhibitory feedback and a subsequent reduction in cortical excitability. In parallel, alpha activity is regarded as an index of cortical excitability, with higher alpha levels reflecting reduced cortical excitability (Iemi et al., 2017; Jensen & Mazaheri, 2010; Klimesch et al., 2007; Romei, Brodbeck, et al., 2008; Romei, Rihs, et al., 2008) and visual attentiveness (Kelly et al., 2006; Sauseng et al., 2005; Thut et al., 2006). Alpha-driven cortical inhibition as a mechanism of neural modulation around the periodic baroreceptor signal has yet to be directly investigated, especially in the context of exercise-induced cardiovascular changes.

Changes in heart rate are also thought to be a key physiological response mediating the effect of exercise on perceptual and cognitive performance (Cantelon & Giles, 2021; Chang et al., 2012). Although this relationship is not well characterised in the context of exercise, existing evidence highlights a link between heart rate dynamics and visual perception. For instance, individuals with lower heart rates demonstrate increased visual stimulus detection accuracy (Sandman et al., 1977). Additionally, studies employing perceptual paradigms performed at rest reveal that heart rate changes occur both prior

to and following perception of an external stimulus (B. C. Lacey & Lacey, 1978; J. I. Lacey, 1967; B. C. Lacey & Lacey, 1974; Jennings & Wood, 1977; B. C. Lacey & Lacey, 1980; Somsen et al., 2004; Park et al., 2014; Cobos et al., 2019; Motyka et al., 2019; Grund et al., 2022; Vila et al., 2007; Skora et al., 2022). Specifically, heart rate typically decelerates in anticipation of an upcoming stimulus, a pattern thought to reflect sustained attention and preparatory processes (B. C. Lacey & Lacey, 1978; Skora et al., 2022; Vila et al., 2007), and then accelerates again, following stimulus detection or response registration.

These instantaneous adjustments in heart rate are thought to fine-tune the balance between internal bodily signals (interoception) and external sensory inputs (exteroception), thereby facilitating perception and action (Skora et al., 2022). Cardiac deceleration has been proposed to reduce the inhibitory influence of baroreceptor activity, enhancing attention to external stimuli, improving sensory processing and perception. Consistent with this notion, preliminary evidence shows that cardiac deceleration tracks active attention during binocular rivalry (Corcoran et al., 2021). Conversely, heart rate acceleration following response registration restores the balance between interoceptive and exteroceptive processing and prepares the system for action (Skora et al., 2022).

Interestingly, this competition between interoception and exteroception, independent of cardiovascular mechanisms, has also been discussed in the context of exercise, where shifts in attentional focus between these domains are thought to modulate the perception of fatigue (Pennebaker & Lightner, 1980; Wallman-Jones et al., 2021). However, while resting heart rates and instantaneous heart rate changes have been linked to the perception of visual stimuli and are thought to reflect an interoceptive-exteroceptive trade off, how sustained heart rate increases during exercise influence visual perceptual dynamics, particularly in relation to alpha oscillations, remains unexplored.

Moving beyond heart rate and alpha activity changes, heartbeat-evoked potentials (HEP) are a neural measure that has not yet been investigated in the context of exercise. HEPs represent transient neural activity observed when electrophysiological data are time-locked to heartbeats, and are thought to serve as a marker of cortical processing of cardiac information (Coll et al., 2021; Gray et al., 2007; Park & Blanke, 2019; Schandry

& Montoya, 1996). HEP amplitudes are increased during interoceptive tasks such as heartbeat counting (Montoya et al., 1993; Petzschner et al., 2019). HEP amplitudes have also been shown to predict conscious perception of visual (Park et al., 2014) and somatosensory (Al et al., 2020) stimuli at threshold, further linking interoceptive and exteroceptive processing. Investigating the effect of cycling on HEPs could offer valuable insights into how exercise modulates heart-brain coupling, potentially illuminating interactions between cardiac and cortical responses. Furthermore, examining whether cycling-related modulation of HEPs influences conscious perception could provide additional insight into the contribution of interoceptive processing to exteroceptive perceptual awareness.

In this study, we investigated the neural and cardiac changes through which exercise influences conscious visual perception in a bistable perceptual suppression paradigm. Specifically, we examined how stationary cycling modulates oscillatory brain activity, heart rate, and heart-brain coupling, and how these responses potentially influence conscious perception in a Generalized Flash Suppression (GFS) paradigm. GFS is a perceptual suppression paradigm in which a salient target is rendered subjectively invisible upon presentation of a random dot motion (RDM) surround (Wilke et al., 2003). Previous work employing GFS performed at rest has shown that parieto-occipital alpha amplitudes in the second prior to the motion onset were significantly decreased preceding target disappearances, compared to when the target remained visible (Poland et al., 2021). Therefore, in the current study, exercise-induced changes in alpha oscillations may serve not only as an index of cortical excitability, but may also predict perceptual suppression.

How might perceptual suppression and related pre-RDM parieto-occipital alpha activity be altered during cycling? Evidence from prior studies suggests that alpha activity often increases during exercise (Bailey et al., 2008; Bullock et al., 2017; Enders et al., 2016; Fumoto et al., 2010; Hosang et al., 2022; Hottenrott et al., 2013), and extending the baroreceptor hypothesis to the exercise context further links elevated heart rates during exercise to decreased cortical excitability and increased alpha oscillations (Crabbe &

Dishman, 2004; Hosang et al., 2022; Koriath et al., 1987; B. C. Lacey & Lacey, 1978). However, decreases in alpha activity during physical activity have also been reported in some studies (Cao & Händel, 2019; Storzer et al., 2016), presenting an alternative possibility. Based on these observations and previous GFS findings (Poland et al., 2021), we hypothesised that decreased pre-RDM (i.e. pre-random dot motion) parieto-occipital alpha amplitudes would be associated with higher subjective target suppression rates, whereas increased pre-RDM parieto-occipital alpha amplitudes would correspond to higher target visibility rates.

We also investigated how cycling modulates HEPs. Given the heightened exteroceptive attention required to perform a perceptual and motor task simultaneously, we hypothesised that interoceptive processing will be reduced, reflected by decreased HEP amplitudes during cycling. Additionally, we explored if HEPs predict perceptual suppression. Given that perceptual suppression is associated with lower pre-RDM occipital alpha activity, which indicates increased external attention (Kelly et al., 2006; Sauseng et al., 2005; Thut et al., 2006), increased exteroceptive attention might be correlated with target suppression during GFS. If increased exteroceptive processing competes with interoceptive processing (Skora et al., 2022), we might expect lower HEP amplitudes when the target disappears.

2.3 Methods

2.3.1 Participants

Forty-nine healthy volunteers, mostly university students, were initially recruited for the current study. To be eligible for participation, individuals were required to have no history of neurological, psychological, cardiovascular, respiratory, metabolic, endocrine, immune, or substance abuse disorders. Further eligibility criteria included not taking regular medications that might alter cardiovascular, autonomic, or cognitive functioning, not being pregnant, and not concurrently participating in pharmacological or stimulation studies. All subjects were also required to have normal or corrected-to-normal vision. Of the recruited participants, two did not complete all sessions of the experiment. During the

practice session on day 1, five participants never perceived the target disappearing, and two perceived it disappearing in every trial; all seven were excluded from further participation in the study on day 2. Ten subjects were excluded from further analysis due to noisy EEG data, largely caused by movement artefacts during the cycling conditions, as their recordings required more than 15% of channels to be interpolated. The final cohort consisted of 30 subjects (14 male, 16 female; mean age ± SD: 23.93 ± 2.41 years, age range: 20 – 29 years). One subject was excluded from the HEP analysis due to a lack of trials that met the inclusion criteria for this analysis in one condition. The study was conducted in accordance with the ethical guidelines of the Declaration of Helsinki. The experimental procedure was approved by the ethics committee of the University Medical Center Göttingen (UMG, Germany). All subjects gave written informed consent before the study and were paid for their participation.

2.3.2 Stimuli and task

The visual stimuli were programmed in MATLAB R2015b (The MathWorks Inc., Natick, MA, USA) using Psychtoolbox-3 (Brainard, 1997; Kleiner et al., 2007). Each trial began with a white fixation cross on a black background that remained visible throughout the trial (**Figure 2-1A**). After two seconds of central fixation, the target, a red disk with a diameter of 3° of visual angle, was presented in the left visual hemifield, positioned 7° horizontally and 3° vertically from the centre. After an additional two seconds, a random dot motion (RDM) pattern of moving blue dots (dot diameter = 0.08°; dot speed = 10°/s; dot density = 1.0 dot/deg^2) appeared for two seconds. A 0.5° buffer zone, set to the background colour, was maintained between the target and the RDM pattern. The target and RDM pattern were each presented monocularly using red-blue anaglyphic glasses. In a subset of trials, the presentation of the RDM stimulus resulted in the subjective disappearance of the target. Following each trial, a blank screen was shown for three seconds as the inter-trial interval (ITI).

Subjects were instructed to maintain fixation on the fixation cross throughout the trial and to use a button box (4 Button Curve Right; Current Designs Inc., Philadelphia, PA, USA) to report their perception of the target. Using the index finger of their dominant hand (27

right-handed, 3 left-handed as assessed by the short version of the Edinburgh Handedness Inventory (Oldfield, 1971)), participants pressed the response button upon target appearance. They were instructed to hold the button down as long as the target was visible, releasing it if the target disappeared. If the target reappeared before the end of the trial, they were asked to report this by pressing and holding the button again.

Two types of control trials (**Figure 2-1A**) were intermixed with the experimental trials: catch trials and RDM_{OFF} trials. In the catch trials, the target was physically removed upon the onset of the RDM pattern, while in the RDM_{OFF} trials, the RDM pattern was never presented.

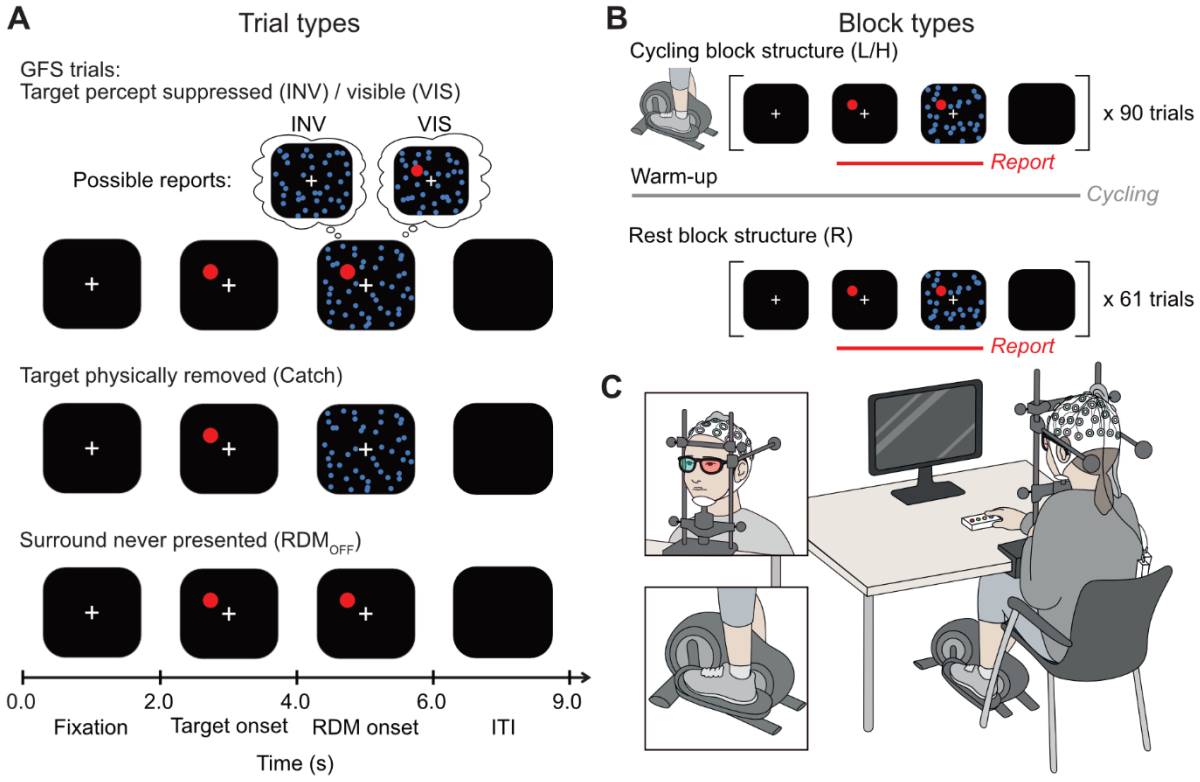

Figure 2-1 – GFS trial types, block design, experimental setup

(**A**) Time courses of GFS, catch and RDM_{OFF} trials. GFS trials began with a 2 s central fixation, followed by the onset of a salient red target in the upper left visual hemifield. After 2 s of target presentation, a random dot motion (RDM) stimulus was presented for a further 2 s, resulting in the disappearance of the target in a subset of trials. During catch trials, the target was physically removed at RDM onset. During RDM_{OFF} trials, the RDM pattern was never presented. Subjects reported their detection of the target by pressing and holding the button for as long as they could see it, and releasing the button to indicate its

disappearance. A blank screen presented for 3 s as the inter-trial interval (ITI). (**B**) The three rest (R) blocks each consisted of 61 trials: 44 GFS, 10 catch, and 7 RDM_{OFF}. The four cycling blocks (2 low-resistance (L) and 2 high-resistance (H)) each consisted of 90 trials: 65 GFS, 15 catch, and 10 RDM_{OFF}. Each cycling block began with a 3-minute warm-up period before the GFS paradigm was presented. (**C**) The experimental setup consisted of the subject seated at a desk facing a computer screen where the perceptual task was presented. They reported their perceptual responses using a button box placed on the desk. They wore red-blue anaglyphic glasses and their head was positioned on a chin rest, stabilised by positioning supports on either side and against their forehead (top inset). During the cycling blocks, they cycled using an ergometer placed under the desk (bottom inset). EEG and ECG were recorded simultaneously.

The subjects performed GFS under three exercise intensity conditions (**Figure 2-1B**): at rest (R), and during low-resistance (L) or high-resistance cycling (H). The two cycling conditions were performed using an ergometer (Sportstech DFX100; Sportstech, Berlin, Germany) placed under the desk. According to the American College of Sports Medicine guidelines (Garber et al., 2011) on exercise intensity, categorised by percentage of maximal heart rate (HRmax, estimated by the formula $211-0.64\times age$) (Nes et al., 2013), the low-resistance condition would be classified as very light (<50% HRmax), while the high-resistance condition would be classified as light (50-60% HRmax) intensity.

Each rest block (**Figure 2-1B**) comprised 61 trials (44 GFS, 10 catch, and 7 RDM_{OFF}) and lasted approximately 12 minutes. Each cycling block (**Figure 2-1B**) comprised 90 trials (65 GFS, 15 catch, and 10 RDM_{OFF}) and lasted a total of 15 minutes, beginning with a 3-minute warm-up period without a perceptual task, followed by 12 minutes of simultaneous cycling and perceptual task performance. During the initial 3-minute warm-up period for each cycling block, participants were instructed to establish a cadence of 60 rotations per minute (rpm), guided by an on-screen clock displaying seconds to help them match the pace. When the clock was replaced by the perceptual task, participants were instructed to maintain this cadence of 60 rpm to the best of their abilities until the end of the block.

2.3.3 Experimental procedure

The study was conducted over two sessions, spaced no more than 10 days apart. Overall, the first session lasted approximately 1 to 1.5 hours, and the second session lasted 3.5

to 4 hours including electrode preparation. In Session 1, participants completed a demographic survey, a questionnaire to assess interoceptive awareness (MAIA) (Mehling et al., 2012), and the Ishihara colour vision test (Clark, 1924). For inclusion in the study, subjects were required to correctly identify at least 19 out of 20 Ishihara plates. Following this, they received instructions for the task and completed one practice block of each of the three exercise intensity conditions.

Participants were instructed to abstain from caffeine, alcohol, or other mind-altering substances for 3 to 4 hours prior to Session 2, and from heavy alcohol consumption for 24 hours before the session. In this session, EEG and ECG data were recorded simultaneously. Respiration data was recorded using a respiration belt measuring thoracic/abdominal movements (Respiration Belt MR; Brain Products GmbH, Gilching, Germany), but was not analysed in the context of this paper due to motion artefacts. Following EEG and ECG preparation, an 8-minute baseline recording with eyes closed was taken, with blood pressure measured at the 7-minute mark. Participants were then reminded of the task instructions and proceeded to perform the experiment.

To perform the experimental task (**Figure 2-1C**), subjects were seated in front of a 60 × 34 cm computer screen with a resolution of 1920 × 1080 pixels and a 60 Hz refresh rate (BenQ XL2411T; BenQ, Taipei, Taiwan), and the eye-to-screen distance was 70 cm. They placed their head on a chin rest, and it was stabilised by positioning supports on each side of the head and a pad to lean their forehead against (HeadLock Ultra Precision Head Positioner; Arrington Research, Scottsdale, AZ, USA), to minimise head movement. The lights in the recording room were turned off during the experiment, and additional curtains were used to protect the subjects from extraneous light.

The experiment consisted of seven GFS blocks, with cycling (low-resistance – L, high-resistance - H) and rest (R) blocks interleaved in one of two sequence orders, either L-R-H-R-L-R-H or H-R-L-R-H-R-L, pseudorandomly assigned for each participant. Subjects were allowed adequate breaks between blocks and special care was taken to allow heart rates to return to baseline after each cycling block. Baseline heart rate was defined as the

rate observed during the initial baseline recording and blood pressure measurement. Live heart rate was monitored throughout the breaks using an armband (TikrFit; Wahoo Fitness, Atlanta, GA, USA). After the experimental blocks, another 8-minute baseline recording with eyes closed was taken.

2.3.4 EEG acquisition and preprocessing

EEG activity was recorded from 64 electrodes distributed over the head according to the International 10-20 system (actiCap Snap, BrainAmp MR, BrainVision Recorder; Brain Products GmbH, Gilching, Germany). Electrode impedances were kept below 20 kΩ throughout the experiment. The data were recorded at a sampling rate of 1000 Hz.

EEG data were preprocessed and analysed using the FieldTrip toolbox (Oostenveld et al., 2011) and custom-written software in MATLAB R2015b (The MathWorks Inc., Natick, MA, USA). The data were downsampled to 256 Hz and bandpass filtered between 0.5 and 110 Hz. A notch filter was applied to remove 50 Hz line noise. The continuous data were then segmented into trials. Trials containing muscle artefacts, jumps or clipping artefacts were identified automatically, visually inspected and then rejected when necessary. Overall, 18% of trials were excluded. An independent component analysis (ICA) was performed to identify eye movement-related artefacts, and the relevant components were removed. The data were then re-referenced to a common average reference. If there were noisy channels that required interpolation, they were removed prior to re-referencing. They were then interpolated after the data were re-referenced.

2.3.5 ECG acquisition, preprocessing, and instantaneous heart rate analysis

The ECG montage used in this study was based on the one described by Petzschner et al., 2019. Two ECG signals were acquired using two electrodes placed on the left and right clavicle (active electrodes), two electrodes placed at the left and the right hip/abdominal regions (reference electrodes), and a ground electrode placed between the shoulder blades (BrainAmp ExG; Brain Products GmbH, Gilching, Germany). The second ECG (left clavicle – right hip) served as a backup in case the signal quality of the

first ECG (right clavicle – left hip) was too low for reliable R-peak or T-wave detection. In the current dataset, the first ECG signal was of high quality for all but one participant, for whom the second ECG was used in the analysis.

R-peaks were identified using the Pan and Tompkins algorithm (Pan & Tompkins, 1985), using code custom-written in MATLAB R2015b (The MathWorks Inc., Natick, MA, USA), combined with code modified from Sedghamiz, 2014. The peaks of the P wave, Q wave, S wave, and T wave were identified using a custom-written code implementing the method proposed in Leutheuser et al., 2016, for detection of these four fiducial points. The end of the T wave was determined using a custom-written code implementing a trapezoidal area algorithm (Vázquez-Seisdedos et al., 2011), and this method was also adapted for detection of the beginning of the P wave. The pre-RDM instantaneous heart rate was obtained by dividing 60 by the inter-beat interval (distance between two R-peaks) preceding RDM onset. Heart rate variability (HRV) during the pre-RDM period was quantified using the root mean square of successive differences (RMSSD), a commonly used time-domain method that reflects short-term parasympathetic activity. RMSSD was calculated over the whole 4-second pre-RDM period using the formula:

$$RMSSD = \sqrt{\frac{1}{N-1}\sum_{i+1}^{N-1}(RR_{i+1} - RR_i)^2}$$

where RR_i represents the i-th interbeat interval, and N is the total number of intervals within that time window.

2.3.6 Behavioural analysis

The behavioural analyses were performed using custom-written scripts in MATLAB R2015b (The MathWorks Inc., Natick, MA, USA). For each subject, the disappearance probability during GFS trials in each of the three exercise intensity conditions was calculated by dividing the number of trials with at least one reported target disappearance by the total number of GFS trials performed. The reaction time for the catch trials was

defined as the average time taken after RDM onset/target removal to report the disappearance of the target. The average disappearance latencies for GFS trials were calculated by subtracting the reaction time for catch trials from the time at which the first disappearance was reported for each of the GFS trials with at least one reported target disappearance. The reappearance probability during GFS trials was calculated by dividing the number of trials with more than one reported target disappearance by the total number of GFS trials performed.

2.3.7 Alpha amplitude analysis

For the analysis of pre-RDM alpha amplitudes, the data of the parieto-occipital electrodes O1, O2, Oz, POz, PO3, PO4, PO7, PO8, and Iz during the course of the whole trial were band-pass filtered at 8–12 Hz with a 4^{th}-order Butterworth filter and subsequently Hilbert transformed. The pre-RDM alpha amplitudes were obtained by taking the absolute values of the Hilbert transform, equivalent to the envelope of the filtered signal, in a time window spanning the second prior to the onset of the RDM stimulus (pre-RDM window), pooled over the parieto-occipital electrodes. The data were baseline-corrected using a baseline window of 0.5 seconds prior to target onset. The electrodes were chosen based on previous research that investigated pre-RDM alpha power during GFS across the same set of electrodes (Poland et al., 2021). The analysis for the other time windows (one second prior to target onset, one second following target onset, one second following RDM onset / post-RDM onset, the last second of RDM onset / 1 s post-RDM onset) was conducted in a similar fashion. The two seconds between target onset and RDM onset were split into two separate windows, instead of taking the whole time period as a pre-RDM window, to be able to distinguish between the response associated with target adaptation and the pre-RDM preparatory processes prior to RDM onset, in other words, the neural factors that might lead to perceptual suppression. Similarly, the two seconds after RDM onset were split into two separate windows (post-RDM onset and 1 s post-RDM onset), to distinguish between neural responses to the RDM onset and any subsequent perceptual response registration (which predominantly took place in the first second after RDM onset), and any post-response neural modulations.

We also report differences in pre-RDM pre-frontal alpha amplitude across the three exercise intensity conditions, calculated over the Fp1, Fp2, AF3, AF7, AFz, AF4, AF8 channels.

For the comparison between exercise intensity conditions (levels: rest, low-resistance cycling, high-resistance cycling), we analysed the alpha amplitudes for all GFS trials for each of the three conditions retained after preprocessing. To determine each subject's individual alpha frequency (IAF), we performed a Fast Fourier Transform (FFT) on the 1 s pre-RDM time window for all parieto-occipital electrodes for each exercise intensity condition, analysing frequencies between 1 and 30 Hz with a resolution of 1 Hz. We then identified the peak frequency within the 8 to 12 Hz range for each subject. For the topographical representations, we calculated the average absolute value of the 8–12 Hz filtered Hilbert transform during the second prior to RDM onset for each channel individually, then subtracted the rest condition values from those of the cycling conditions.

For the two-factor comparison of target visibility (levels: visible, invisible) and exercise intensity, we analysed the alpha amplitudes separately for trials in which subjects reported the target's disappearance and trials in which that target was reported to have remained visible, across each of the three exercise intensity conditions.

2.3.8 Heartbeat-evoked potentials analysis

Heartbeat-evoked potentials (HEPs) were computed on EEG signals locked to the T-peak of the ECG. Only trials with T-peaks occurring at least 300 ms after target onset up to 400 ms before RDM onset were chosen to avoid the HEPs from being contaminated by responses to the target or the RDM onset. The EEG signals were segmented from 1000 ms before the T-peak to 2000 ms after the T-peak and then averaged to generate the pre-RDM T-locked responses to heartbeats.

Nine subjects had no trials that met the inclusion criteria for this analysis in the high-resistance condition. Additionally, eight subjects (not mutually exclusive from the nine previously mentioned) had heart rates in the high-resistance condition that were too high

(R-to-R interval < 550 ms) to allow for a sufficient time window between heartbeats for statistical analysis. Consequently, the high-resistance condition was excluded from this analysis. One subject had no trials meeting the inclusion criteria for this analysis in the low-resistance condition and was therefore also excluded from this analysis, resulting in a sample size of 29.

For the HEP analysis, the significantly different heart rates between the two conditions exercise intensity conditions (rest vs. low-resistance) were taken into account when selecting the statistical window. To account for variations in the timing of T-waves and P-waves and their respective cardiac field artefacts, the ends of the T-waves and the beginnings of the subsequent P-waves were carefully inspected on each trial. Based on this inspection, a 133 ms to 234 ms post-T-peak time window was chosen to ensure HEPs submitted for further statistical analysis are free from cardiac electrical artefacts.

For the analysis of the effect of exercise intensity on HEPs, the selected window and all electrodes were submitted to a cluster-based permutation *t*-test (Maris & Oostenveld, 2007) as implemented in the FieldTrip toolbox (Oostenveld et al., 2011). This test compared the HEP amplitudes between conditions (rest vs. low-resistance), identifying clusters of significant differences across electrodes and time points. The Monte Carlo method was used to generate the permutation distribution by randomly shuffling the condition labels 5000 times to calculate cluster-level statistics. Clusters were formed based on a *t*-statistic threshold of $p < 0.05$, with adjacent electrodes considered neighbours; a minimum of two neighbouring channels was required for a cluster to be considered. Significant differences in clusters were identified if the cluster-level *p* value, corrected using the maximum cluster sum statistic, was below 0.05.

To test for a 2×2 interaction effect of target visibility (visible vs. invisible) and exercise intensity (rest vs. low-resistance) on HEP amplitudes, a similar procedure was adopted, but a repeated measures permutation *F*-test was employed instead of a *t*-test. This analysis compared the target visibility effect at rest (Rest(visible-invisible)) against the target visibility effect at low-resistance (Low-resistance(visible-invisible)) to assess

whether the target visibility effect differed significantly between exercise intensity conditions.

For any significant clusters identified by the cluster-based permutation tests, the average HEP amplitudes over the electrodes and time points within the cluster were extracted. These average amplitudes were then submitted to paired samples *t*-tests to further validate the observed differences between conditions.

2.3.8.1 Control analyses for possible effects of cardiovascular artefacts

HEPs represent neural responses to cardiac signals but can also include cardiac field artefacts and pulse-related artefacts (Kern et al., 2013). One commonly used approach to mitigate any associated volume conduction effects of these artefacts is independent component analysis (ICA). However, this approach has been criticised for its limited ability to completely eliminate the cardiac field artefacts and for the potential risk of removing relevant task-related signals (Petzschner et al., 2019). To ensure that the observed effects in HEP amplitudes were not due to differences in cardiac electrical activity directly affecting EEG data by volume conduction, we submitted the mean ECG amplitudes to the same cluster-based permutation tests as the observed effects.

Several studies have also controlled for heart rate when differences in HEPs were observed (Coll et al., 2021; Park & Blanke, 2019). By using exercise as an intervention, the rest and low-resistance conditions have significantly different heart rates by design. We thus fitted a linear mixed-effect model (LME) to investigate the effects of exercise intensity conditions and heart rate on HEP amplitude. The model examined the main effects of exercise intensity condition and heart rate on HEP amplitude, with condition and heart rate as fixed effects and subject included as a random intercept to account for repeated measures within participants. Assumptions of linearity, homoscedasticity, and no multicollinearity were evaluated prior to model fitting, while the normality of residuals was assessed *post hoc*. Model fitting and parameter estimation were conducted using maximum likelihood estimation in MATLAB R2015b (The MathWorks Inc., Natick, MA, USA). Model fit was assessed using the Akaike Information Criterion (AIC), Bayesian

Information Criterion (BIC), and log-likelihood values, with statistical significance set at α = 0.05.

2.3.9 Statistical analyses

Statistical analyses were conducted in SPSS Statistics for Windows, Version 27.0 (IBM Corp., Armonk, NY, USA). Data were tested for the normality assumption using the Shapiro-Wilk test.

When testing for the effects of exercise intensity (3 levels: rest, low-resistance cycling, high-resistance cycling), data that met the normality assumption were analysed using repeated-measures ANOVA (RM-ANOVA), followed by Bonferroni-corrected *post hoc* pairwise comparisons when significant effects were found. When testing for the effects of target visibility and exercise intensity, if normality was satisfied, a 2 (factor: target visibility; levels: visible, invisible) × 3 (factor: exercise intensity; levels: rest, low-resistance cycling, high-resistance cycling) repeated-measures ANOVA was applied. Mauchly's test was used to assess sphericity, and if this assumption was violated, the Greenhouse-Geisser correction was applied. If the test revealed significant effects, *post hoc* Bonferroni-corrected pairwise comparisons were performed.

Data that did not satisfy the normality assumption were analysed using the Friedman test to assess differences across conditions. When the Friedman test indicated a significant effect, *post hoc* pairwise comparisons were conducted using the Wilcoxon signed-rank test to identify specific differences between conditions, with a Bonferroni correction applied for multiple comparisons. For the analysis of the effects of exercise intensity and target visibility on alpha amplitudes, a Bonferroni-Holm correction was applied due to the larger number of comparisons in this analysis.

Partial eta-squared (η_p^2), Cohen's *d*, Kendall's *W*, and rank-biserial correlation (*r*) were calculated as the effect sizes for the repeated-measures ANOVAs, *t*-tests, Friedman tests, and Wilcoxon signed-rank tests, respectively.

For comparisons against zero, a one-sample *t*-test was used for data meeting the normality assumption, while a Wilcoxon signed-rank test was applied for data that did not meet this assumption.

For correlation analyses, Pearson correlation was employed for normally distributed data, while Kendall's Tau-b was applied for data that did not meet the normality assumption.

2.4 Results

2.4.1 Behavioural analysis

Subjects performed a Generalized Flash Suppression (GFS) task under three exercise intensity conditions: at rest, and during low-resistance or high-resistance cycling. In the GFS task, a salient target stimulus is typically completely suppressed, i.e. rendered subjectively invisible, after the onset of a random dot motion (RDM) stimulus (see **section 2.3.2** - **Stimuli and task**). We tested whether there is an effect of exercise on the probability of target suppression during GFS trials (**Figure 2-2A**). The RM-ANOVA revealed an effect of exercise intensity on disappearance (i.e. target suppression) probability ($F(2, 58) = 6.40$, $p = 3.08\times10^{-3}$, $\eta_p^2 = 0.18$). *Post hoc* Bonferroni-corrected pairwise comparisons showed that the disappearance probability was lower for the low-resistance (mean $\pm$ SEM: 0.43 $\pm$ 0.04; $p = 0.02$) and high-resistance (mean $\pm$ SEM: 0.41 $\pm$ 0.04; $p = 0.01$) cycling conditions compared with rest (mean $\pm$ SEM: 0.50 $\pm$ 0.03), but there was no difference between the two cycling conditions ($p = 1.00$). On average, this corresponded to a 14.99% decrease in disappearance probability for the low-resistance condition (one-sample *t*-test, $t(29) = -2.92$, $p = 6.78\times10^{-3}$, Cohen's $d = -0.53$) and an 18.45% decrease for the high-resistance condition (one-sample *t*-test, $t(29) = -3.15$, $p = 3.74\times10^{-3}$, Cohen's $d = -0.58$) compared to rest (**Figure 2-2B**).

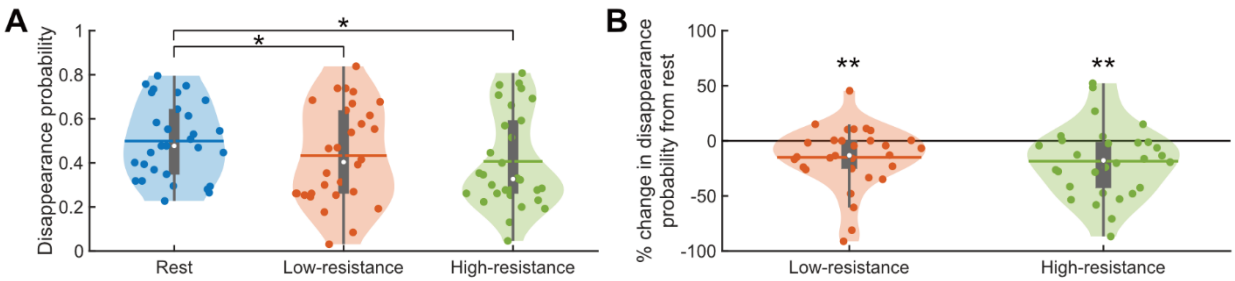

Figure 2-2 – Disappearance probability decreases for cycling conditions compared to rest

(**A**) Violin plots showing the mean disappearance probabilities during GFS performed at rest (blue), low-resistance (orange), and high-resistance (green) cycling. Statistical significance between the conditions, as assessed by *post hoc* Bonferroni-corrected pairwise comparisons, is indicated at the $p \leq 0.05$ (*) level. (**B**) Violin plots showing the percent change in disappearance probability for low-resistance (orange) and high-resistance (green) cycling compared to rest. Statistical significance, as assessed by one-sample *t*-tests, is indicated at the $p \leq 0.01$ (**) level. For both panels, vertical grey boxes indicate the interquartile range (IQR), with grey whiskers indicating 1.5 × IQR, surrounded on each side by the kernel density estimation in the colour corresponding to each group. Horizontal lines, in the colour corresponding to each group, denote means, and white dots indicate medians. Each dot in a given condition represents the average value of a single subject. $N = 30$ for all plots.

No significant differences between the three exercise intensity conditions were observed in the percentage of correct reports during both RDM_{OFF} trials (Friedman test, $\chi^2(2) = 0.19$, $p = 0.91$, Kendall's $W = 3.11 \times 10^{-3}$; overall mean ± SD: 96.52 ± 4.98%; median: 100%) and catch trials (Friedman test, $\chi^2(2) = 3.08$, $p = 0.22$, Kendall's $W = 0.05$; overall mean ± SD: 97.32 ± 4.90%; median: 100%). The high detection rates across these control trials suggest subjects' percept detection and reporting abilities remained unimpaired across the exercise intensity conditions.

2.4.2 Alpha amplitude analysis

Given that cycling modulates alpha activity (8–12 Hz) (Crabbe & Dishman, 2004; Hosang et al., 2022) and pre-RDM parieto-occipital alpha amplitudes are predictive of perceptual suppression (Poland et al., 2021), we analysed the effect of exercise intensity on parieto-occipital alpha amplitudes during the second preceding RDM onset. There was a statistically significant difference in the mean parieto-occipital alpha amplitude over this time window (**Figure 2-3** and **Figure 2-4A**) between exercise intensity conditions

(Friedman test, $\chi^2(2) = 16.80$, $p = 2.25\times10^{-4}$, Kendall's W = 0.29). Parieto-occipital alpha amplitudes were lower during cycling compared to rest (Bonferroni-corrected Wilcoxon signed-rank tests, low-resistance: $Z = -3.86$, $p = 3.45\times10^{-4}$, $r = 0.50$; high-resistance: $Z = -2.89$, $p = 0.01$, $r = 0.37$), but there was no difference between the two cycling conditions ($Z = -0.85$, $p = 1.18$, $r = 0.11$).

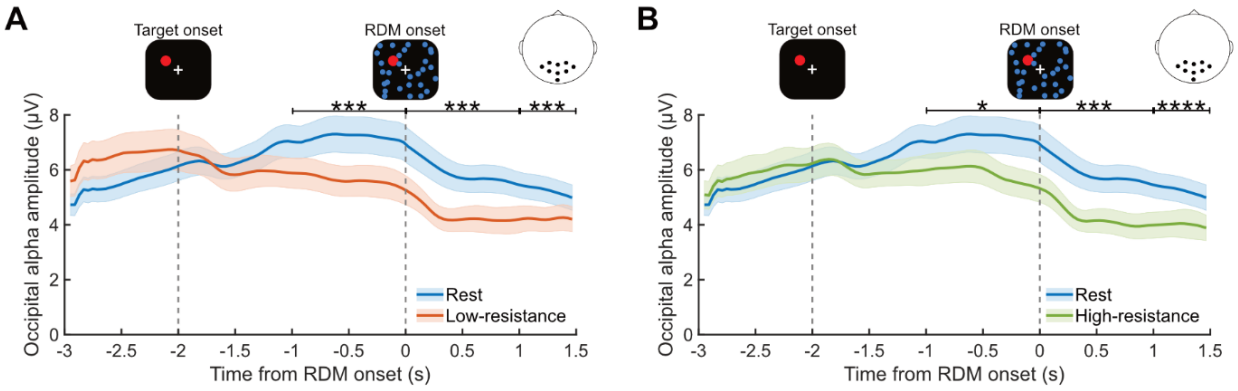

Figure 2-3 – Decreased parieto-occipital alpha amplitude during cycling compared to rest

Average time courses of alpha band (8–12 Hz) amplitudes for GFS performed during (**A**) low-resistance (orange) and (**B**) high-resistance (green) cycling compared to rest (blue) ($N = 30$). The shaded areas denote the SEM for each time course. The zero mark denotes the onset of the RDM stimulus, after which the target was potentially perceptually suppressed. The data represent the mean of all parieto-occipital electrodes. Statistical significance between the conditions for different time windows, as assessed by Bonferroni-corrected Wilcoxon signed-rank tests, is indicated at the $p \leq 0.05$ (*), $p \leq 0.001$ (***), and $p \leq 0.0001$ (****) levels.

We also found differences in parieto-occipital alpha amplitude due to exercise intensity in other time windows (**Figure 2-3**); specifically, during the first second of RDM presentation (post-RDM onset; Friedman test, $\chi^2(2) = 29.07$, $p = 4.88\times10^{-7}$, Kendall's W = 0.48) and the subsequent half-second (1 s post-RDM onset, Friedman test, $\chi^2(2) = 26.87$, $p = 1.47\times10^{-6}$, Kendall's W = 0.45). *Post hoc* Bonferroni-corrected Wilcoxon signed-rank tests revealed a significant decrease in parieto-occipital alpha amplitude during cycling, compared with rest, also in both later time windows (post-RDM onset results: low-resistance, $Z = -3.92$, $p = 2.68\times10^{-4}$, $r = 0.50$; high-resistance, $Z = -3.98$, $p = 2.07\times10^{-4}$, $r = 0.51$; 1 s post-RDM onset results: low-resistance, $Z = -3.63$, $p = 8.49\times10^{-4}$, $r = 0.47$; high-resistance, $Z = -4.19$, $p = 8.53\times10^{-4}$, $r = 0.54$). No significant differences were

observed between the two cycling conditions (post-RDM onset results: Z = -0.09, p = 2.78, r = 0.01; 1 s post-RDM onset results: Z = -0.92, p = 0.36, r = 0.12).

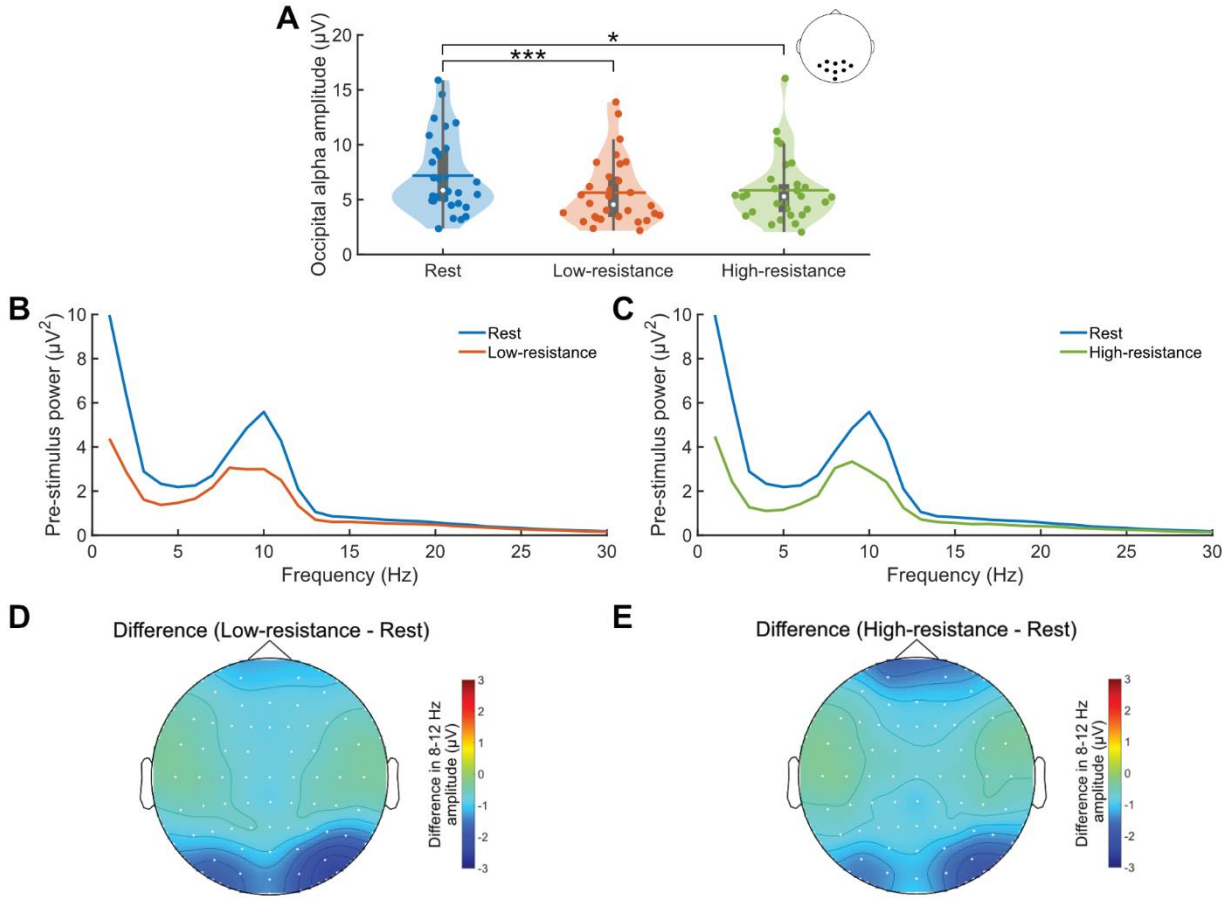

Figure 2-4 – Decreased pre-RDM parieto-occipital alpha power for cycling conditions compared to rest

(**A**) Violin plots showing the mean pre-RDM parieto-occipital alpha during GFS performed at rest (blue), low-resistance (orange), and high-resistance (green) cycling. Vertical grey boxes indicate the interquartile range (IQR), with grey whiskers indicating 1.5 × IQR, surrounded on each side by the kernel density estimation in the colour corresponding to each group. Horizontal lines, in the colour corresponding to each group, denote means, and white dots indicate medians. Each dot in a given condition represents the average value of a single subject. Statistical significance between conditions, as assessed by Bonferroni-corrected Wilcoxon signed-rank tests, is indicated at the $p \leq 0.05$ (*) and $p \leq 0.001$ (***) levels. Power spectra for the second preceding the RDM stimulus for GFS performed at rest and during (**B**) low-resistance and (**C**) high-resistance cycling across subjects. Topographies of the (**D**) low-resistance – rest and (**E**) high-resistance – rest differences in 8–12 Hz amplitude in the second prior to RDM onset. N = 30 for all plots.

The power spectra of the second prior to RDM onset revealed that the peak individual alpha frequency (IAF) did not differ across the three exercise intensity conditions (Friedman test, $\chi^2(2) = 5.26$, $p = 0.07$, Kendall's W = 0.09), and the mean IAF across subjects was 9.62 Hz $\pm$ SD 1.05 Hz. However, the cycling conditions led to a downshift of the EEG power spectrum compared to rest, and an analysis of the power at peak IAF (**Figure 2-4**Error! Reference source not found.**B** and **C**) revealed a difference between t he three conditions (Friedman test, $\chi^2(2) = 15.27$, $p = 4.84\times10^{-4}$, Kendall's W = 0.25). Corroborating the pre-RDM, cycling-induced decrease in alpha amplitude, decreased power was observed for low-resistance (Bonferroni-corrected Wilcoxon signed-rank test, $Z = -3.67$, $p = 7.24\times10^{-4}$, $r = 0.47$) and high-resistance ($Z = -2.77$, $p = 0.02$, $r = 0.36$) cycling compared to rest, but there was no difference in power between the cycling conditions ($Z = -0.36$, $p = 2.16$, $r = 0.05$). The topographies of the cycling – rest difference in alpha amplitude (**Figure 2-4D** and **E**) suggested that the decrease in alpha activity was most prominent in the parieto-occipital cortex.

In addition to parieto-occipital alpha amplitudes, we examined pre-RDM prefrontal alpha amplitudes, since exercise has been reported to elicit prominent effects in the alpha band in anterior regions (Hosang et al., 2022). A significant effect of exercise intensity on pre-RDM prefrontal alpha was observed (Friedman test, $\chi^2(2) = 18.07$, $p = 1.19\times10^{-4}$, Kendall's W = 0.30). However, *post hoc* Bonferroni-corrected Wilcoxon signed-rank tests revealed that both low-resistance ($Z = -4.10$, $p = 1.22\times10^{-4}$, $r = 0.75$) and high-resistance ($Z = -3.65$, $p = 7.84\times10^{-4}$, $r = 0.67$) cycling conditions resulted in significantly *lower* prefrontal alpha amplitudes compared to rest. No significant difference was found between the two cycling conditions ($Z = -0.61$, $p = 1.63$, $r = 0.11$). We also examined whether changes in prefrontal alpha amplitude correlated with changes in disappearance probability. No significant correlation was observed between the percentage change in pre-RDM prefrontal alpha amplitude from rest and the percentage change in disappearance probability, for either low-resistance (Kendall's Tau-b, $\tau_b(30) = -0.05$, $p = 0.78$) or high-resistance cycling ($\tau_b(30) = -0.08$, $p = 0.56$).

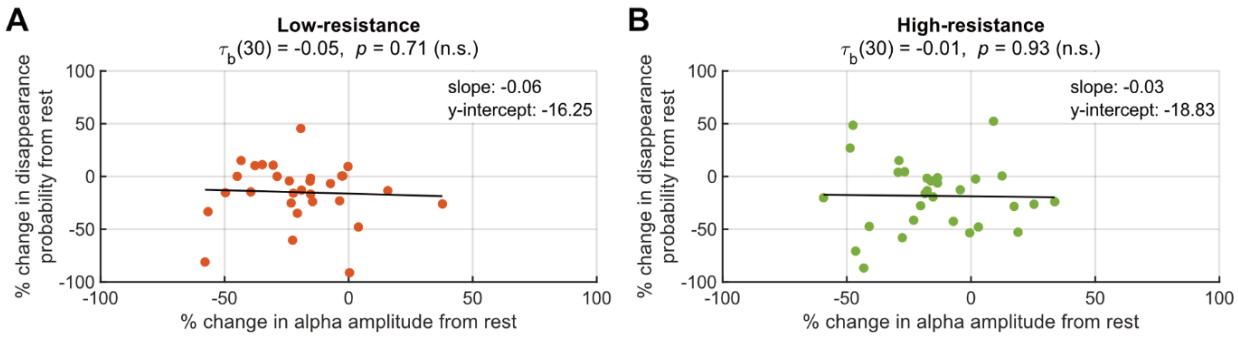

Figure 2-5 – No correlation between pre-RDM parieto-occipital alpha amplitude and disappearance probability

Correlations, as assessed by Kendall's Tau-b, between percent change in parieto-occipital alpha amplitude from rest and percent change in disappearance probability from rest for (**A**) low-resistance and (**B**) high-resistance cycling. *N* = 30 for all plots.

In an analysis of the relationship between cycling-related changes in alpha amplitude and changes in disappearance probability (**Figure 2-5**), we observed no statistically significant correlations for either the low-resistance and high-resistance cycling conditions (Kendall's Tau-b, all *p*s > 0.05).

Based on previous work on GFS performed at rest (Poland et al., 2021), we hypothesized that pre-RDM parieto-occipital alpha would be lower when the target becomes perceptually suppressed compared to when it remains visible. To investigate this, we assessed whether pre-RDM, parieto-occipital alpha activity reflects the subjective visibility of the target in GFS trials (**Figure 2-6**) and examined how this relationship interacted with the effect of cycling. A Friedman test revealed a statistically significant difference in pre-RDM, parieto-occipital alpha activity across the exercise intensity and target visibility conditions ($\chi^2(5) = 42.74$, $p = 4.17\times10^{-8}$, Kendall's W = 0.29). In the *post hoc* analysis, we performed nine pairwise comparisons with the Bonferroni-Holm-corrected Wilcoxon signed-rank test (**Figure 2-6D**), with three comparisons testing for the effect of exercise intensity on pre-RDM alpha amplitudes and six comparisons testing for the effect of alpha amplitudes on target visibility. This analysis suggests alpha amplitude-linked effects of both target visibility and exercise intensity. Violin plots in **Figure 2-6E** show that, for most subjects, pre-RDM alpha amplitude was consistently higher for trials where the target remained visible compared to when it was rendered invisible across all

exercise intensity conditions, in line with the findings in Poland et al., 2021. However, the target visibility-related effects did not survive the correction for multiple comparisons (rest: Z = -2.03, p = 0.17; low-resistance: Z = -2.07, p = 0.19; high-resistance: Z = -1.98, p = 0.14; Uncorrected p values reported in **2.7 Supplementary Information**, **Table S2-1**).

As for the cycling-related effects on pre-RDM alpha, we observed significant reductions in alpha amplitude during visible trials for both low-resistance (Z = -3.82, $p = 1.09\times10^{-3}$, r = 0.49) and high-resistance cycling (Z = -2.95, p = 0.02, r = 0.38) compared to rest, with no significant difference between the two cycling conditions (Z = -1.41, p = 0.32, r = 0.18). Similarly, in the invisible trials, a significant reduction was found between rest and low-resistance cycling (Z = -3.90, $p = 8.74\times10^{-4}$, r = 0.50), but not between rest and high-resistance cycling (Z = -2.58, p = 0.06, r = 0.33), or between the two cycling conditions (Z = -1.08, p = 0.28, r = 0.14). These results suggest that while cycling decreases pre-RDM alpha amplitude, this exercise-induced modulation is not specifically linked to perceptual suppression.

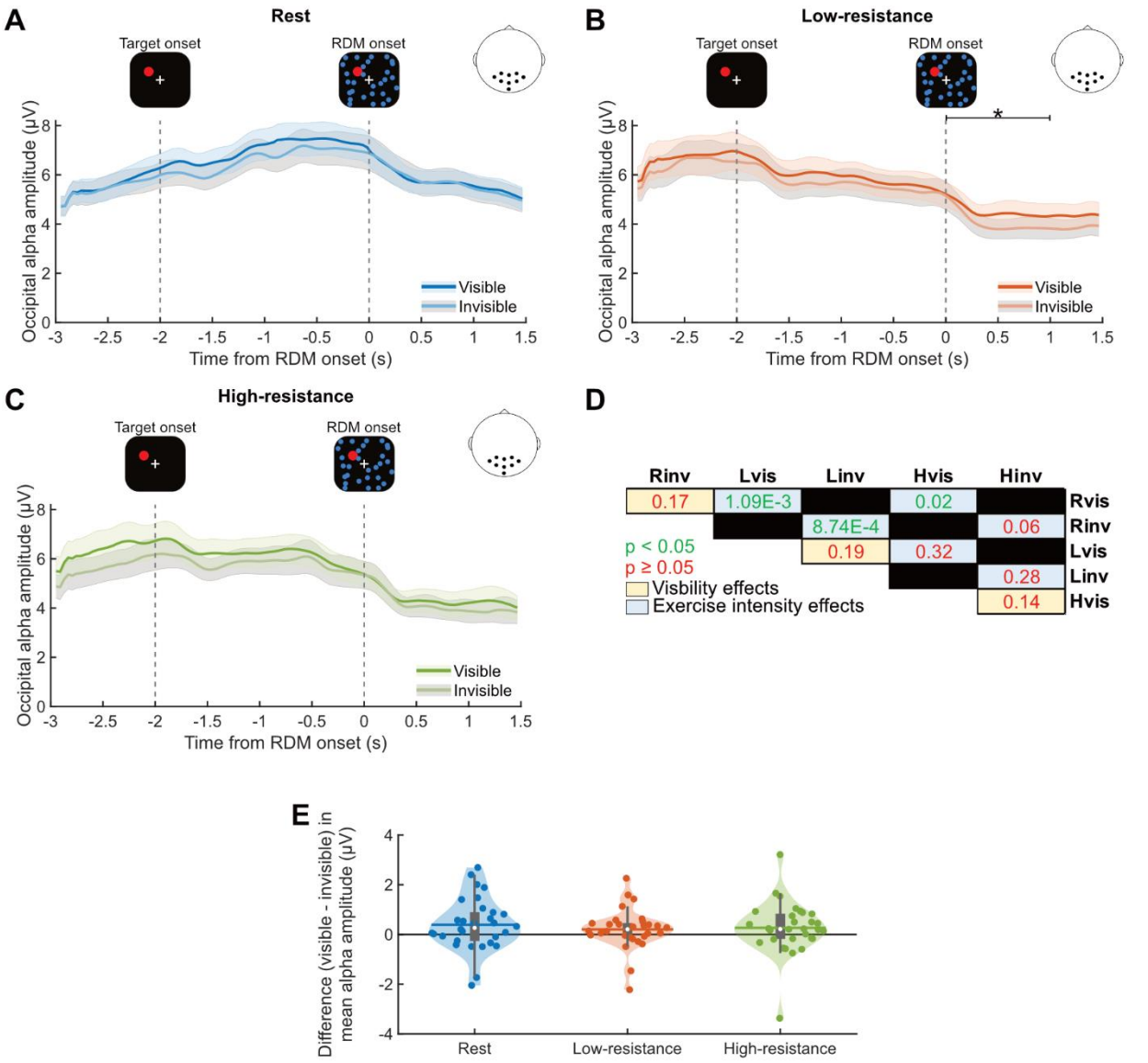

Figure 2-6 – Pre-RDM parieto-occipital alpha amplitude as a function of perceptual suppression and cycling

Average time courses of alpha band (8–12 Hz) amplitudes for GFS trials where the target remained visible and trials where the target was rendered invisible, when the task was performed during (**A**) rest, (**B**) low-resistance, and (**C**) high-resistance cycling. The SEM is plotted for each time course in corresponding colour. The zero mark denotes the onset of the RDM stimulus, after which the target was potentially perceptually suppressed. The data represent the mean of all parieto-occipital electrodes. Statistical significance between the conditions for different time windows, as assessed by Wilcoxon signed-rank tests, is indicated at the $p \leq 0.05$ (*) level. (**D**) Bonferroni-Holm-corrected Wilcoxon signed-rank test *p*-values for pairwise comparisons reflecting the effect of target visibility and exercise intensity on parieto-occipital alpha amplitude in the second prior to RDM onset (Rest – R, Low-resistance – L,

High-resistance – H, Visible – vis, Invisible - inv). (**E**) Violin plots showing the visible – invisible difference in mean pre-RDM alpha during GFS performed at rest (blue), and during low-resistance (orange), and high-resistance (green) cycling. Vertical grey boxes indicate the interquartile range (IQR), with grey whiskers indicating 1.5 × IQR, surrounded on each side by the kernel density estimation in the colour corresponding to each group. Horizontal lines, in the colour corresponding to each group, denote means, and white dots indicate medians. Each dot in a given condition represents the average value of a single subject. *N* = 30 for all plots.

2.4.3 Heart rate analysis

To investigate how the pre-RDM instantaneous heart rate interacts with exercise intensity and conscious visual perception of the target, we conducted a two-way repeated measures ANOVA with two factors: exercise intensity (levels: rest, low-resistance cycling, high-resistance cycling) and target visibility (levels: visible, invisible). The analysis revealed a significant main effect of exercise intensity (Greenhouse-Geisser corrected; $F(1.25, 36.26) = 269.24$, $p = 1.09\times10^{-19}$, $\eta_p^2 = 0.90$), confirming the efficacy of the exercise intervention. *Post hoc* Bonferroni-corrected pairwise comparisons indicated that both low-resistance and high-resistance cycling elicited significantly higher heart rates compared to rest (**Figure 2-7A**; low-resistance: 10.81 bpm difference, $p = 2.78\times10^{-16}$; high-resistance: 28.59 bpm difference, $p = 4.53\times10^{-17}$). Additionally, high-resistance cycling resulted in a significantly higher heart rate than low-resistance cycling (17.77 bpm difference, $p = 3.11\times10^{-13}$). On average, the heart rate increased by 15.56% during low-resistance cycling compared to rest, and by 41.32% during high-resistance cycling compared to rest. However, there was no significant main effect of target visibility: the instantaneous pre-RDM heart rate did not differ significantly between trials in which the target remained visible and those in which it disappeared ($F(1, 29) = 0.99$, $p = 0.33$, $\eta_p^2 = 0.03$). Furthermore, no significant interaction between exercise intensity and target visibility was observed ($F(2, 58) = 0.47$, $p = 0.63$, $\eta_p^2 = 0.02$).

We investigated whether these heart rate changes were associated with the cycling-related changes in disappearance probability and pre-RDM alpha amplitude. For the relationship between heart rate and disappearance probability, there were no statistically significant correlations for either low-resistance or high-resistance cycling (**Figure 2-7B** and **C**; Kendall's tau-b, all *p*s > 0.05). Similarly, for the relationship between heart rate and alpha amplitude, no statistically significant correlations emerged for either condition (**Figure 2-7D** and **E**; Kendall's tau-b, all *p*s > 0.05). An analysis using pre-RDM heart rate variability (HRV), quantified with the RMSSD time-domain method, yielded similar results. RMSSD HRV significantly decreased with increasing exercise intensity but did not vary with target disappearance/visibility, and showed no significant correlations with

disappearance probability or pre-RDM alpha amplitude (**2.7 Supplementary Information**, **Figure S2-1**).

We also assessed phasic heart rate changes across the course of a trial, and found a deceleration in heart rate over the trial duration, which occurred irrespective of target visibility (**2.7 Supplementary Information**, **Figure S2-2** and **Table S2-2**). This deceleration aligns with the well-characterized phenomenon of cardiac deceleration following a warning stimulus, which reflects anticipation of an upcoming stimulus or response registration (B. C. Lacey & Lacey, 1978; J. I. Lacey, 1967; B. C. Lacey & Lacey, 1974; Jennings & Wood, 1977; B. C. Lacey & Lacey, 1980; Somsen et al., 2004; Park et al., 2014; Cobos et al., 2019; Motyka et al., 2019; Grund et al., 2022). Interestingly, in our paradigm, this phenomenon emerged despite the absence of an explicit warning stimulus, likely driven instead by the presence of stereotyped, predictable events that may have acted as implicit cues for anticipation. Furthermore, this deceleration appears to be robust, persisting even under the cycling conditions.

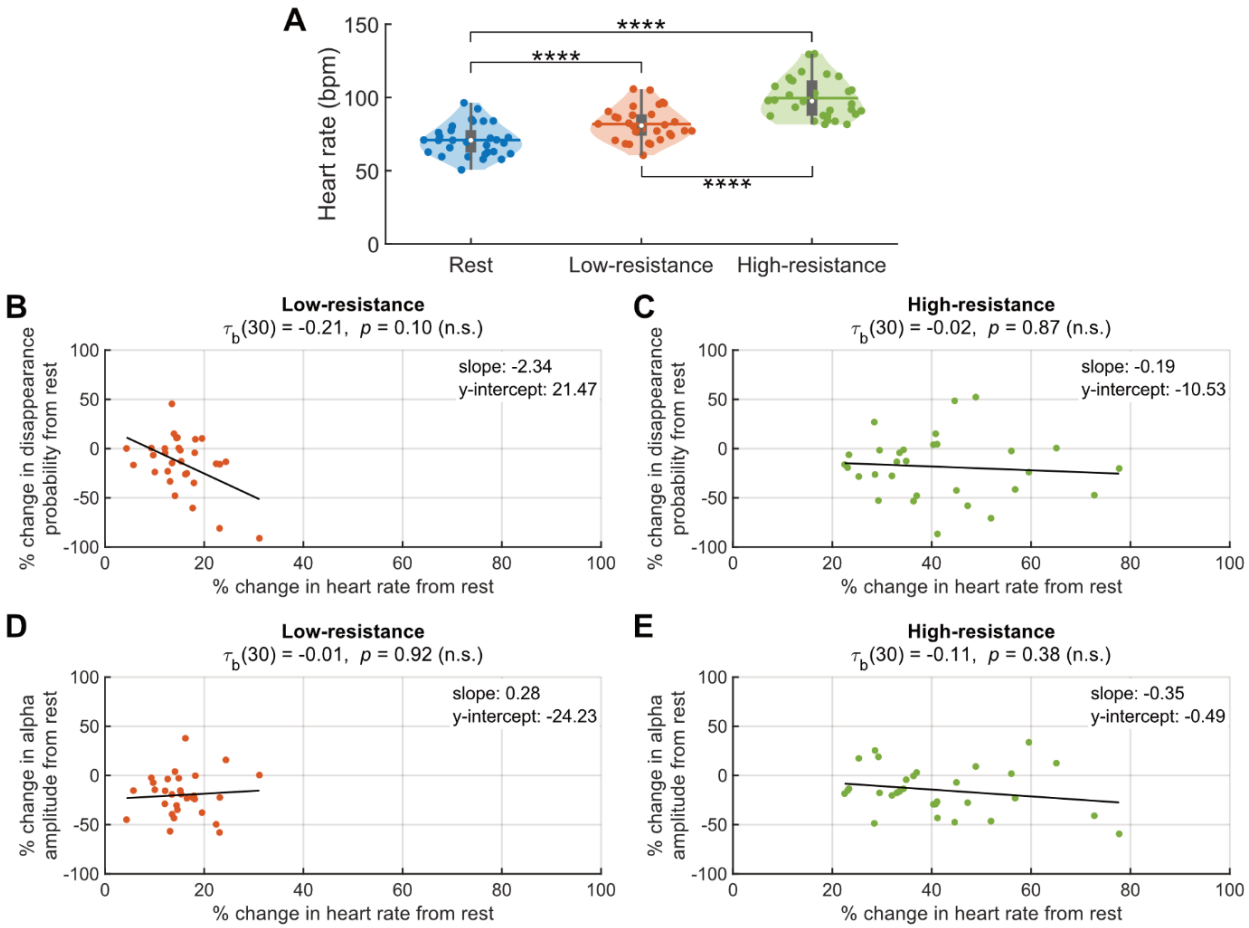

Figure 2-7 – Heart rate increases with cycling intensity

(**A**) Violin plots showing the pre-RDM instantaneous heart rate during GFS performed at rest (blue), low-resistance (orange), and high-resistance (green) cycling. Vertical grey boxes indicate the interquartile range (IQR), with grey whiskers indicating 1.5 × IQR, surrounded on each side by the kernel density estimation in the colour corresponding to each group. Horizontal lines, in the colour corresponding to each group, denote means, and white dots indicate medians. Each dot in a given condition represents the average value of a single subject. Statistical significance between the conditions, as assessed by a *post hoc* analysis with a Bonferroni adjustment, is indicated at the $p \leq 0.0001$ (****) level. Correlations as assessed by Kendall's Tau-b between percent change in heart rate from rest and percent change in disappearance probability from rest for (**B**) low-resistance and (**C**) high-resistance cycling. Correlations between percent change in heart rate from rest and percent change in alpha amplitude from rest for (**D**) low-resistance and (**E**) high-resistance cycling. None of the correlations are significant. N = 30 for all plots.

2.4.4 Heartbeat-evoked potentials analysis

To explore if and how neural processing of heartbeats is altered during exercise, we analysed the effect of cycling on heartbeat-evoked potential (HEP) amplitudes. EEG data locked to the T-peak preceding RDM onset was averaged for the rest and low-resistance cycling conditions. The high-resistance cycling condition was excluded from this analysis because the heart rates were too high to allow for a sufficient time window between heartbeats for statistical analysis. For the other two conditions, a 133 to 234 ms post-T-peak time window, chosen to avoid overlap with the end of the previous T wave and the beginning of the subsequent P wave, ensuring HEPs are free from cardiac artefacts, was submitted to a cluster-based permutation *t*-test. Pre-RDM HEPs significantly differed between rest and low-resistance cycling (**Figure 2-8A**, **B**, **C**) over central, parietal, and occipital electrodes in a 152 to 203 ms post-T-peak time window (cluster-level statistic = 337.85, p = 0.02, N = 29; **2.7 Supplementary Information**, **Figure S2-3**). The HEP amplitudes during low-resistance cycling were lower than at rest (Wilcoxon signed-rank test, Z = -2.26, p = 0.02, r = 0.42; **Figure 2-8C, D**).

The control for volume conduction, i.e. comparison of the ECG waveforms for rest and low-resistance in the same time window as the observed effect, revealed no significant differences (**2.7 Supplementary Information**, **Figure S2-4**). Thus, the observed differences in HEP amplitudes between the two conditions cannot be attributed to differences in cardiac electrical activity. The linear mixed-effects model (**2.7 Supplementary Information**, **Table S2-3**) used to investigate the effects of exercise intensity conditions on HEP amplitude, while controlling for heart rate, revealed no significant difference in HEP amplitudes between rest and low-resistance cycling (b = 0.20, p = 0.43). Heart rate also did not significantly predict HEP amplitude (b = -0.03, p = 0.17), though the direction of the effect suggests a possible trend toward lower HEP amplitudes at higher heart rates. Random intercepts for subject (σ = 0.39) accounted for individual variability, and the residual standard deviation was 0.84. Model fit statistics included AIC = 164.87 and BIC = 175.17. These results suggest that heart rate is an unlikely contributor to the observed difference in HEP amplitudes between conditions.

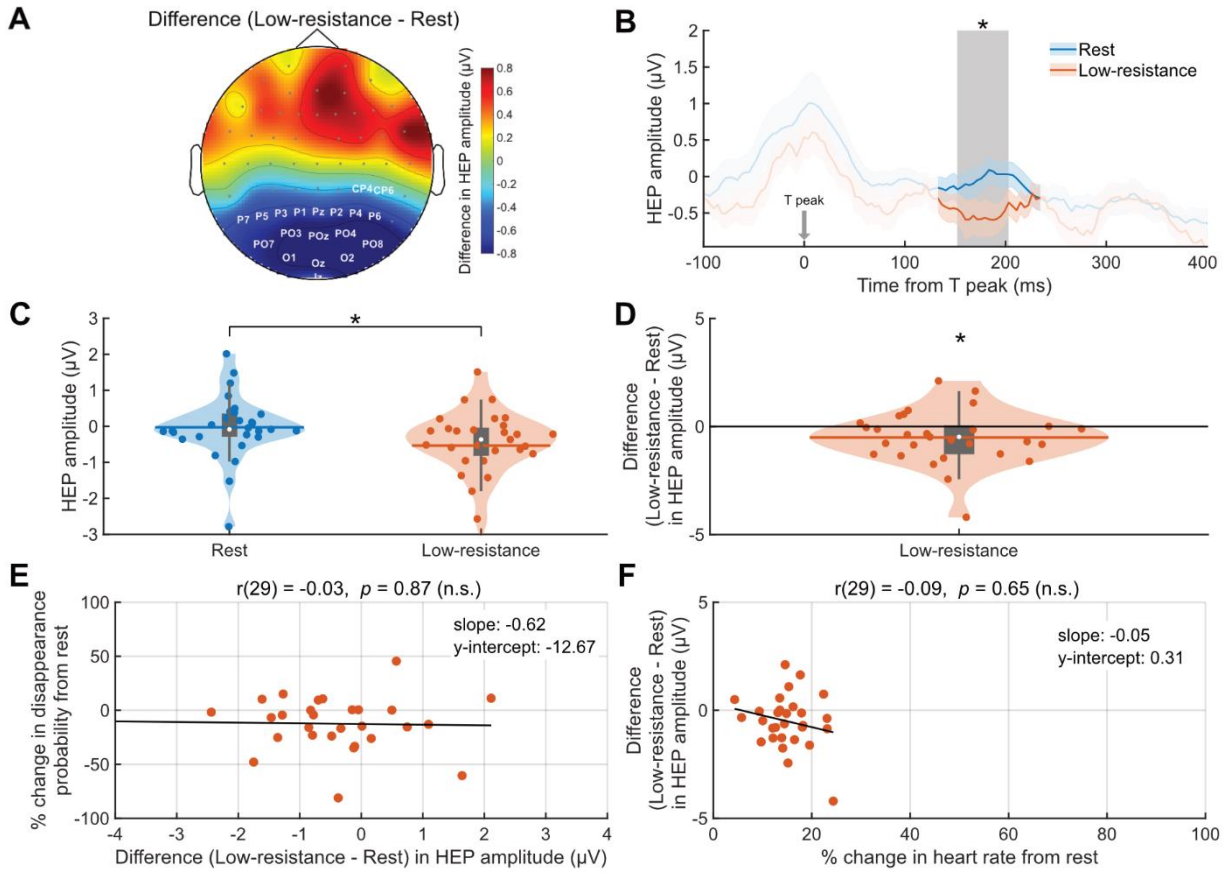

Figure 2-8 – Heartbeat-evoked potential amplitudes decrease during cycling

(**A**) Topographical map of heartbeat-evoked potential (HEP) amplitude difference between low-resistance and rest conditions in the 152 to 203 ms post-T-peak time window during which a statistically significant difference was observed. White labels indicate the channels contributing to the significant cluster. (**B**) Pre-RDM HEPs for the two conditions averaged across the cluster. The shaded areas denote the SEM for each time course. The signal contaminated by T-wave and P-wave cardiac artefacts appears in a lighter colour. The grey bar highlights the time window in which a significant difference was observed as the $p \leq 0.05$ (*) level. (**C**) Violin plots of the HEP amplitude averaged across the cluster for rest (blue) and low-resistance cycling (orange). Vertical grey boxes indicate the interquartile range (IQR), with grey whiskers indicating 1.5 × IQR, surrounded on each side by the kernel density estimation in the colour corresponding to each group. Horizontal lines, in the colour corresponding to each group, denote means, and white dots indicate medians. Each dot in a given condition represents the average value of a single subject. For both (**B**) and (**C**), statistical significance between the conditions was assessed by a Wilcoxon signed-rank test and is indicated at the $p \leq 0.05$ (*) level. (**D**) Difference from rest in HEP amplitudes for low-resistance cycling. Statistical significance was assessed by one-sample *t*-test ($t(28) = -2.22$, $p = 0.04$, Cohen's $d = 0.41$) and is indicated at the $p \leq 0.05$ (*) level. Correlations as assessed by Pearson correlation between (**E**) change in HEP amplitude and percent change in disappearance probability and

(**F**) change in heart rate and change in HEP amplitude for cycling from rest. Neither correlation is significant. *N* = 29 for all plots.

We investigated whether these modulations in HEPs were associated with cycling-related changes in disappearance probability (Error! Reference source not found.**E**) and found n o statistically significant correlation (Pearson correlation, r(29) = -0.03, *p* = 0.87). We also investigated the relationship between the cycling-related changes in heart rate and the changes in HEP amplitude (**Figure 2-8F**), and again, no statistically significant correlation was found (Pearson correlation, r(29) = -0.09, *p* = 0.65). A corresponding analysis using cycling-related changes in RMSSD HRV instead of heart rate also revealed no significant correlation with changes in HEP amplitude (**2.7 Supplementary Information**, **Figure S2-5**).

Additionally, HEP amplitude has been linked to conscious perception of sensory stimuli at threshold (Al et al., 2020; Park et al., 2014), suggesting a role for interoceptive processing in the perception of external stimuli. To investigate this, we employed a cluster-based permutation *F*-test to assess the 2×2 interaction effect of target visibility (levels: visible, invisible) and exercise intensity (levels: rest, low-resistance) on HEP amplitudes. This analysis revealed five positive spatio-temporal clusters, however, neither cluster reached statistical significance (smallest cluster-level *p* = 0.22). We also assessed whether pre-RDM HEP amplitude reflected the subjective visibility of the target in GFS trials (**Figure 2-9**) within the same time window as the exercise intensity effect described above, as well as its interaction with the cycling effect. A Friedman test revealed a statistically significant difference in HEP amplitudes across the exercise intensity and target visibility conditions ($\chi^2(3) = 8.79$, *p* = 0.03, Kendall's W = 0.10). In the *post hoc* analysis, we performed four pairwise comparisons with Bonferroni-corrected Wilcoxon signed-rank tests (**Figure 2-9C**), with two comparisons testing for the effect of exercise intensity on pre-RDM HEP amplitudes and two comparisons testing for the effect of pre-RDM HEP amplitudes on target visibility. However, neither the effect of target visibility nor the effect of cycling survived the correction for multiple comparisons (all *p*s > 0.05; Uncorrected *p* values are reported in the **2.7 Supplementary Information**, **Table S2-4**). The difference between HEP amplitudes for trials in which the target remained visible and

the trials in which it was perceptually suppressed (**Figure 2-9D**) was not significant for rest ($t(28) = -0.83$, $p = 0.41$, Cohen's $d = -0.16$) or for low-resistance cycling ($t(28) = -0.22$, $p = 0.83$, Cohen's $d = -0.04$).

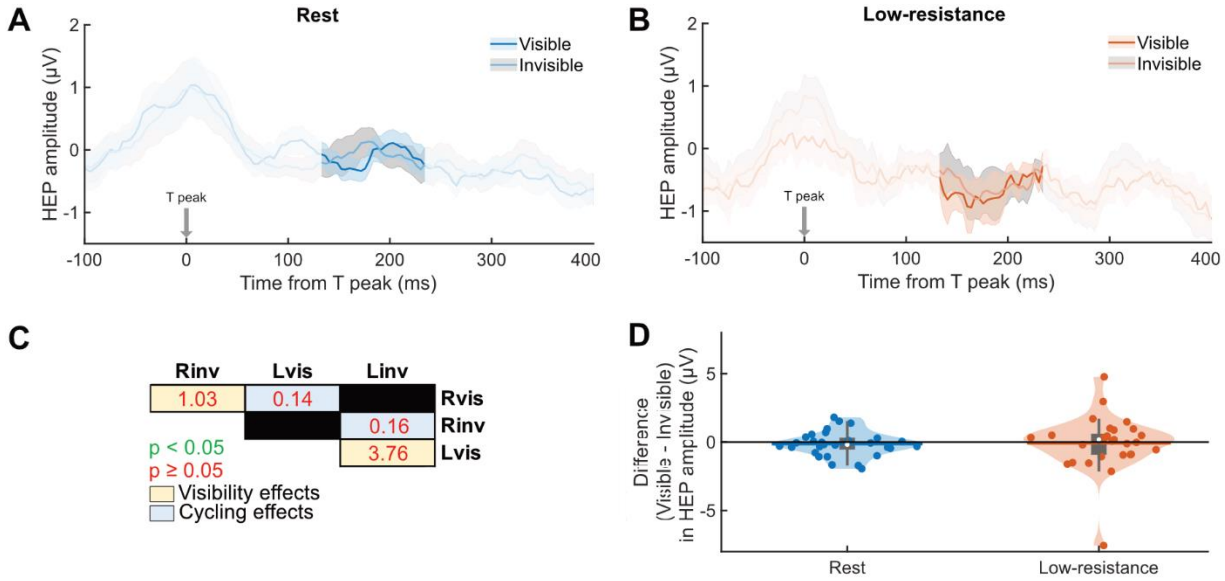

Figure 2-9 – Heartbeat-evoked potentials as a function of perceptual suppression and cycling

Pre-RDM HEPs averaged across the significant cluster for the trials where the target remained visible and those where it was rendered invisible during GFS are shown for (**A**) rest and (**B**) low-resistance cycling conditions. (**C**) Bonferroni-corrected Wilcoxon signed-rank test *p*-values for pairwise comparisons reflecting the effect of target visibility and exercise on pre-RDM HEP amplitude (Rest – R, Low-resistance – L, Visible – vis, Invisible - inv). (**D**) Violin plots showing the visible – invisible difference in mean pre-RDM HEP amplitude (from the same time window as the exercise intensity analysis) during GFS performed at rest (blue) and during low-resistance (orange) cycling. Vertical grey boxes indicate the interquartile range (IQR), with grey whiskers indicating 1.5 × IQR, surrounded on each side by the kernel density estimation in the colour corresponding to each group. Horizontal lines, in the colour corresponding to each group, denote means, and white dots indicate medians. Each dot in a given condition represents the average value of a single subject. $N = 29$ for all plots.

2.5 Discussion

2.5.1 Alpha activity and perception during exercise

In the current study, we investigated behavioural, neural, and cardiovascular responses to Generalized Flash Suppression (GFS) performed during light-intensity cycling. We found that the disappearance probability, i.e. the rate of perceptual suppression, decreased during cycling. In parallel, pre-RDM parieto-occipital alpha activity was lower during cycling compared to rest. When comparing pre-RDM alpha modulations between visible and invisible trials, we observed that parieto-occipital alpha amplitudes were lower prior to target disappearance compared to when the target remained visible, consistently across all three exercise intensity conditions. While this difference did not reach significance after correction for multiple comparisons, the direction of the effect aligns with our previous EEG GFS study (Poland et al., 2021). These results, along with the absence of a correlation between cycling-related modulation of alpha amplitude and disappearance probability, suggest that while pre-RDM alpha amplitudes index target visibility, they do not account for the decreased rate of perceptual suppression during cycling.

Modulations of alpha activity have been shown to reflect fluctuations in attentional states, with the processing of attended stimuli being linked to reduced alpha activity compared to unattended stimuli (Kelly et al., 2006; Sauseng et al., 2005; Thut et al., 2006). Such reductions in alpha activity are thought to indicate heightened neural excitability (Iemi et al., 2017; Jensen & Mazaheri, 2010; Klimesch et al., 2007; Romei, Brodbeck, et al., 2008; Romei, Rihs, et al., 2008) and are linked to the suppression of distracting stimuli (Foxe & Snyder, 2011; Kelly et al., 2006; Worden et al., 2000; Wöstmann et al., 2019). In the previous GFS study linking alpha decreases to target disappearance at rest, it was proposed that these functions of alpha were responsible for enhancing the processing of the surrounding motion stimulus, thereby increasing its effectiveness in suppressing GFS targets (Poland et al., 2021). As in the previous study (Poland et al., 2021), we cannot distinguish between neural modulations associated with the target and the surround, which would be of interest to investigate in future studies. Understanding whether the

observed alpha reductions during cycling reflect attentional shifts specific to the target, the surrounding stimulus, or a combination of both could provide further insights into the neural mechanisms underlying the reduced rate of perceptual suppression in exercise-related contexts.

While the observed decreases in alpha activity indicate increased visual attention (Kelly et al., 2006; Sauseng et al., 2005; Thut et al., 2006), they may not be solely attributable to either target or surround processing. Instead, these reductions could reflect the dual-task demands of dividing external attention between perceptual and motor task performance. Similar alpha modulations have been observed during walking, where reductions in parietal alpha are thought to reflect sensorimotor integration during visually guided walking in a virtual reality paradigm (Wagner et al., 2014).

Walking has been linked to more pronounced alpha power decreases than cycling, potentially reflecting the unique somatosensory and proprioceptive demands of gait (Storzer et al., 2016). Correspondingly, unique patterns of visual processing have been associated with walking and cycling. For example, studies employing orientation discrimination paradigms report different outcomes during walking and cycling. Concurrent decreases in both pre-RDM alpha power and orientation discrimination accuracy are reported during natural walking (as opposed to stationary walking on a treadmill), with the changes in alpha suggesting a change in attentional state linked to visual awareness (Chen et al., 2022). Meanwhile, during cycling, increases in parieto-occipital alpha relative to rest have been associated with a decrease in orientation discrimination accuracy (Bullock et al., 2017). These differing findings suggest that changes in alpha activity may vary depending on the type of exercise, potentially leading to different perceptual outcomes based on the sensory and attentional demands associated with each exercise.

2.5.2 Heart rate and heart rate variability during exercise and their effect on alpha activity and perception

In addition to neural and behavioural effects, our study examined exercise-mediated cardiac influences on neural activity and perceptual outcomes in GFS. As expected, there was an increase in heart rate / decrease in heart rate variability (HRV) associated with the physical activity of cycling. However, neither the increase in heart rate nor the decrease in HRV correlated with the observed decreases in disappearance probability or pre-RDM alpha activity. Also, none of these parameters differed significantly between trials in which the target remained visible and those in which it disappeared. The decrease in alpha observed in parallel to the increase in heart rate, argues against the baroreceptor hypothesis theory of cardiovascular influences on cortical excitability during exercise (Crabbe & Dishman, 2004; Hosang et al., 2022).

The absence of a correlation between heart rate and perceptual or neural outcomes also suggests that the sustained heart rate increases during cycling may reflect a general sympathetic arousal state that does not directly map onto perceptual processing. This stands in contrast to the phasic heart rate decelerations associated with attentional orienting and stimulus anticipation (B. C. Lacey & Lacey, 1978; J. I. Lacey, 1967; B. C. Lacey & Lacey, 1974; Jennings & Wood, 1977; B. C. Lacey & Lacey, 1980; Somsen et al., 2004; Park et al., 2014; Cobos et al., 2019; Motyka et al., 2019; Grund et al., 2022), which were also observed in this study. It is possible that the tonic sympathetic dominance induced by exercise may override or mask the more subtle interoceptive effects that might otherwise influence perceptual suppression.

A further consideration is the interplay between respiration and cardiac function. While increased heart rate is often associated with increased baroreceptor firing due to greater cardiac output and arterial stretch, in some situations there is a context-dependent dissociation between heart rate and baroreceptor signalling. One such case is respiratory sinus arrhythmia (RSA), the natural fluctuation in heart rate across the respiratory cycle. RSA reflects cyclic autonomic modulation aimed at optimising pulmonary gas exchange: heart rate increases during inhalation, driven by sympathetic activation and vagal

withdrawal, and decreases during exhalation due to baroreflex-mediated vagal engagement (Berntson et al., 1993; Noble & Hochman, 2019). Importantly, this means that during inhalation, heart rate is high but baroreceptor activity is relatively low. It follows that inhalation has sometimes also been associated with enhanced perception and reduced alpha power, indicating increased cortical excitability (Kluger et al., 2021), despite this being a phase of elevated heart rate and lower baroreceptor firing. This supports the idea that cortical excitability can increase even when baroreceptor activity is low, depending on the respiratory phase and overall autonomic state.

A previous study showed that RSA systematically decreases during exercise, although it can still be observed at heart rates (HR) above 100 beats per minute (Hatfield et al., 1998). Together with the observed exercise-induced reduction of HRV it means that exercise further complicates this relationship by reducing RSA and HRV, effectively narrowing the dynamic range of autonomic modulation. This diminished capacity for autonomic variation may limit the brain's ability to flexibly shift between interoceptive and exteroceptive modes, potentially affecting perceptual outcomes. In this sense, it may not be just the level of baroreceptor activity that matters, or the extent of parasympathetic/sympathetic dominance, but also the autonomic variability and adaptability.

2.5.3 Exercise-induced effects on HEP amplitudes

In addition to changes in heart rate and alpha activity, we also observed cycling-related differences in HEPs, reflecting a change in the neural responses to cardiac signals during exercise. Increased HEP amplitudes have been linked to enhanced interoceptive attention, reflecting both explicit attention to (Montoya et al., 1993; Petzschner et al., 2019; Pollatos et al., 2005; Pollatos & Schandry, 2004; Schandry et al., 1986; Villena-González et al., 2017), and unconscious processing of heartbeats (Kern et al., 2013; Perogamvros et al., 2019). We observed a decrease in HEP amplitudes during cycling compared to rest, suggesting that interoceptive processing is attenuated during exercise, potentially reflecting an attentional shift away from interoceptive information and towards exteroceptive information required for the simultaneous performance of a perceptual and

a motor task. Our results also indicate that the difference in heart rate between the rest and low-resistance cycling conditions does not contribute to the observed difference in HEP amplitudes between them.

Furthermore, in our study, the HEPs did not predict perceptual suppression in GFS at rest or during cycling, nor did cycling-induced changes in HEPs correlate with changes in disappearance probability. These results suggest that while HEPs are sensitive to changes in physiological state, their role in mediating perceptual outcomes may be limited, at least in the context of GFS. This contrasts with preliminary evidence from previous research suggesting that increased HEP amplitudes were associated with increased detection of a target in a visual threshold paradigm (Park et al., 2014). The absence of such a link in our study suggests that the influence of interoceptive processing as indexed by HEPs on perceptual processing may vary depending on the perceptual task, highlighting the need for further investigation into the contribution of HEPs to conscious perception.

The observed exercise-linked reductions in perceptual suppression, alpha activity, and HEP amplitude highlight a complex interplay between interoception and exteroception during physical activity. While exercise appears to enhance exteroceptive processing, as reflected in reduced perceptual suppression and reduced alpha amplitudes, it simultaneously attenuates cardiac interoceptive processing, as indexed by reduced HEPs. These findings support the idea of a dynamic trade-off between interoceptive and exteroceptive domains, modulated by task demands and physiological state.

2.6 References

Al, E., Iliopoulos, F., Forschack, N., Nierhaus, T., Grund, M., Motyka, P., Gaebler, M., Nikulin, V. V., & Villringer, A. (2020). Heart–Brain Interactions Shape Somatosensory Perception and Evoked Potentials. *Proceedings of the National Academy of Sciences*, *117*(19), 10575–10584. https://doi.org/10.1073/pnas.1915629117

Bailey, S. P., Hall, E. E., Folger, S. E., & Miller, P. C. (2008). Changes in EEG During Graded Exercise on a Recumbent Cycle Ergometer. *Journal of Sports Science & Medicine*, *7*(4), 505.

Berntson, G. G., Cacioppo, J. T., & Quigley, K. S. (1993). Respiratory sinus arrhythmia: Autonomic origins, physiological mechanisms, and psychophysiological implications. *Psychophysiology*, *30*(2), 183–196. https://doi.org/10.1111/j.1469-8986.1993.tb01731.x

Berntson, G. G., Quigley, K. S., & Lozano, D. (2007). Cardiovascular Psychophysiology. In G. Berntson, J. T. Cacioppo, & L. G. Tassinary (Eds.), *Handbook of Psychophysiology* (3rd ed., pp. 182–210). Cambridge University Press. https://www.cambridge.org/core/books/handbook-of-psychophysiology/cardiovascular-psychophysiology/CAB9D08704751D5A26A58C442B3F2BB8

Birznieks, I., Boonstra, T. W., & Macefield, V. G. (2012). Modulation of Human Muscle Spindle Discharge by Arterial Pulsations—Functional Effects and Consequences. *PLOS ONE*, *7*(4), e35091. https://doi.org/10.1371/journal.pone.0035091

Bishop, V. S., Malliani, A., & Thorén, P. (1983). Cardiac Mechanoreceptors. In J. T. Shephard & F. M. Abbound (Eds.), *Handbook of Physiology* (pp. 497–555). Waverly Press. https://doi.org/10.1002/cphy.cp020315

Brainard, D. H. (1997). The Psychophysics Toolbox. *Spatial Vision*, *10*(4), 433–436.

Bullock, T., Cecotti, H., & Giesbrecht, B. (2015). Multiple Stages of Information Processing Are Modulated During Acute Bouts of Exercise. *Neuroscience*, *307*, 138–150. https://doi.org/10.1016/j.neuroscience.2015.08.046

Bullock, T., Elliott, J. C., Serences, J. T., & Giesbrecht, B. (2017). Acute Exercise Modulates Feature-selective Responses in Human Cortex. *Journal of Cognitive Neuroscience*, *29*(4), 605–618. https://doi.org/10.1162/jocn_a_01082

Cantelon, J. A., & Giles, G. E. (2021). A Review of Cognitive Changes During Acute Aerobic Exercise. *Frontiers in Psychology*, *12*. https://doi.org/10.3389/fpsyg.2021.653158

Cao, L., & Händel, B. (2019). Walking Enhances Peripheral Visual Processing in Humans. *PLoS Biology*, *17*(10), e3000511. https://doi.org/10.1371/journal.pbio.3000511

Chang, Y. K., Labban, J. D., Gapin, J. I., & Etnier, J. L. (2012). The Effects of Acute Exercise on Cognitive Performance: A Meta-Analysis. *Brain Research*, *1453*, 87–101. https://doi.org/10.1016/j.brainres.2012.02.068

Chen, X., Cao, L., & Haendel, B. F. (2022). Human Visual Processing During Walking: Dissociable Pre- and Post-Stimulus Influences. *NeuroImage*, *264*, 119757. https://doi.org/10.1016/j.neuroimage.2022.119757

Ciria, L. F., Luque-Casado, A., Sanabria, D., Holgado, D., Ivanov, P. Ch., & Perakakis, P. (2019). Oscillatory Brain Activity During Acute Exercise: Tonic and Transient Neural Response to an Oddball Task. *Psychophysiology*, *56*(5), e13326. https://doi.org/10.1111/psyp.13326

Clark, J. H. (1924). The Ishihara Test for Color Blindness. *American Journal of Physiological Optics*, *5*, 269–276.

Cobos, M. I., Guerra, P. M., Vila, J., & Chica, A. B. (2019). Heart-Rate Modulations Reveal Attention and Consciousness Interactions. *Psychophysiology*, *56*(3), e13295. https://doi.org/10.1111/psyp.13295

Coll, M.-P., Hobson, H., Bird, G., & Murphy, J. (2021). Systematic Review and Meta-Analysis of the Relationship Between the Heartbeat-Evoked Potential and Interoception. *Neuroscience & Biobehavioral Reviews*, *122*, 190–200. https://doi.org/10.1016/j.neubiorev.2020.12.012

Corcoran, A. W., Macefield, V. G., & Hohwy, J. (2021). Be Still My Heart: Cardiac Regulation as a Mode of Uncertainty Reduction. *Psychonomic Bulletin & Review*, *28*(4), 1211–1223. https://doi.org/10.3758/s13423-021-01888-y

Crabbe, J. B., & Dishman, R. K. (2004). Brain Electrocortical Activity During and After Exercise: A Quantitative Synthesis. *Psychophysiology*, *41*(4), 563–574. https://doi.org/10.1111/j.1469-8986.2004.00176.x

Dampney, R. A. L., Polson, J. W., Potts, P. D., Hirooka, Y., & Horiuchi, J. (2003). Functional Organization of Brain Pathways Subserving the Baroreceptor Reflex: Studies in Conscious Animals Using Immediate Early Gene Expression. *Cellular and Molecular Neurobiology*, *23*(4), 597–616. https://doi.org/10.1023/A:1025080314925

De Sanctis, P., Butler, J. S., Malcolm, B. R., & Foxe, J. J. (2014). Recalibration of Inhibitory Control Systems During Walking-Related Dual-Task Interference: A Mobile Brain-Body Imaging (MOBI) Study. *NeuroImage*, *94*, 55–64. https://doi.org/10.1016/j.neuroimage.2014.03.016

Enders, H., Cortese, F., Maurer, C., Baltich, J., Protzner, A. B., & Nigg, B. M. (2016). Changes in Cortical Activity Measured with EEG During a High-Intensity Cycling Exercise. *Journal of Neurophysiology*, *115*(1), 379–388. https://doi.org/10.1152/jn.00497.2015

Ferris, L. T., Williams, J. S., & Shen, C.-L. (2007). The Effect of Acute Exercise on Serum Brain-Derived Neurotrophic Factor Levels and Cognitive Function. *Medicine and Science in Sports and Exercise*, *39*(4), 728–734. https://doi.org/10.1249/mss.0b013e31802f04c7

Ford, T. W., & Kirkwood, P. A. (2018). Cardiac Modulation of Alpha Motoneuron Discharges. *Journal of Neurophysiology*, *119*(5), 1723–1730. https://doi.org/10.1152/jn.00025.2018

Foxe, J. J., & Snyder, A. C. (2011). The Role of Alpha-Band Brain Oscillations as a Sensory Suppression Mechanism During Selective Attention. *Frontiers in Psychology*, *2*. https://doi.org/10.3389/fpsyg.2011.00154

Fumoto, M., Oshima, T., Kamiya, K., Kikuchi, H., Seki, Y., Nakatani, Y., Yu, X., Sekiyama, T., Sato-Suzuki, I., & Arita, H. (2010). Ventral Prefrontal Cortex and Serotonergic System Activation During Pedaling Exercise Induces Negative Mood Improvement and Increased Alpha Band in EEG. *Behavioural Brain Research*, *213*(1), 1–9. https://doi.org/10.1016/j.bbr.2010.04.017

Garber, C. E., Blissmer, B., Deschenes, M. R., Franklin, B. A., Lamonte, M. J., Lee, I.-M., Nieman, D. C., & Swain, D. P. (2011). Quantity and Quality of Exercise for Developing and Maintaining Cardiorespiratory, Musculoskeletal, and Neuromotor Fitness in Apparently Healthy Adults: Guidance for Prescribing Exercise. *Medicine & Science in Sports & Exercise*, *43*(7), 1334. https://doi.org/10.1249/MSS.0b013e318213fefb

Garrett, J., Chak, C., Bullock, T., & Giesbrecht, B. (2024). A Systematic Review and Bayesian Meta-Analysis Provide Evidence for an Effect of Acute Physical Activity on Cognition in Young Adults. *Communications Psychology*, *2*(1), 82. https://doi.org/10.1038/s44271-024-00124-2

Gray, M. A., Taggart, P., Sutton, P. M., Groves, D., Holdright, D. R., Bradbury, D., Brull, D., & Critchley, H. D. (2007). A Cortical Potential Reflecting Cardiac Function. *Proceedings of the National Academy of Sciences*, *104*(16), 6818–6823. https://doi.org/10.1073/pnas.0609509104

Grund, M., Al, E., Pabst, M., Dabbagh, A., Stephani, T., Nierhaus, T., Gaebler, M., & Villringer, A. (2022). Respiration, Heartbeat, and Conscious Tactile Perception. *Journal of Neuroscience*, *42*(4), 643–656. https://doi.org/10.1523/JNEUROSCI.0592-21.2021

Hatfield, B. D., Spalding, T. W., Santa Maria, D. L., Porges, S. W., Potts, J. T., Byrne, E. A., Brody, E. B., & Mahon, A. D. (1998). Respiratory Sinus Arrhythmia During Exercise in Aerobically Trained and Untrained Men. *Medicine and Science in Sports and Exercise*, *30*(2), 206–214. https://doi.org/10.1097/00005768-199802000-00006

Heinonen, I., Kalliokoski, K. K., Hannukainen, J. C., Duncker, D. J., Nuutila, P., & Knuuti, J. (2014). Organ-Specific Physiological Responses to Acute Physical Exercise and Long-Term Training in Humans. *Physiology*, *29*(6), 421–436. https://doi.org/10.1152/physiol.00067.2013

Hosang, L., Mouchlianitis, E., Guérin, S. M. R., & Karageorghis, C. I. (2022). Effects of Exercise on Electroencephalography-Recorded Neural Oscillations: A Systematic Review. *International Review of Sport and Exercise Psychology*, *0*(0), 1–54. https://doi.org/10.1080/1750984X.2022.2103841

Hottenrott, K., Taubert, M., & Gronwald, T. (2013). Cortical Brain Activity Is Influenced by Cadence in Cyclists. *The Open Sports Sciences Journal*, *6*, 9–14. https://doi.org/10.2174/1875399X01306010009

Iemi, L., Chaumon, M., Crouzet, S. M., & Busch, N. A. (2017). Spontaneous Neural Oscillations Bias Perception by Modulating Baseline Excitability. *The Journal of*

Neuroscience: The Official Journal of the Society for Neuroscience, *37*(4), 807–819. https://doi.org/10.1523/JNEUROSCI.1432-16.2016

Jammal Salameh, L., Bitzenhofer, S. H., Hanganu-Opatz, I. L., Dutschmann, M., & Egger, V. (2024). Blood Pressure Pulsations Modulate Central Neuronal Activity Via Mechanosensitive Ion Channels. *Science*, *383*(6682), eadk8511. https://doi.org/10.1126/science.adk8511

Jänig, W. (1996). Neurobiology of Visceral Afferent Neurons: Neuroanatomy, Functions, Organ Regulations and Sensations. *Biological Psychology*, *42*(1–2), 29–51. https://doi.org/10.1016/0301-0511(95)05145-7

Jennings, J. R., & Wood, C. C. (1977). Cardiac Cycle Time Effects on Performance, Phasic Cardiac Responses, and Their Intercorrelation in Choice Reaction Time. *Psychophysiology*, *14*(3), 297–307. https://doi.org/10.1111/j.1469-8986.1977.tb01179.x

Jensen, O., & Mazaheri, A. (2010). Shaping Functional Architecture by Oscillatory Alpha Activity: Gating by Inhibition. *Frontiers in Human Neuroscience*, *4*. https://doi.org/10.3389/fnhum.2010.00186

Kefauver, J. M., Ward, A. B., & Patapoutian, A. (2020). Discoveries in Structure and Physiology of Mechanically Activated Ion Channels. *Nature*, *587*(7835), 567–576. https://doi.org/10.1038/s41586-020-2933-1

Kelly, S. P., Lalor, E. C., Reilly, R. B., & Foxe, J. J. (2006). Increases in Alpha Oscillatory Power Reflect an Active Retinotopic Mechanism for Distracter Suppression During Sustained Visuospatial Attention. *Journal of Neurophysiology*, *95*(6), 3844–3851. https://doi.org/10.1152/jn.01234.2005

Kern, M., Aertsen, A., Schulze-Bonhage, A., & Ball, T. (2013). Heart Cycle-Related Effects on Event-Related Potentials, Spectral Power Changes, and Connectivity Patterns in the Human Ecog. *NeuroImage*, *81*, 178–190. https://doi.org/10.1016/j.neuroimage.2013.05.042

Kim, K. J., Ramiro Diaz, J., Iddings, J. A., & Filosa, J. A. (2016). Vasculo-Neuronal Coupling: Retrograde Vascular Communication to Brain Neurons. *The Journal of Neuroscience*, *36*(50), 12624–12639. https://doi.org/10.1523/JNEUROSCI.1300-16.2016

Kleiner, M., Brainard, D., Pelli, D., Ingling, A., Murray, R., & Broussard, C. (2007). What's New in Psychtoolbox-3. *Perception*, *36*(14), 1–16.

Klimesch, W., Sauseng, P., & Hanslmayr, S. (2007). EEG Alpha Oscillations: The Inhibition–Timing Hypothesis. *Brain Research Reviews*, *53*(1), 63–88. https://doi.org/10.1016/j.brainresrev.2006.06.003

Kluger, D. S., Balestrieri, E., Busch, N. A., & Gross, J. (2021). Respiration Aligns Perception with Neural Excitability. *eLife*, *10*, e70907. https://doi.org/10.7554/eLife.70907

Koriath, J. J., Lindholm, E., & Landers, D. M. (1987). Cardiac-Related Cortical Activity During Variations in Mean Heart Rate. *International Journal of Psychophysiology*, *5*(4), 289–299. https://doi.org/10.1016/0167-8760(87)90060-2

Lacey, B. C., & Lacey, J. I. (1974). Studies of Heart Rate and Other Bodily Processes in Sensorimotor Behavior. In *Cardiovascular psychophysiology: Current issues in response mechanisms, biofeedback and methodology* (pp. 538–564). AldineTransaction.

Lacey, B. C., & Lacey, J. I. (1978). Two-Way Communication Between the Heart and the Brain: Significance of Time Within the Cardiac Cycle. *American Psychologist*, *33*(2), 99–113. https://doi.org/10.1037/0003-066X.33.2.99

Lacey, B. C., & Lacey, J. I. (1980). Cognitive Modulation of Time-Dependent Primary Bradycardia. *Psychophysiology*, *17*(3), 209–221. https://doi.org/10.1111/j.1469-8986.1980.tb00137.x

Lacey, J. I. (1967). Somatic Response Patterning and Stress: Some Revisions of Activation Theory. In M. H. Appley & R. Trimbull (Eds.), *Pyschological Stress: Issues in Research*. Appleton Century-Crofts.

Lacey, J. I., & Lacey, B. C. (1958). The Relationship of Resting Autonomic Activity to Motor Impulsivity. *Research Publications of the Association for Research in Nervous & Mental Disease*, *36*, 144–209.

Lacey, J. I., & Lacey, B. C. (1970). Some Autonomic-Central Nervous System Interrelationships. In P. Black (Ed.), *Physiological Correlates of Emotion* (pp. 205–227). Academic Press. https://doi.org/10.1016/B978-0-12-102850-3.50016-5

Lambourne, K., & Tomporowski, P. (2010). The Effect of Exercise-Induced Arousal on Cognitive Task Performance: A Meta-Regression Analysis. *Brain Research*, *1341*, 12–24. https://doi.org/10.1016/j.brainres.2010.03.091

Leutheuser, H., Gradl, S., Anneken, L., Arnold, M., Lang, N., Achenbach, S., & Eskofier, B. M. (2016, July 21). *Instantaneous P- and T-Wave Detection: Assessment of Three ECG Fiducial Points Detection Algorithms*. 2016 IEEE 13th International Conference on Wearable and Implantable Body Sensor Networks (BSN), San Francisco, CA, USA. https://doi.org/10.1109/BSN.2016.7516283

Macefield, V. G. (2003). Cardiovascular and Respiratory Modulation of Tactile Afferents in the Human Finger Pad. *Experimental Physiology*, *88*(5), 617–625. https://doi.org/10.1113/eph8802548

Marina, N., Christie, I. N., Korsak, A., Doronin, M., Brazhe, A., Hosford, P. S., Wells, J. A., Sheikhbahaei, S., Humoud, I., Paton, J. F. R., Lythgoe, M. F., Semyanov, A., Kasparov, S., & Gourine, A. V. (2020). Astrocytes Monitor Cerebral Perfusion and Control Systemic Circulation to Maintain Brain Blood Flow. *Nature Communications*, *11*(1), 131. https://doi.org/10.1038/s41467-019-13956-y

Maris, E., & Oostenveld, R. (2007). Nonparametric Statistical Testing of EEG- and MEG-Data. *Journal of Neuroscience Methods*, *164*(1), 177–190. https://doi.org/10.1016/j.jneumeth.2007.03.024

Meeusen, R., & De Meirleir, K. (1995). Exercise and Brain Neurotransmission. *Sports Medicine (Auckland, N.Z.)*, *20*(3), 160–188. https://doi.org/10.2165/00007256-199520030-00004

Mehling, W. E., Price, C., Daubenmier, J. J., Acree, M., Bartmess, E., & Stewart, A. (2012). The Multidimensional Assessment of Interoceptive Awareness (MAIA). *PLOS ONE*, *7*(11), e48230. https://doi.org/10.1371/journal.pone.0048230

Mongin, D., Chabert, C., Extremera, M. G., Hue, O., Courvoisier, D. S., Carpena, P., & Galvan, P. A. B. (2022). Decrease of Heart Rate Variability During Exercise: An Index of Cardiorespiratory Fitness. *PloS One*, *17*(9), e0273981. https://doi.org/10.1371/journal.pone.0273981

Montoya, P., Schandry, R., & Müller, A. (1993). Heartbeat Evoked Potentials (HEP): Topography and Influence of Cardiac Awareness and Focus of Attention. *Electroencephalography and Clinical Neurophysiology/Evoked Potentials Section*, *88*(3), 163–172. https://doi.org/10.1016/0168-5597(93)90001-6

Motyka, P., Grund, M., Forschack, N., Al, E., Villringer, A., & Gaebler, M. (2019). Interactions Between Cardiac Activity and Conscious Somatosensory Perception. *Psychophysiology*, *56*(10), e13424. https://doi.org/10.1111/psyp.13424

Nes, B. M., Janszky, I., Wisløff, U., Støylen, A., & Karlsen, T. (2013). Age-Predicted Maximal Heart Rate in Healthy Subjects: The HUNT Fitness Study. *Scandinavian Journal of Medicine & Science in Sports*, *23*(6), 697–704. https://doi.org/10.1111/j.1600-0838.2012.01445.x

Noble, D. J., & Hochman, S. (2019). Hypothesis: Pulmonary Afferent Activity Patterns During Slow, Deep Breathing Contribute to the Neural Induction of Physiological Relaxation. *Frontiers in Physiology*, *10*, 1176. https://doi.org/10.3389/fphys.2019.01176

Oldfield, R. C. (1971). The Assessment and Analysis of Handedness: The Edinburgh Inventory. *Neuropsychologia*, *9*(1), 97–113. https://doi.org/10.1016/0028-3932(71)90067-4

Oostenveld, R., Fries, P., Maris, E., & Schoffelen, J.-M. (2011). FieldTrip: Open Source Software for Advanced Analysis of MEG, EEG, and Invasive Electrophysiological Data. *Computational Intelligence and Neuroscience*, *2011*, 1–9. https://doi.org/10.1155/2011/156869

Pan, J., & Tompkins, W. J. (1985). A Real-Time QRS Detection Algorithm. *IEEE Transactions on Bio-Medical Engineering*, *32*(3), 230–236. https://doi.org/10.1109/TBME.1985.325532

Park, H.-D., & Blanke, O. (2019). Heartbeat-Evoked Cortical Responses: Underlying Mechanisms, Functional Roles, and Methodological Considerations. *NeuroImage*, *197*, 502–511. https://doi.org/10.1016/j.neuroimage.2019.04.081

Park, H.-D., Correia, S., Ducorps, A., & Tallon-Baudry, C. (2014). Spontaneous Fluctuations in Neural Responses to Heartbeats Predict Visual Detection. *Nature Neuroscience*, *17*(4), Article 4. https://doi.org/10.1038/nn.3671

Pennebaker, J. W., & Lightner, J. M. (1980). Competition of Internal and External Information in an Exercise Setting. *Journal of Personality and Social Psychology*, *39*(1), 165–174. https://doi.org/10.1037/0022-3514.39.1.165

Perogamvros, L., Park, H.-D., Bayer, L., Perrault, A. A., Blanke, O., & Schwartz, S. (2019). Increased Heartbeat-Evoked Potential During REM Sleep in Nightmare Disorder. *NeuroImage: Clinical*, *22*, 101701. https://doi.org/10.1016/j.nicl.2019.101701

Petzschner, F. H., Weber, L. A., Wellstein, K. V., Paolini, G., Do, C. T., & Stephan, K. E. (2019). Focus of Attention Modulates the Heartbeat Evoked Potential. *NeuroImage*, *186*, 595–606. https://doi.org/10.1016/j.neuroimage.2018.11.037

Poland, E., Bhonsle, A., Steinmann, I., & Wilke, M. (2021). Reduced Alpha Amplitudes Predict Perceptual Suppression. *Scientific Reports*, *11*(1), Article 1. https://doi.org/10.1038/s41598-021-92404-8

Pollatos, O., Kirsch, W., & Schandry, R. (2005). Brain Structures Involved in Interoceptive Awareness and Cardioafferent Signal Processing: A Dipole Source Localization Study. *Human Brain Mapping*, *26*(1), 54–64. https://doi.org/10.1002/hbm.20121

Pollatos, O., & Schandry, R. (2004). Accuracy of Heartbeat Perception Is Reflected in the Amplitude of the Heartbeat-Evoked Brain Potential. *Psychophysiology*, *41*(3), 476–482. https://doi.org/10.1111/1469-8986.2004.00170.x

Querido, J. S., & Sheel, A. W. (2007). Regulation of Cerebral Blood Flow During Exercise. *Sports Medicine (Auckland, N.Z.)*, *37*(9), 765–782. https://doi.org/10.2165/00007256-200737090-00002

Romei, V., Brodbeck, V., Michel, C., Amedi, A., Pascual-Leone, A., & Thut, G. (2008). Spontaneous Fluctuations in Posterior Alpha-Band EEG Activity Reflect Variability in Excitability of Human Visual Areas. *Cerebral Cortex*, *18*(9), 2010–2018. https://doi.org/10.1093/cercor/bhm229

Romei, V., Rihs, T., Brodbeck, V., & Thut, G. (2008). Resting Electroencephalogram Alpha-Power Over Posterior Sites Indexes Baseline Visual Cortex Excitability. *Neuroreport*, *19*(2), 203–208. https://doi.org/10.1097/WNR.0b013e3282f454c4

Sandman, C. A., McCanne, T. R., Kaiser, D. N., & Diamond, B. (1977). Heart Rate and Cardiac Phase Influences on Visual Perception. *Journal of Comparative and Physiological Psychology*, *91*(1), 189–202. https://doi.org/10.1037/h0077302

Sauseng, P., Klimesch, W., Stadler, W., Schabus, M., Doppelmayr, M., Hanslmayr, S., Gruber, W. R., & Birbaumer, N. (2005). A Shift of Visual Spatial Attention Is Selectively Associated with Human EEG Alpha Activity. *The European Journal of Neuroscience*, *22*(11), 2917–2926. https://doi.org/10.1111/j.1460-9568.2005.04482.x

Schandry, R., & Montoya, P. (1996). Event-Related Brain Potentials and the Processing of Cardiac Activity. *Biological Psychology*, *42*(1), 75–85. https://doi.org/10.1016/0301-0511(95)05147-3

Schandry, R., Sparrer, B., & Weitkunat, R. (1986). From the Heart to the Brain: A Study of Heartbeat Contingent Scalp Potentials. *International Journal of Neuroscience*, *30*(4), 261–275. https://doi.org/10.3109/00207458608985677

Sedghamiz, H. (2014). *Matlab Implementation of Pan Tompkins ECG QRS detector.* [Computer software]. https://doi.org/10.13140/RG.2.2.14202.59841

Skora, L. I., Livermore, J. J. A., & Roelofs, K. (2022). The Functional Role of Cardiac Activity in Perception and Action. *Neuroscience & Biobehavioral Reviews*, *137*, 104655. https://doi.org/10.1016/j.neubiorev.2022.104655

Somsen, R. J. M., Jennings, J. R., & Van der Molen, M. W. (2004). The Cardiac Cycle Time Effect Revisited: Temporal Dynamics of the Central-Vagal Modulation of Heart Rate in Human Reaction Time Tasks. *Psychophysiology*, *41*(6), 941–953. https://doi.org/10.1111/j.1469-8986.2004.00241.x

Storzer, L., Butz, M., Hirschmann, J., Abbasi, O., Gratkowski, M., Saupe, D., Schnitzler, A., & Dalal, S. S. (2016). Bicycling and Walking are Associated with Different Cortical Oscillatory Dynamics. *Frontiers in Human Neuroscience*, *10*. https://doi.org/10.3389/fnhum.2016.00061

Thut, G., Nietzel, A., Brandt, S. A., & Pascual-Leone, A. (2006). Alpha-Band Electroencephalographic Activity Over Occipital Cortex Indexes Visuospatial Attention Bias and Predicts Visual Target Detection. *The Journal of Neuroscience: The Official Journal of the Society for Neuroscience*, *26*(37), 9494–9502. https://doi.org/10.1523/JNEUROSCI.0875-06.2006

Vázquez-Seisdedos, C. R., Neto, J. E., Marañón Reyes, E. J., Klautau, A., & Limão de Oliveira, R. C. (2011). New Approach for T-Wave End Detection on Electrocardiogram: Performance in Noisy Conditions. *BioMedical Engineering OnLine*, *10*(1), 77. https://doi.org/10.1186/1475-925X-10-77

Vila, J., Guerra, P., Muñoz, M. Á., Vico, C., Viedma-del Jesús, M. I., Delgado, L. C., Perakakis, P., Kley, E., Mata, J. L., & Rodríguez, S. (2007). Cardiac Defense: From Attention to Action. *International Journal of Psychophysiology*, *66*(3), 169–182. https://doi.org/10.1016/j.ijpsycho.2007.07.004

Villena-González, M., Moënne-Loccoz, C., Lagos, R. A., Alliende, L. M., Billeke, P., Aboitiz, F., López, V., & Cosmelli, D. (2017). Attending to the Heart Is Associated with Posterior Alpha Band Increase and a Reduction in Sensitivity to Concurrent Visual Stimuli. *Psychophysiology*, *54*(10), 1483–1497. https://doi.org/10.1111/psyp.12894

Wagner, J., Solis-Escalante, T., Scherer, R., Neuper, C., & Müller-Putz, G. (2014). It's How You Get There: Walking down a Virtual Alley Activates Premotor and Parietal Areas. *Frontiers in Human Neuroscience*, *8*. https://doi.org/10.3389/fnhum.2014.00093

Wallman-Jones, A., Perakakis, P., Tsakiris, M., & Schmidt, M. (2021). Physical Activity and Interoceptive Processing: Theoretical Considerations for Future Research. *International Journal of Psychophysiology: Official Journal of the International Organization of Psychophysiology*, *166*, 38–49. https://doi.org/10.1016/j.ijpsycho.2021.05.002

Wang, J., & Hamill, O. P. (2021). Piezo2-Peripheral Baroreceptor Channel Expressed in Select Neurons of the Mouse Brain: A Putative Mechanism for Synchronizing Neural

Networks by Transducing Intracranial Pressure Pulses. *Journal of Integrative Neuroscience*, *20*(4), 825–837. https://doi.org/10.31083/j.jin2004085

Wilke, M., Logothetis, N. K., & Leopold, D. A. (2003). Generalized Flash Suppression of Salient Visual Targets. *Neuron*, *39*(6), 1043–1052. https://doi.org/10.1016/j.neuron.2003.08.003

Worden, M. S., Foxe, J. J., Wang, N., & Simpson, G. V. (2000). Anticipatory Biasing of Visuospatial Attention Indexed by Retinotopically Specific Alpha-Band Electroencephalography Increases Over Occipital Cortex. *The Journal of Neuroscience: The Official Journal of the Society for Neuroscience*, *20*(6), RC63.

Wöstmann, M., Alavash, M., & Obleser, J. (2019). Alpha Oscillations in the Human Brain Implement Distractor Suppression Independent of Target Selection. *Journal of Neuroscience*, *39*(49), 9797–9805. https://doi.org/10.1523/JNEUROSCI.1954-19.2019

Zeng, W.-Z., Marshall, K. L., Min, S., Daou, I., Chapleau, M. W., Abboud, F. M., Liberles, S. D., & Patapoutian, A. (2018). PIEZOs mediate neuronal sensing of blood pressure and the baroreceptor reflex. *Science*, *362*(6413), 464–467. https://doi.org/10.1126/science.aau6324

2.7 Supplementary Information

Table S2-1 - Table of uncorrected *p* values for pairwise comparison of pre-RDM parieto-occipital alpha amplitudes across exercise intensity and visibility conditions

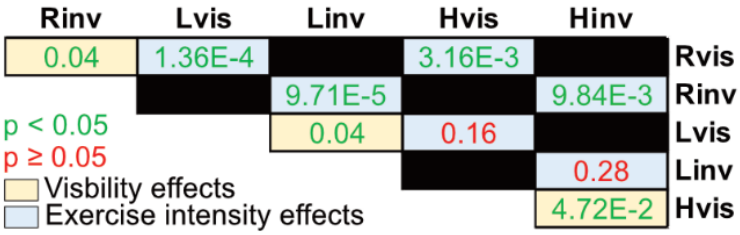

These uncorrected *p* values correspond to the comparisons reported in **Figure 6**, testing for the effects of target visibility (visible – vis; invisible - inv) and exercise intensity (rest – R; low-resistance – L, high-resistance - H) on pre-RDM parieto-occipital alpha amplitudes using Wilcoxon signed-rank tests. These results indicate that alpha amplitudes reflect target visibility and that exercise influences alpha amplitudes compared to rest, although no significant differences were observed between the two cycling conditions.

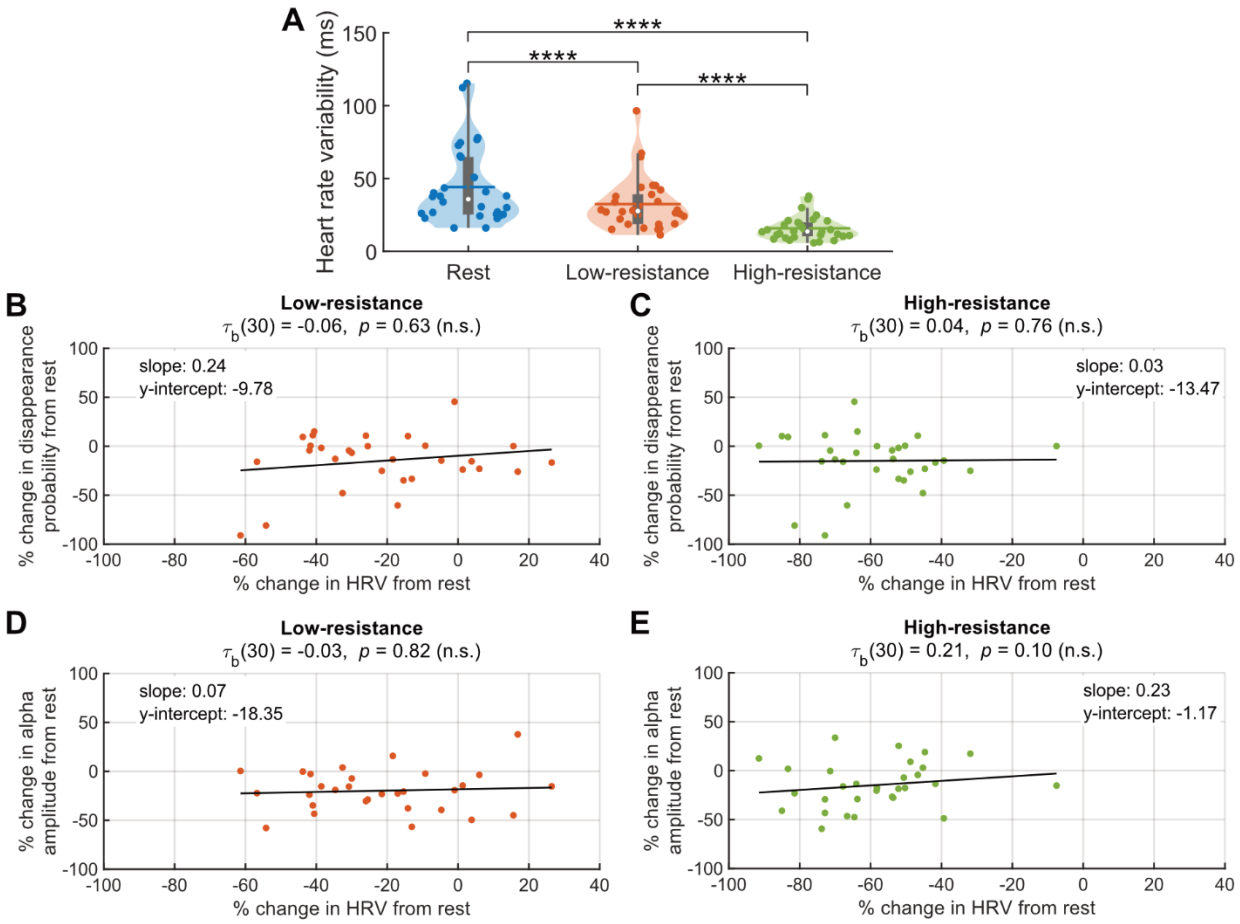

Figure S2-1 – RMSSD heart rate variability (HRV) decreases with cycling intensity

(**A**) Violin plots showing the pre-RDM RMSSD HRV during GFS performed at rest (blue), low-resistance (orange), and high-resistance (green) cycling. Vertical grey boxes indicate the interquartile range (IQR), with grey whiskers indicating 1.5 × IQR, surrounded on each side by the kernel density estimation in the colour corresponding to each group. Horizontal lines, in the colour corresponding to each group, denote means, and white dots indicate medians. Each dot in a given condition represents the average value of a single subject. Statistical significance between conditions, as assessed by Wilcoxon signed-rank tests with a Bonferroni adjustment, is indicated at the $p \leq 0.0001$ (****) level. Correlations as assessed by Kendall's Tau-b between percent change in HRV from rest and percent change in disappearance probability from rest for (**B**) low-resistance and (**C**) high-resistance cycling. Correlations between percent change in HRV from rest and percent change in alpha amplitude from rest for (**D**) low-resistance and (**E**) high-resistance cycling. All correlations are not significant. $N = 30$ for all plots.

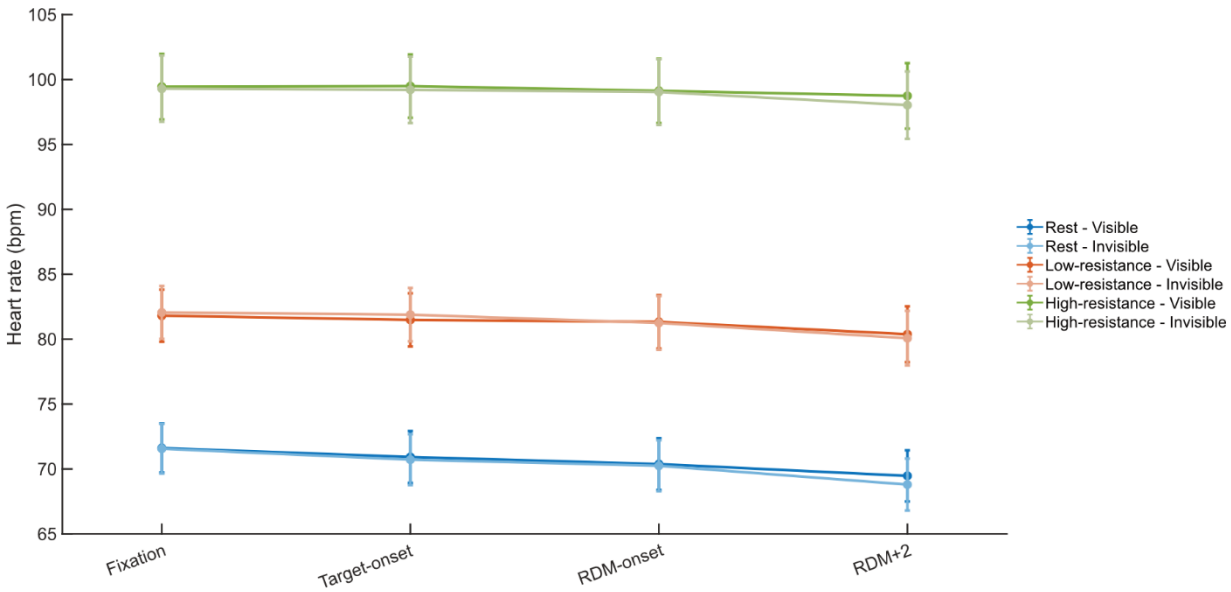

Figure S2-2 – Phasic heart rate deceleration over the course of the GFS trial

Phasic heart rate changes across the course of a trial were assessed using a three-way repeated measures ANOVA with exercise intensity (levels: rest, low-resistance cycling, high-resistance cycling), target visibility (levels: visible, invisible), and time (levels: fixation onset, target onset, RDM onset, trial end (RDM + 2s)) as factors. The analysis showed significant main effects of exercise intensity (Greenhouse-Geisser corrected; $F(1.25, 36.38) = 269.60$, $p = 9.28\times10^{-20}$, $\eta_p^2 = 0.90$) and time (Greenhouse-Geisser corrected; $F(1.68, 48.64) = 22.65$, $p = 4.83\times10^{-7}$, $\eta_p^2 = 0.49$), but not target visibility ($F(1, 29) = 1.26$, $p = 0.27$, $\eta_p^2 = 0.04$). There were significant two-way interactions between exercise intensity and time (Greenhouse-Geisser corrected; $F(3.56, 103.30) = 4.30$, $p = 4.20\times10^{-3}$, $\eta_p^2 = 0.13$) and target visibility and time (Greenhouse-Geisser corrected; $F(2.60, 75.25) = 5.74$, $p = 2.23\times10^{-3}$, $\eta_p^2 = 0.17$), but not between exercise intensity and target visibility ($F(2, 58) = 0.92$, $p = 0.40$, $\eta_p^2 = 0.03$). There was also no significant three-way interaction between the factors ($F(6, 174) = 0.57$, $p = 0.76$, $\eta_p^2 = 0.02$).

The table of the Bonferroni-corrected pairwise comparisons for the factor of time is presented below. These results indicate that there was a decrease in heart rate from fixation to target onset, indicative of the well-characterised phenomenon of cardiac deceleration in anticipation of an upcoming stimulus or response registration, with fixation serving as a 'warning' of an upcoming stimulus, i.e. the onset of a target, which in turn requires a response. Similarly, there is also a slight, non-significant decrease in heart rate from target onset to RDM onset. It is likely that the cardiac acceleration typically reported after response registration does not occur in this case since the target onset acts as a warning of the upcoming RDM onset. Furthermore, there is a potential for an additional response registration after RDM onset if the target is perceptually suppressed. However, since subjects were instructed to also report if the target

reappeared, the cardiac acceleration typically reported after response registration, is not observed; rather, it appears that the heart rate continues to decrease after RDM onset until the end of the trial.

Table S2-2 - Bonferroni-corrected pairwise comparisons for the factor of time

Factor: Time					95% Confidence Interval for difference	
Level (I)	Level (J)	Mean difference in heart rate (I-J)	Std. Error	*p*	Lower bound	Upper bound
Fixation	Target onset	0.34	0.11	0.03	0.02	0.67
	RDM onset	0.76	0.27	0.06	-0.03	1.50
	End of trial	1.72	0.26	2.24×10^{-6}	0.97	2.46
Target onset	RDM onset	0.39	0.22	5.02×10^{-2}	-0.23	1.01
	End of trial	1.37	0.25	4.31×10^{-5}	0.66	2.08
RDM onset	End of trial	0.98	0.16	8.31×10^{-6}	0.52	1.44

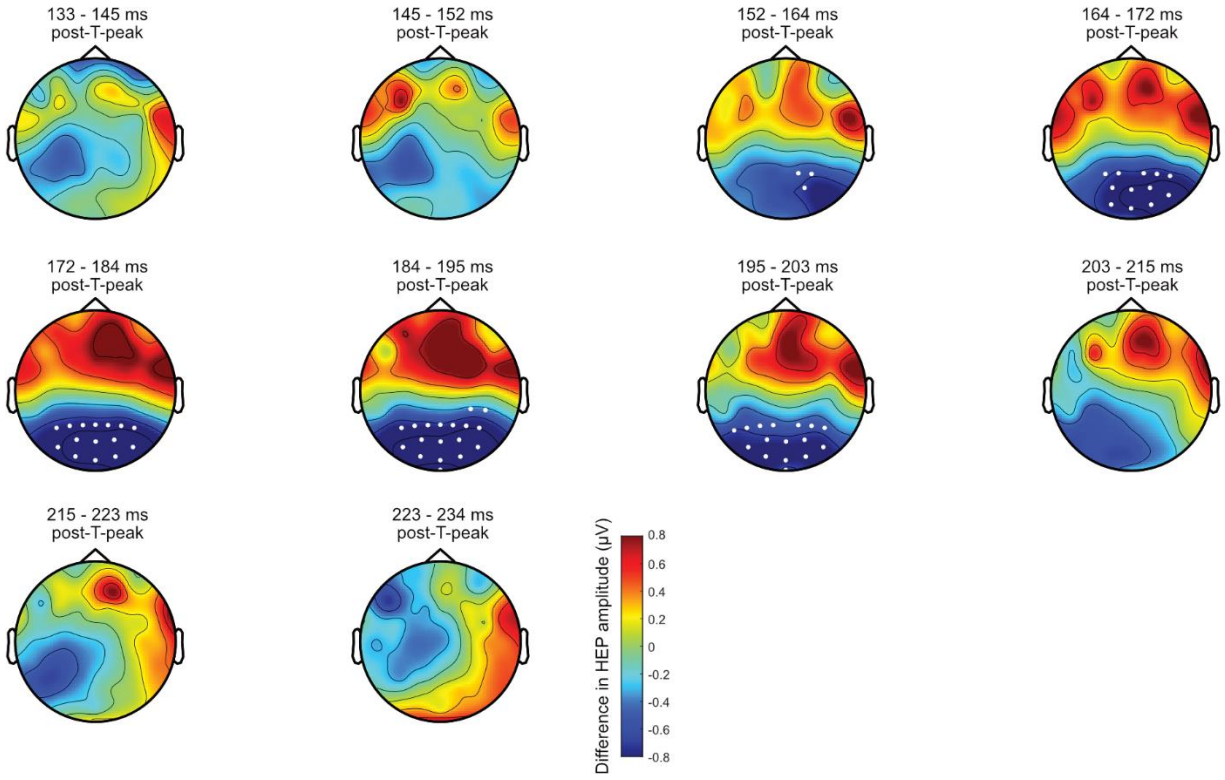

Figure S2-3 – Cluster based permutation analysis of Heartbeat Evoked Potentials (HEP) investigating effect of exercise on HEP amplitude

Scalp topographies of the low-resistance – rest difference in HEP amplitude for 12 ms windows spanning the 133 ms to 234 ms post-T-peak time window. The T-peaks chosen for this analysis were at least 300 ms after target onset and up to 400 ms before RDM onset, to avoid the HEPs from being contaminated by responses to the target or the RDM onset. Spatio-temporal clusters showing a significant difference between the two exercise intensity conditions are indicated by white dots ($p < 0.05$).

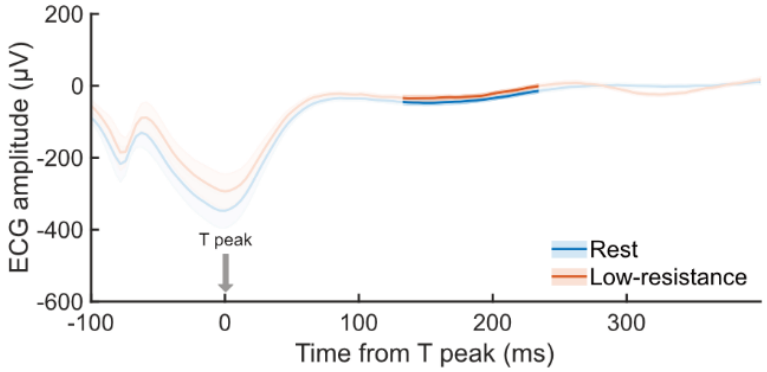

Figure S2-4 – Control for volume conduction

T-peak-locked ECG, grand-average across subjects for the rest and low-resistance cycling conditions in the same time window as the HEP analysis. The shaded areas denote the SEM for each time course. There were no significant differences between the two conditions.

Table S2-3 – Linear mixed-effects model examining the main effects of exercise intensity condition and heart rate on HEP amplitude

Fixed and random effect results from the LME. The two exercise intensity conditions are rest and low-resistance cycling. The model revealed no significant effect of condition on HEP amplitude after controlling for heart rate (p = 0.43), while heart rate showed a marginal negative association with HEP amplitude (p = 0.17). Random intercepts for subjects accounted for individual variability in HEP amplitude.

HEP amplitude ~ 1 + Exercise Intensity condition + Heart Rate + (1|Subject)

Model fit statistics

AIC	BIC	LogLikelihood	Deviance
164.87	175.17	-77.44	154.87

Fixed Effects

Predictor	Estimate (*b*)	SE	*t*-value	*p*-value	95% CI (lower, upper)
Intercept	1.85	0.99	1.87	0.07	(-0.13, 3.83)
Condition (Rest vs. Low-resistance cycling)	0.20	0.25	0.80	0.43	(-0.31, 0.71)
Heart rate	-0.03	0.01	-2.45	0.17	(-0.05, 0.01)

Random Effects

Group	Random Effect	Estimate	95% CI (lower, upper)
Subject (Intercept)	Standard deviation	0.39	(0.14, 1.12)
Residuals	Standard deviation	0.84	(0.65, 1.09)

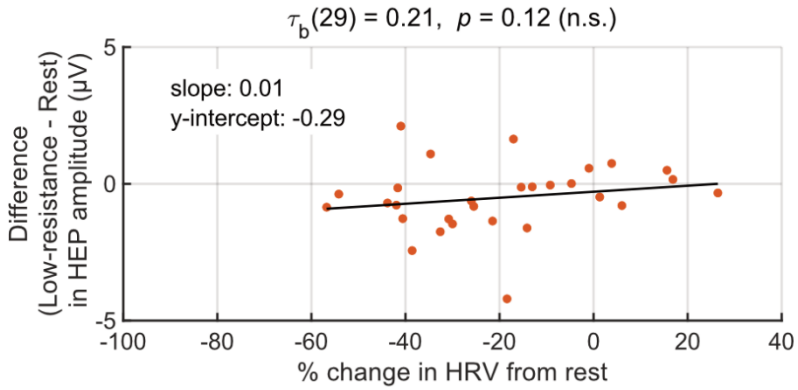

Figure S2-5 – No statistically significant correlation between cycling-related changes in RMSSD heart rate variability (HRV) and the change in HEP amplitude

Correlation as assessed by Kendall's Tau-b between exercise-induced change in HRV and change in HEP amplitude for low-resistance cycling from rest. *N* = 29.

Table S2-4 - Table of uncorrected *p* values for pairwise comparison of HEP amplitudes across exercise intensity and visibility conditions

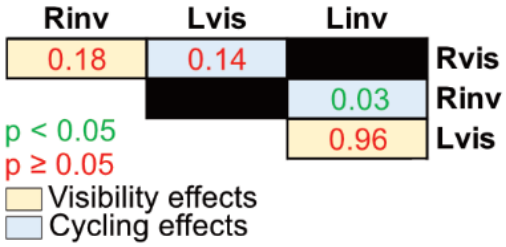

These uncorrected *p* values correspond to the comparisons reported in **Figure 9**, testing for the effects of target visibility (levels: visible – vis; invisible - inv) and exercise intensity (levels: rest – R; low-resistance – L) on HEP amplitudes with Wilcoxon signed-rank tests. There is a significant difference in HEP amplitudes between the rest and low-resistance conditions in trials where the target is rendered invisible.

Author contributions / CRediT statement

Aishwarya Bhonsle: Conceptualization; Data curation; Formal analysis; Investigation; Methodology; Software; Visualization; Writing – original draft; Writing – review & editing

Melanie Wilke: Conceptualization; Methodology; Resources; Supervision; Writing – review & editing, Funding acquisition

Funding information

This research was supported by the Hermann and Lilly Schilling Foundation, the Else-Kröner-Fresenius Foundation and the DFG GRK 2824: 'Heart and Brain Diseases'.

Conflict of interest statement

The authors declare no conflicts of interest.

Data availability statement

Data available on request.

Acknowledgements

We would like to thank Greta Wippich for the illustration of the experimental setup; Alina Seidel for help with data collection; Severin Heumüller for providing technical support; the UMG Statistische Betreuung team for advice on the statistical analyses; Carsten Schmidt-Samoa, Shirin Mahdavi, Ulrich Parlitz and Roberto Goya-Maldonado for helpful discussions.

Chapter 3 Interplay of Interoceptive and Exteroceptive Processing: Investigating Cardiac Dynamics in Motion-Induced Blindness

Aishwarya Bhonsle[1,2] and Melanie Wilke[1,2,3*]

[1.] Department of Cognitive Neurology, University Medical Center Göttingen, Göttingen, Germany

[2.] MR-Research in Neurosciences, University Medical Center Göttingen, Göttingen, Germany

[3.] Cognitive Neurology Group, Department of Cognitive Neuroscience, German Primate Center, Leibniz Institute for Primate Research, Göttingen, Germany

*Corresponding author:

Prof. Dr. Melanie Wilke, Department of Cognitive Neurology, Heart & Brain Center, University Medicine Göttingen, Robert-Koch-Strasse 42, 37073 Göttingen, Germany

Email: melanie.wilke@med.uni-goettingen.de

3.1 Abstract

Interoception, the brain's processing of internal bodily signals, and exteroception, the perception of external stimuli, interact dynamically to shape conscious perception. Theoretical frameworks propose that these interactions may reflect either a competition for attentional resources or facilitation through integration. Here, we investigated this interplay in the context of motion-induced blindness (MIB), a multistable perception paradigm. We examined whether exercise-induced changes in heart rate modulate MIB dynamics and whether heartbeat-evoked potentials (HEPs), an index of cardiac interoception, reflect perceptual suppression or response registration. Participants performed the MIB task under three exercise-intensity conditions: rest, low-resistance cycling, and high-resistance cycling. Neither the duration nor the rate of perceptual suppression in MIB was influenced by exercise intensity or by increased heart rates. Stimulus-locked analyses of HEPs in a Replay condition revealed significantly lower amplitudes during physical target removal compared to target presence, indicating interoceptive processing differences during the physical presence and absence of a stimulus. However, response-locked analyses of HEPs for both MIB and Replay conditions revealed no significant differences. This study underscores the complexity of interoceptive-exteroceptive interactions and the challenges of disentangling these dynamics, especially within multistable perception paradigms.

3.2 Introduction

The brain receives and processes signals both from the external environment (exteroception) and the body (interoception). Interoceptive signals, such as those generated by the heart, can influence the processing of exteroceptive stimuli (Engelen et al., 2023; Tallon-Baudry, 2023). Individuals with lower heart rates have been shown to exhibit enhanced visual stimulus detection (Sandman et al., 1977). Additionally, cardiac activity adapts in response to environmental demands and interacts with higher-order processing, including perception. For example, in forewarned perceptual reaction-time tasks (Jennings & Wood, 1977; B. C. Lacey & Lacey, 1974, 1980; J. I. Lacey, 1967; Somsen et al., 2004) or threshold detection tasks (Cobos et al., 2019; Motyka et al., 2019;

Grund et al., 2022; Park et al., 2014), heart rate decelerates in anticipation of an upcoming stimulus following a warning cue and accelerates again after stimulus detection or response registration. This pattern of deceleration followed by acceleration reflects the central regulation of heart rate through reciprocal parasympathetic and sympathetic activity that is thought to fine-tune the balance between interoceptive and exteroceptive processing in response to situational demands (Skora et al., 2022).

One perspective is that baroreceptor activity, which relays information about cardiac contractions to the brain, inhibits exteroceptive processing (B. C. Lacey & Lacey, 1974; J. I. Lacey, 1967; J. I. Lacey & Lacey, 1958, 1970), as interoceptive and exteroceptive signals compete for attentional resources (Berntson & Khalsa, 2021; Critchley & Garfinkel, 2018; Skora et al., 2022). Cardiac deceleration, driven by parasympathetic activity, might therefore reflect enhanced attention to external stimuli, playing a role in optimising sensory processing (Skora et al., 2022). Supporting this idea, cardiac deceleration has been shown to track active attention during binocular rivalry, linking heart rate dynamics to visual sensitivity (Corcoran et al., 2021). Conversely, cardiac acceleration, indicative of sympathetic dominance, is proposed to restore the balance between interoception and exteroception, preparing the system for action (Skora et al., 2022).

Among studies reporting this deceleration-acceleration pattern, some have found that cardiac deceleration is more pronounced preceding stimulus detection compared to when no detection occurs (Cobos et al., 2019; Motyka et al., 2019), while others have observed less pronounced cardiac acceleration following stimulus detection when the stimulus is missed rather than detected (Grund et al., 2022; Park et al., 2014). Thus, cardiac responses are theorised to be dynamically regulated to align with environmental and bodily demands, reflecting an attentional trade-off framework in which interoception and exteroception compete for limited resources (Berntson & Khalsa, 2021; Critchley & Garfinkel, 2018; Skora et al., 2022).

Another, diametrically opposed perspective is that interoceptive processing facilitates exteroceptive processing, either directly or indirectly. Direct facilitation may occur through

combining interoceptive and exteroceptive inputs to produce larger responses than the sum of their individual effects (Engelen et al., 2023; Park & Blanke, 2019a; Stein & Stanford, 2008). Indirect facilitation, on the other hand, is thought to arise through the generation of a sense of experiential (Tallon-Baudry et al., 2018), emotional (Damasio, 2010), or bodily (Park & Blanke, 2019a; Seth, 2013) self, providing a framework for integrating and interpreting exteroceptive signals. Preliminary evidence for the facilitation of exteroceptive processing by interoception comes from research on heartbeat-evoked potentials (HEP). The HEP is a transient neural signal time-locked to a heartbeat and is considered an index of cardiac interoceptive processing (Coll et al., 2021; Gray et al., 2007; Park & Blanke, 2019b; Schandry & Montoya, 1996). A study demonstrated that higher HEP amplitude predicted conscious perception of visual stimuli presented at threshold, suggesting that increased interoceptive processing coincides with enhanced visual sensitivity (Park et al., 2014). However, contrasting findings from another study using somatosensory stimuli presented at threshold showed the opposite pattern, where increased HEP amplitude was associated with reduced sensory detection (Al et al., 2020). These differences may reflect how attentional resources are allocated to interoception depending on the sensory modality being processed (Al et al., 2020).

To better understand the interaction between interoception and exteroception, our study seeks to address two key gaps in the existing literature. First, previous research has largely relied on threshold paradigms (Al et al., 2020; Cobos et al., 2019; Park et al., 2014), which involve the detection of stimuli at the edge of perceptual awareness. In contrast, we focus on motion-induced blindness (MIB), a multistable perception paradigm in which salient stimuli are intermittently suppressed from awareness (Bonneh et al., 2001). While phasic changes in heart rate leading to perceptual changes have been studied in the context of multistable perception (Corcoran et al., 2021), such paradigms have not been investigated under conditions of sustained changes in heart rate.

In the first part of our study, we address this gap by employing cycling as an intervention to increase heart rate and therefore, modulate interoceptive signals. This allows us to investigate the dynamic balance between interoceptive and exteroceptive processing,

specifically under an altered physiological state of sympathetic dominance and to examine how these changes influence the dynamics of perceptual suppression in MIB. Based on the attentional trade-off framework, we hypothesize that sustained increases in heart rate during cycling will enhance interoceptive processing at the expense of exteroception, resulting in longer disappearance durations and increased rates of perceptual suppression. Alternatively, if interoceptive signals facilitate exteroceptive processing, we predict that higher heart rates will be associated with shorter disappearance durations and decreased suppression, reflecting enhanced integration of interoceptive and exteroceptive inputs.

The second gap we address concerns the role of heartbeat-evoked potentials (HEPs) in interoceptive-exteroceptive dynamics. While HEPs have been studied in the pre-stimulus period (Al et al., 2020; Park et al., 2014), their role during perceptual changes or after response registration remains unexplored. Thus, in the second part of our study, we examine HEPs concurrently with physical stimulus changes, subjective perceptual changes and following response registration. If interoception and exteroception compete for attentional resources, we hypothesize that HEP amplitudes will be higher during perceptual suppression, reflecting increased interoceptive processing and therefore, potentially decreased attention to exteroceptive signals. Conversely, if interoceptive signals facilitate exteroceptive processing, we predict lower HEP amplitudes during perceptual suppression.

3.3 Methods

3.3.1 Participants

Thirty-six healthy volunteers were initially recruited for the current study. Eligibility criteria required participants to be generally healthy, have no history of neurological, psychological, cardiovascular, respiratory, metabolic, endocrine, immune, or substance abuse disorders. Participants were also ineligible if they were taking regular medications that might alter cardiovascular, autonomic, or cognitive functioning, were pregnant, or concurrently participating in pharmacological or stimulation studies. All subjects were also

required to have normal or corrected-to-normal vision. Of the initial cohort, one subject was excluded for not following the task instructions and three did not complete the study session. In this experiment, trials were defined based on subjects' subjective reports of target disappearance and visibility (see the **Trial extraction** section **below**). Six subjects were excluded due to an insufficient number of target disappearance/reappearance reports, with fewer than 20 trials defined based on their responses during the experimental task. The final cohort consisted of 26 subjects (15 male, 11 female; mean age $\pm$ SD: 25.23 $\pm$ 4.88 years, age range: 21 – 46 years). For the ECG and HEP analyses, two subjects were excluded due to poor ECG data quality, resulting in a final sample of 24 subjects for these analyses. The study was conducted in accordance with the ethical guidelines of the Declaration of Helsinki. The experimental procedure was approved by the ethics committee of University Medicine Göttingen (UMG, Germany). All subjects gave written informed consent before the study and were paid for their participation.

3.3.2 Stimuli and task

The visual stimuli were programmed in MATLAB R2015b (The MathWorks Inc., Natick, MA, USA) using Psychtoolbox-3 (Brainard, 1997; Kleiner et al., 2007). The target was a salient yellow disc (full contrast, diameter: 0.1° of visual angle), surrounded by a moving mask (square, equally spaced grid of 9 × 9 full-contrast blue crosses, 17° width/length; **Figure 3-1A**). Both stimuli and a central fixation mark (red outline, white inside, 0.8° in width and length) were superimposed on a black background. The target was located on the bottom right visual field diagonal at an eccentricity of 7°. The mask rotated around the fixation square (speed: 120°/s), and the direction of rotation was randomised over runs to reduce motion after-effects (McEwen et al., 2020). The target was separated from the mask by a black "protection zone" subtending about 0.5° around the target. These stimulus parameters were chosen to yield high percentages of target invisible time across subjects.

The MIB stimulus was continuously presented for several runs of 2-minute duration each, with a blank screen presented for 30 seconds as the inter-run interval. The subjects were

instructed to maintain stable fixation and to report the spontaneous disappearance and reappearance of the target by pressing or releasing a response button (4 Button Curve Right; Current Designs Inc., Philadelphia, PA, USA) with their index finger (left or right, counterbalanced across subjects). The mapping between perceptual switch and motor response was also counterbalanced across subjects: button press for indicating target disappearance (release for reappearance) or button release for disappearance (press for reappearance), both for as long as the percept did not switch again.

A Replay run in which the target was intermittently physically removed from the screen was randomly intermixed with the MIB runs. The timing and durations of these physical removals corresponded to actual disappearances reported during one of the previous MIB runs completed by the corresponding subject. The physical removals of the target were instantaneous, consistent with the typically abrupt perceptual switches in MIB runs.

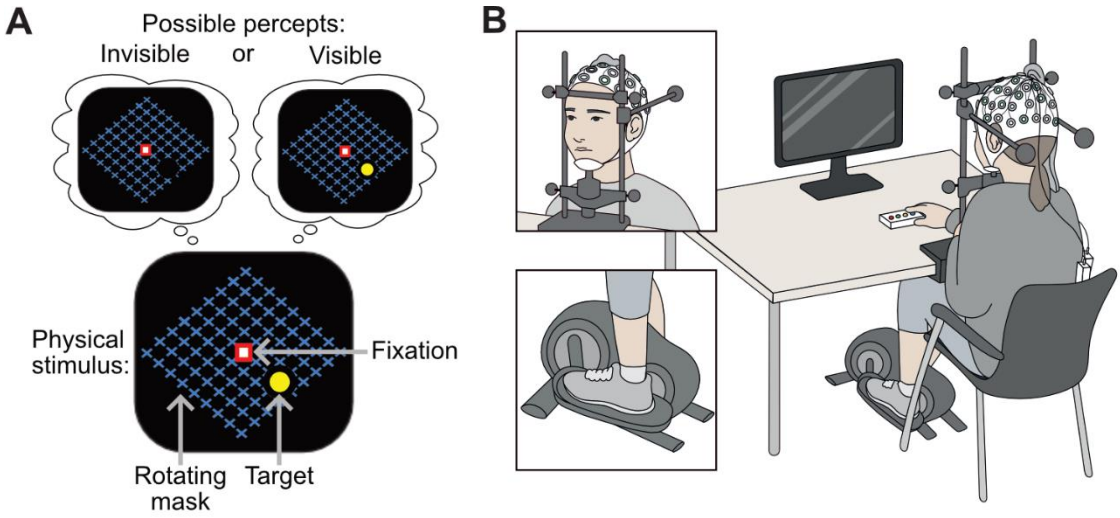

Figure 3-1 – Motion Induced Blindness (MIB) run schematic and experimental setup

(**A**) Stimulus configuration of the MIB trials. A small but salient yellow target was presented on the bottom-right visual field diagonal and was surrounded by a rotating grid of blue crosses on a black background. The perception of the target alternated: it was either visible (VIS) or rendered invisible (INV). (**B**) The experimental setup consisted of the subject seated at a desk facing a computer screen where the task was presented. They reported their perceptual responses using a button box placed on the desk. Their head was positioned on a chin rest, and stabilised by positioning supports on either side and against their

forehead (top inset). During the cycling blocks, they cycled using an ergometer placed under the desk (bottom inset). ECG and EEG data were recorded simultaneously.

The subjects performed the perceptual task under three exercise-intensity conditions: at rest (R), and during low-resistance (L) or high-resistance cycling (H). The two cycling conditions were performed using an ergometer (Sportstech DFX100; Sportstech, Berlin, Germany) placed under the desk. According to the American College of Sports Medicine guidelines (Garber et al., 2011) on exercise intensity, categorised by percentage of maximal heart rate (HRmax, estimated by the formula $211 - 0.64 \times \text{age}$) (Nes et al., 2013) the low-resistance condition would be classified as very light (<50% HRmax), while the high-resistance condition would be classified as light (50-60% HRmax) intensity.

Each rest block comprised 3 MIB runs, and each cycling block comprised 4 MIB runs. Regardless of block type, there was always one Replay run intermixed among the MIB runs. Each cycling block started with an initial 3-minute warm-up period during which participants were instructed to establish a cadence of 60 rotations per minute (rpm), guided by an on-screen clock displaying seconds to help them match the pace. When the clock was replaced by the perceptual task, participants were instructed to maintain this cadence of 60 rpm to the best of their abilities until the end of the block.

3.3.3 Experimental procedure

The study was conducted in a single session lasting 3 to 3.5 hours in total. Participants were instructed to abstain from caffeine, alcohol, or other mind-altering substances for 3 to 4 hours prior to the session, and from heavy alcohol consumption for 24 hours before the session. Prior to the experiment, participants completed a demographic survey and questionnaires to assess physical activity (IPAQ) (Craig et al., 2003) and interoceptive awareness (MAIA) (Mehling et al., 2012). In this experiment, EEG and ECG data were recorded simultaneously. Breathing data were recorded using a respiration belt measuring thoracic/abdominal movements (Respiration Belt MR; Brain Products GmbH, Gilching, Germany) but was not analysed in the context of this paper. Following EEG and ECG preparation, an 8-minute baseline recording with eyes closed was taken, with blood

pressure measured at the 7-minute mark. Participants were instructed on how to perform the task and proceeded to perform the experiment.

Subjects performed the task in a sound-insulated cabin with a Faraday cage. They were seated in front of a 60 × 34 cm computer screen with a resolution of 1920 × 1080 pixels and a 60 Hz refresh rate (BenQ XL2411T; BenQ, Taipei, Taiwan), at an eye-to-screen distance of 70 cm (**Figure 3-1B**). They placed their head on a chin rest, and it was stabilised by positioning supports on each side of the head and one to lean their forehead against (HeadLock Ultra Precision Head Positioner; Arrington Research, Scottsdale, AZ, USA). The lights in the cabin were turned off during the experiment.

The experiment consisted of seven blocks, with cycling and rest blocks interleaved in one of two sequence orders: either L-R-H-R-L-R-H or H-R-L-R-H-R-L, randomly assigned for each participant. Subjects were allowed adequate breaks between blocks, and special care was taken to allow heart rates to return to baseline after each cycling block. Baseline heart rate was defined as the rate observed during the initial baseline recording and blood pressure measurement. Live heart rate was monitored throughout the breaks using an armband (TikrFit; Wahoo Fitness, Atlanta, GA, USA). After the experimental blocks, another 8-minute baseline recording with eyes closed was taken.

3.3.4 Behavioural analysis

All behavioural, ECG, and EEG analyses were performed using custom-written scripts in MATLAB R2015b (The MathWorks Inc., Natick, MA, USA), and all statistical analyses were conducted in SPSS Statistics for Windows, Version 27.0 (IBM Corp., Armonk, NY, USA).

The percentage of target invisible time was calculated by summing all of a subject's disappearance durations within a run and determining what percentage of the total MIB run time they constituted. This metric was used to confirm that the illusion was working effectively, with a target invisible time of at least 20%, generally considered indicative of a robust MIB effect (Kloosterman et al., 2015).

The disappearance duration for each disappearance report in a MIB run was calculated by subtracting the time of the disappearance report from the time of the subsequent reappearance report. The disappearance rate for a given MIB run was determined by dividing the number of disappearance reports in the run by the duration of the run.

The assumption of normality for these metrics was assessed using the Shapiro-Wilk test, and sphericity was evaluated using Mauchly's test. To test the effect of exercise intensity (levels: rest, low-resistance cycling, and high-resistance cycling) on disappearance duration, disappearance rate, and percentage of target invisible time, repeated-measures ANOVAs (RM ANOVAs) were conducted. Partial eta-squared (η_p^2) was calculated as the effect size for all repeated-measures ANOVAs. If the ANOVAs revealed significant effects, *post hoc* Bonferroni-corrected pairwise comparisons were performed to examine differences between levels of the within-subjects factors.

3.3.5 ECG acquisition, preprocessing, and average heart rate analysis

The ECG montage used in this study was inspired by Petzschner et al., 2019. Two ECG signals were acquired using two electrodes placed on the left and right clavicle (active electrodes), two electrodes placed at the left and the right hip/abdomin (reference electrodes), and a ground electrode placed between the shoulder blades (BrainAmp ExG; Brain Products GmbH, Gilching, Germany). The second ECG (left clavicle – right hip) served as a back-up in case the signal quality of the first ECG (right clavicle – left hip) was too low for reliable R-peak or T-wave detection. In the current dataset, the first ECG signal was of high quality for all participants; therefore, the second ECG was not used in this analysis. R-peaks were identified using the Pan and Tompkins algorithm (Pan & Tompkins, 1985), using code modified from Sedghamiz, 2014. The peaks of the P wave, Q wave, S wave, and T wave were identified using a custom-written code implementing the method proposed in Leutheuser et al., 2016 for detection of these four fiducial points. The end of the T wave was determined using a custom code implementing a trapezoidal area algorithm (Vázquez-Seisdedos et al., 2011), and was also adapted for detection of the beginning of the P wave.

The average heart rate for a given condition was obtained by dividing 60 by the mean of all inter-beat intervals (the distance between two R-peaks). To examine the effect of exercise intensity (levels: rest, low-resistance cycling, and high-resistance cycling) on heart rate, a Friedman test was conducted, as the data violated the assumption of normality. Kendall's *W* was reported as a measure of effect size for the Friedman test. *Post hoc* pairwise comparisons were performed using Wilcoxon signed-rank tests, with Bonferroni correction applied to control for multiple comparisons. Rank-biserial correlation (*r*) was calculated as the effect size for the Wilcoxon signed-rank tests.

To examine the relationships between percent changes in heart rate and percent changes in disappearance duration, as well as percent changes in heart rate and percent changes in disappearance rate (calculated as the percent change from rest for each cycling condition), Kendall's tau-b correlation coefficients were computed.

3.3.6 EEG acquisition and preprocessing

EEG activity was recorded from 64 electrodes distributed over the head according to the international 10-20 system (actiCap Snap, BrainAmp MR, BrainVision Recorder; Brain Products GmbH, Gilching, Germany). Electrode impedances were kept below 20 kΩ throughout the experiment. The data were recorded at a sampling rate of 1000 Hz.

EEG data were preprocessed and analysed using the FieldTrip toolbox (Oostenveld et al., 2011). The data were down-sampled to 256 Hz and band-pass filtered between 0.5 and 110 Hz. A band-stop filter was applied to remove 50 Hz line noise. The continuous data were then segmented into trials (see the **Trial extraction** section **below**). Trials containing muscle artifacts, jumps or clipping artifacts were identified automatically, visually inspected and then rejected when necessary. An independent component analysis (ICA) was performed to identify eye movement related artifacts and the relevant components were removed. The data were then re-referenced to a common average reference. If there were noisy channels that required interpolation, they were removed before the data were re-referenced. They were then interpolated with the re-referenced data.

3.3.6.1 Trial extraction

For both the MIB and Replay conditions involving subjects' reports, we extracted trials based on subjects' button presses or releases, from the 2-min runs of continuous stimulus presentation. Therefore, in this context, the term "trial" refers to an epoch of constant stimulation defined by subjects' subjective reports of target disappearance and reappearance. The following constraints were used for trial extraction to avoid mixing data segments from different percepts when averaging across trials: 1) the maximum trial duration was 1.5 s following the report; 2) when another report occurred within this interval, no trial was defined. For the Replay condition, only reports that were preceded by a physical change of the target stimulus within 0.2 s to 1 s were included, thus discarding those following spontaneous target disappearances. For an additional analysis, trials for the Replay condition were defined similarly but aligned to physical target stimulus on- and offsets instead of behavioural reports. The report-locked trials aimed to investigate post-report modulations in HEPs, while the stimulus-locked Replay trials focused on HEP modulations associated with physical target changes.

3.3.7 Heartbeat-evoked potentials analysis

HEPs were computed on EEG signals locked to the T-peak of the ECG. Trials with T-peaks occurring at least 600 ms after report onset (MIB and Replay trials) or physical target on/offsets (Replay trials) up to 400 ms before the end of the trial were chosen. The EEG signals were segmented from 600 ms before the T-peak to 400 ms after the T-peak, baseline corrected based on a -600 ms to -500 ms time window relative to the T-peak, then averaged to generate the T-locked responses to heartbeats. Choosing T-peaks in this window ensured that neither the HEP nor the baseline window was contaminated by report or physical on/offsets. The HEP analysis was conducted only for the rest condition to avoid potential contamination of the HEP window by elevated heart rates during cycling.

A 200 ms to 400 ms post-T-peak time window was chosen to ensure HEPs submitted for further statistical analysis were free from cardiac electrical artifacts. HEP data from all electrodes in the selected window were submitted to a cluster-based permutation *t*-test

(Maris & Oostenveld, 2007) as implemented in the FieldTrip toolbox (Oostenveld et al., 2011). These tests compared the HEP amplitudes between perceptual conditions (target visible vs. target invisible) for all three trial types: report-locked MIB trials, report-locked Replay trials, and stimulus-locked Replay trials. The Monte-Carlo method was used to generate the permutation distribution by randomly shuffling the condition labels 5000 times to calculate cluster-level statistics. Clusters were formed based on a *t*-statistic threshold of $p < 0.05$, with adjacent electrodes considered neighbours. Significant differences in clusters were identified if the cluster-level *p* value, corrected using the maximum cluster sum statistic, was below 0.05. For any significant clusters identified by the cluster-based permutation tests, the average HEP amplitudes over the electrodes and time points within the cluster were extracted. These average amplitudes were then submitted to paired samples *t*-tests to further validate the observed differences between perceptual conditions (target visible vs. target invisible).

3.3.7.1 Control analyses for possible effects of cardiovascular artifacts

HEPs represent neural responses to cardiac signals but can also include cardiac field artifacts and pulse-related artifacts (Kern et al., 2013). One commonly used approach to mitigate any associated volume conduction effects of these artifacts is independent component analysis (ICA). However, this approach has been criticised for its limited ability to completely eliminate the cardiac field artifacts and for the potential risk of removing task-related signals (Petzschner et al., 2019). To ensure that the observed effects in HEP amplitudes were not due to differences in cardiac electrical activity directly affecting EEG data by volume conduction, we submitted the mean ECG amplitudes to the same cluster-based permutation tests as the observed effects.

3.4 Results

3.4.1 Behavioural analysis

A defining characteristic of MIB disappearances, like other multistable illusions, is the unpredictable variation in the duration of each percept between consecutive perceptual transitions, as demonstrated by the average frequency distributions of target invisible and

target visible durations (**3.7 Supplementary Information**, **Figure S3-1**). The average percentage of target invisible time across conditions was 23.41% ± SEM 2.73%, indicating that the illusion worked effectively. There was no significant effect of exercise intensity on the percentage of target invisible time ($F(2, 50) = 0.16$, $p = 0.86$, $\eta_p^2 = 0.01$).

We examined whether exercise intensity influenced the duration and rate of target suppression/disappearance in MIB runs (**Figure 3-2**). No significant differences were observed for either the duration ($F(2, 50) = 0.76$, $p = 0.47$, $\eta_p^2 = 0.03$; **Figure 3-2A**) or the rate ($F(2, 50) = 0.22$, $p = 0.80$, $\eta_p^2 = 0.01$; **Figure 3-2B**) of target disappearance across the three exercise intensity conditions. The average disappearance duration across the conditions was 1.46 ± 0.10 s (mean ± SEM), and the average disappearance rate was 0.16 ± 0.02 events per minute (mean ± SEM).

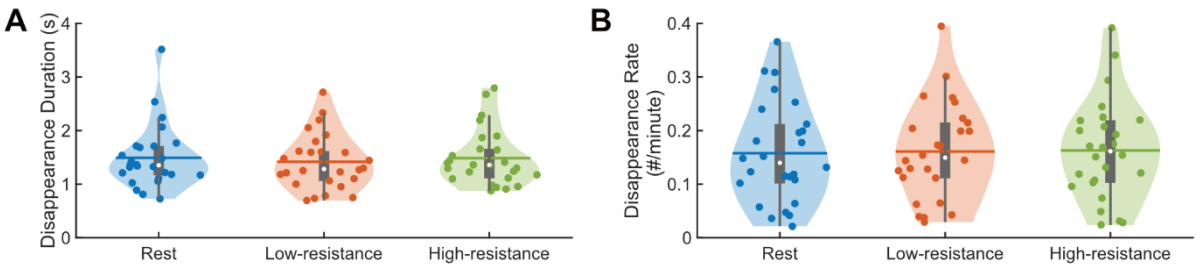

Figure 3-2 – Disappearance duration and rate remain consistent across rest and cycling conditions

Violin plots showing the mean (**A**) disappearance durations and (**B**) disappearance rate in MIB trials performed at rest (blue), low-resistance (orange), and high-resistance (green) cycling. For both panels, vertical grey boxes indicate the interquartile range (IQR), with grey whiskers indicating 1.5 x IQR, surrounded on each side by the kernel density estimation in the colour corresponding to each group. Horizontal lines in the colour corresponding to each group denote means and white dots indicate medians. Each dot in a given condition represents the average value of a single subject. *N* = 26 for all plots.

3.4.2 Heart rate analysis

Examining the effect of exercise intensity on heart rate (**Figure 3-3A**) revealed a significant effect of exercise intensity ($\chi^2(2) = 42.75$, $p = 5.21\times10^{-10}$, Kendall's W = 0.89). *Post hoc* pairwise comparisons showed significant increases in heart rate from rest to

low-resistance cycling (Z = -4.29, p = 5.46×10^{-5}, r = 0.87), from rest to high-resistance cycling (Z = -4.29, p = 5.46×10^{-5}, r = 0.87), and from low- and high-resistance cycling (Z = -3.63, p = 8.55×10^{-4}, r = 0.74), confirming the efficacy of the exercise intervention.

We further investigated whether these increases in heart rate were associated with changes in disappearance duration (**Figure 3-3B** and **C**) and rate (**Figure 3-3D** and **E**) for the two cycling conditions compared to rest, however no significant correlations were observed (all ps > 0.05).

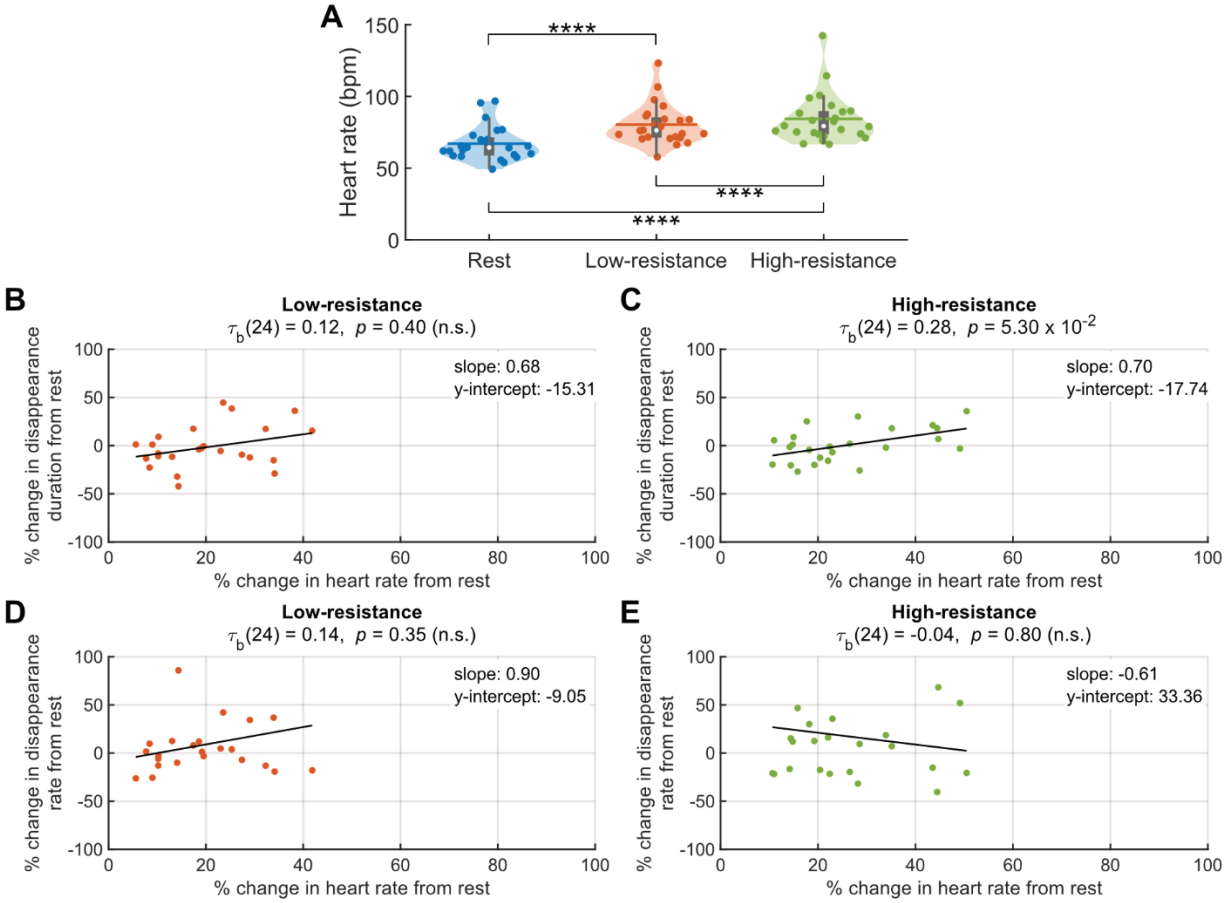

Figure 3-3 – Heart rate increases during cycling conditions, while changes in disappearance duration and rate remain uncorrelated with changes in heart rate

(**A**) Violin plots showing the average heart rate during the MIB runs performed at rest (blue), low-resistance (orange), and high-resistance (green) cycling. Statistical significance between the conditions as assessed by Bonferroni-corrected Wilcoxon signed-rank tests is indicated at the $p \leq 0.0001$ (****) level. Vertical grey boxes indicate the interquartile range (IQR), with grey whiskers indicating 1.5 x IQR,

surrounded on each side by the kernel density estimation in the colour corresponding to each group. Horizontal lines in the colour corresponding to each group denote means, and white dots indicate medians. Each dot in a given condition represents the average value of a single subject. Correlations as assessed by Kendall's Tau-b between percent change in heart rate from rest and percent change in disappearance duration from rest for (**B**) low-resistance and (**C**) high-resistance cycling. Correlations between percent change in heart rate from rest and percent change in disappearance rate from rest for (**D**) low-resistance and (**E**) high-resistance cycling. No correlations are significant. *N* = 24 for all plots.

3.4.3 Heartbeat-evoked potentials analysis

We examined whether neural processing of heartbeats is altered following a physical target change using a stimulus-locked analysis of the Replay condition (**Figure 3-4A** and **B**). Additionally, we examined whether cardiac interoceptive processing is altered concurrently with perceptual suppression and/or following response registration, a response-locked analysis of the MIB (**Figure 3-4C**) and Replay (**Figure 3-4D**) conditions. For each analysis, a 100 to 400 ms post-T peak time window for the visible and invisible conditions was submitted to a cluster-based permutation *t*-test. HEP amplitudes significantly differed between the visible and invisible (physical target removal) conditions in the stimulus-locked analysis of the Replay condition (**Figure 3-4A**) over temporal, parietal, and occipital electrodes in a 189 to 279 ms post-T peak time window (cluster-level statistic = 392.06, $p = 0.04$, $N = 24$; **3.7 Supplementary Information**, **Figure S3-2**). The HEP amplitudes were lower when the target was physically removed (invisible) compared to when the target was visible ($t(24) = 2.50$, $p = 0.02$, Cohen's $d = 0.51$; **Figure 3-4B**).

Control analyses comparing the ECG waveforms for visible and invisible conditions revealed no significant differences (**3.7 Supplementary Information, Figure S3-3**), confirming that the observed HEP differences in the stimulus-locked Replay analysis were not attributable to cardiac electrical activity.

Response-locked HEP analyses of both MIB and Replay conditions revealed no significant differences between the visible and invisible conditions in either MIB (smallest

cluster-level p = 0.11; **Figure 3-4C**) or Replay (smallest cluster-level p = 0.49; **Figure 3-4D**) trials.

In sum, these results suggest that cardiac interoceptive processing differs between the physical presence and absence of a target, but no significant differences are observed between subjective disappearances and reappearances or following response registration.

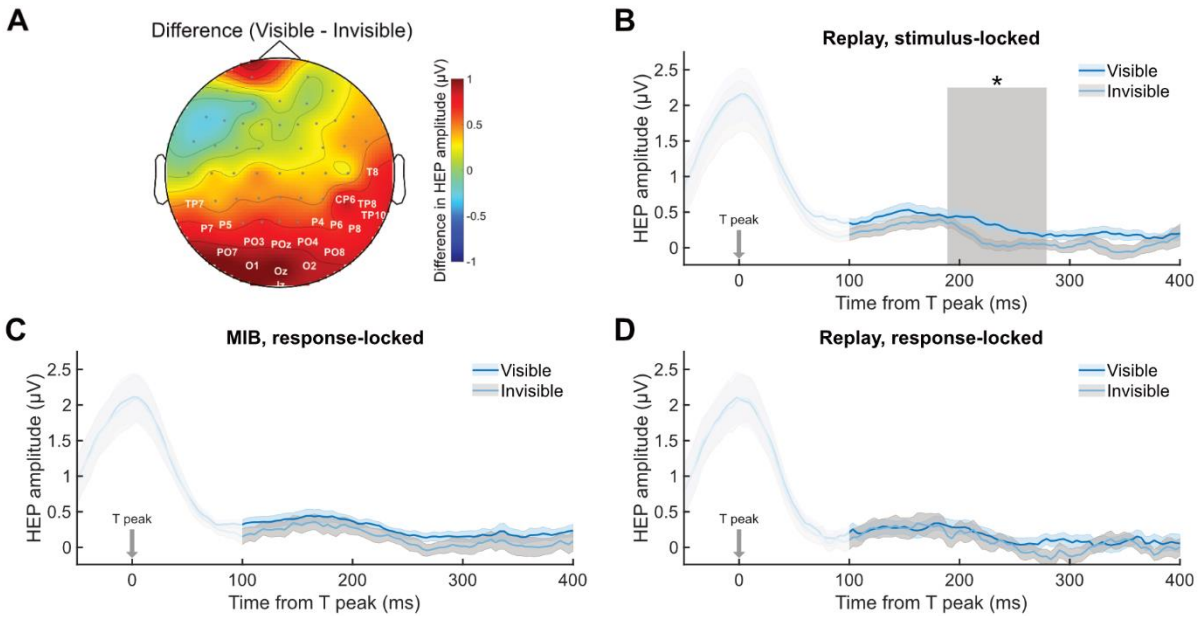

Figure 3-4 – HEP amplitude is reduced during physical target removal compared to when the target remains visible, while response-locked analyses show no differences for physical target removals or spontaneous target disappearances

(**A**) Topographical map of heartbeat-evoked potential (HEP) amplitude difference between conditions where the target remains visible and where the target is physically removed (invisible) for the stimulus-locked analysis of the Replay condition, over the 189 to 279 ms post-T peak time window during which a statistically significant difference was observed. White labels indicate the channels contributing to the significant cluster. (**B**) HEP time courses averaged across the cluster for the visible and invisible conditions in the stimulus-locked analysis of the Replay condition. The shaded areas denote the SEM for each time course. The grey bar highlights the time window in which a significant difference was observed at the $p \leq 0.05$ (*) level. HEP time courses averaged across the cluster for the visible and invisible condition in the response-locked analyses of (**C**) MIB trials and (**D**) Replay trials. The signal contaminated by T-wave cardiac artifact, prior to +100 ms, appears in lighter colour for all HEP time courses. N = 24 for all plots.

3.5 Discussion

This study investigated the interplay between interoception and exteroception by examining the effects of exercise-induced changes in heart rate on MIB dynamics. Our findings revealed no significant effects of exercise intensity on MIB disappearance duration or rate. Contrary to our hypotheses, sustained increases in heart rate during cycling did not influence the dynamics of perceptual suppression in MIB either. These null findings challenge the interoceptive-exteroceptive attentional trade-off framework and nor do they support the proposal of interoceptive facilitation of exteroception in the context of multistable perception paradigms like MIB. A similar lack of effect has been reported in a study examining presence detection in a backward masking paradigm, where the absence of an effect during exercise was attributed to this aspect of visual perception relying on neural mechanisms that are not modulated by acute exercise (Komiyama et al., 2023), although the same study observed an exercise-linked increase in feature detection. Similarly, it is possible that perceptual suppression in MIB depends on neural processes that are not readily influenced by moderate changes in physiological states, such as those induced by light-intensity cycling. Alternatively, the sustained heart rate changes and sympathetic dominance during cycling might overshadow subtle interoceptive effects contributing to perceptual suppression. These effects might be better captured by phasic changes, such as the cardiac deceleration-acceleration pattern observed in threshold detection paradigms (Cobos et al., 2019; Grund et al., 2022; Motyka et al., 2019; Park et al., 2014), and phasic cardiac dynamics should also be examined in the context of multistable paradigms like MIB.

Additionally, while significant HEP differences were observed during the stimulus-locked Replay condition, with lower amplitudes during target disappearance, no significant HEP differences emerged in the response-locked analyses for either the MIB or the Replay conditions. These results suggest that cardiac interoceptive processing may differ during the physical change of a target but appears unaltered following subjective perceptual changes/response registration. The stimulus-locked analysis captures interoceptive processing slightly earlier than the report-locked analysis, perhaps better reflecting the neural dynamics associated with perceptual decisions about the stimulus. In contrast, the

response-locked analysis likely cannot disentangle the neural processing concurrent with perceptual suppression from the processing associated with post-response registration. This overlap might obscure any distinct interoceptive contributions during perceptual suppression, explaining the absence of significant HEP differences in the response-locked analyses. The post-decisional cardiac acceleration observed in threshold detection tasks is thought to indicate a restoration of the balance between interoceptive and exteroceptive processing (Skora et al., 2022). Likewise, the absence of significant differences in response-locked HEP analyses might suggest that the interoceptive-exteroceptive balance normalizes after response registration, resulting in similar HEP responses regardless of the perceptual change just reported. It is also possible that our study was underpowered to detect subtle effects of cardiac interoception on perceptual suppression. Capturing small true effects in proxies of cardiac interoception, such as HEP amplitudes or heart rate changes, may require larger sample sizes or more sensitive methods (Coll et al., 2021).

The possibility that cardiac-related fluctuations in perception are epiphenomenal, arising as a byproduct of physiological and anatomical constraints, rather than being functionally adaptive, may also help explain the inconsistencies in findings about the role of interoception in exteroceptive processing. If interoceptive signals, such as those indexed by HEPs, do not actively influence exteroceptive perception but rather reflect inherent physiological rhythms, this could lead to variability across studies depending on task paradigms, measurement approaches, or individual differences. For instance, studies showing facilitation of exteroceptive processing by interoception may capture coincidental alignment of physiological and perceptual rhythms, while others reporting competition may reflect specific task demands or contexts that amplify attentional trade-offs. These inconsistencies highlight the need for further comparative investigations across sensory modalities and experimental paradigms to disentangle whether interoceptive contributions to perception are mechanistic or merely reflective of underlying biological constraints.

Additionally, other physiological factors, such as arousal and breathing, might play a role in modulating the interplay between interoception and exteroception. For instance, changes in arousal levels during cycling could influence attention allocation and perceptual suppression independently of heart rate (Kuwamizu et al., 2022). Similarly, respiration is tightly linked to both cardiac and neural activity and may modulate interoceptive and exteroceptive processes (Molle & Coste, 2022; Parviainen et al., 2022). Incorporating measures of arousal and respiration in future research could provide a more complete understanding of the physiological underpinnings of perceptual dynamics.

It is important to note that the conclusions drawn in this study are inherently indirect. While changes in heart rate and HEP amplitudes provide valuable insights into the interplay between interoception and exteroception, these measures serve as proxies for underlying physiological mechanisms, such as baroreceptor activity. As baroreceptor influences on central sensory processing were not directly measured, any interpretation regarding their role in modulating perceptual suppression or interoceptive-exteroceptive interplay remains speculative. Future studies employing direct measures of baroreceptor activity or pharmacological manipulations are needed to establish a more definitive link between cardiac signals and sensory processing.

Overall, this study highlights the complexity of the interoceptive-exteroceptive interplay and underscores the challenges of isolating these dynamics in the context of multistable perception paradigms. While our findings raise important questions about the functional role of cardiac interoception in perceptual processes, they also emphasize the need for a multifaceted approach integrating physiological, neural, and behavioural measures to unravel the intricate mechanisms governing interoceptive-exteroceptive interplay.

Author contributions / CRediT statement

Aishwarya Bhonsle: Conceptualization; Data curation; Formal analysis; Investigation; Methodology; Software; Visualization; Writing – original draft; Writing – review & editing

Melanie Wilke: Conceptualization; Methodology; Resources; Supervision; Writing – review & editing, Funding acquisition

Funding information

This research was supported by the Hermann and Lilly Schilling Foundation, the Else-Kröner-Fresenius Foundation and the DFG GRK 2824: 'Heart and Brain Diseases' (to M.W.)

Conflict of interest statement

The authors declare no conflicts of interest.

Acknowledgements

We would like to thank Greta Wippich for the illustration of the experimental setup; Sukanya Chakraborty and Ege Kingir for help with piloting the experiment; Sarah-Denise De Buhr for help with data collection; Severin Heumüller for providing technical support; Ulrich Parlitz and Roberto Goya-Maldonado for helpful discussions.

ORCID

Aishwarya Bhonsle https://orcid.org/0000-0002-7848-3845

Melanie Wilke https://orcid.org/0000-0002-2883-6593

3.6 References

Al, E., Iliopoulos, F., Forschack, N., Nierhaus, T., Grund, M., Motyka, P., Gaebler, M., Nikulin, V. V., & Villringer, A. (2020). Heart–Brain Interactions Shape Somatosensory Perception and Evoked Potentials. *Proceedings of the National Academy of Sciences*, *117*(19), 10575–10584. https://doi.org/10.1073/pnas.1915629117

Berntson, G. G., & Khalsa, S. S. (2021). Neural Circuits of Interoception. *Trends in Neurosciences*, *44*(1), 17–28. https://doi.org/10.1016/j.tins.2020.09.011

Bonneh, Y. S., Cooperman, A., & Sagi, D. (2001). Motion-Induced Blindness in Normal Observers. *Nature*, *411*(6839), 798–801. https://doi.org/10.1038/35081073

Brainard, D. H. (1997). The Psychophysics Toolbox. *Spatial Vision*, *10*(4), 433–436.

Cobos, M. I., Guerra, P. M., Vila, J., & Chica, A. B. (2019). Heart-Rate Modulations Reveal Attention and Consciousness Interactions. *Psychophysiology*, *56*(3), e13295. https://doi.org/10.1111/psyp.13295

Coll, M.-P., Hobson, H., Bird, G., & Murphy, J. (2021). Systematic Review and Meta-Analysis of the Relationship Between the Heartbeat-Evoked Potential and Interoception. *Neuroscience & Biobehavioral Reviews*, *122*, 190–200. https://doi.org/10.1016/j.neubiorev.2020.12.012

Corcoran, A. W., Macefield, V. G., & Hohwy, J. (2021). Be Still My Heart: Cardiac Regulation as a Mode of Uncertainty Reduction. *Psychonomic Bulletin & Review*, *28*(4), 1211–1223. https://doi.org/10.3758/s13423-021-01888-y

Craig, C. L., Marshall, A. L., Sjöström, M., Bauman, A. E., Booth, M. L., Ainsworth, B. E., Pratt, M., Ekelund, U., Yngve, A., Sallis, J. F., & Oja, P. (2003). International Physical Activity Questionnaire: 12-Country Reliability and Validity. *Medicine & Science in Sports & Exercise*, *35*(8), 1381. https://doi.org/10.1249/01.MSS.0000078924.61453.FB

Critchley, H. D., & Garfinkel, S. N. (2018). The Influence of Physiological Signals on Cognition. *Current Opinion in Behavioral Sciences*, *19*, 13–18. https://doi.org/10.1016/j.cobeha.2017.08.014

Damasio, A. (2010). *Self Comes to Mind: Constructing the Conscious Brain*. Knopf Doubleday Publishing Group.

Engelen, T., Solcà, M., & Tallon-Baudry, C. (2023). Interoceptive Rhythms in the Brain. *Nature Neuroscience*, *26*(10), 1670–1684. https://doi.org/10.1038/s41593-023-01425-1

Garber, C. E., Blissmer, B., Deschenes, M. R., Franklin, B. A., Lamonte, M. J., Lee, I.-M., Nieman, D. C., & Swain, D. P. (2011). Quantity and Quality of Exercise for Developing and Maintaining Cardiorespiratory, Musculoskeletal, and Neuromotor Fitness in Apparently Healthy Adults: Guidance for Prescribing Exercise. *Medicine & Science in Sports & Exercise*, *43*(7), 1334. https://doi.org/10.1249/MSS.0b013e318213fefb

Gray, M. A., Taggart, P., Sutton, P. M., Groves, D., Holdright, D. R., Bradbury, D., Brull, D., & Critchley, H. D. (2007). A Cortical Potential Reflecting Cardiac Function.

Proceedings of the National Academy of Sciences, *104*(16), 6818–6823. https://doi.org/10.1073/pnas.0609509104

Grund, M., Al, E., Pabst, M., Dabbagh, A., Stephani, T., Nierhaus, T., Gaebler, M., & Villringer, A. (2022). Respiration, Heartbeat, and Conscious Tactile Perception. *Journal of Neuroscience*, *42*(4), 643–656. https://doi.org/10.1523/JNEUROSCI.0592-21.2021

Jennings, J. R., & Wood, C. C. (1977). Cardiac Cycle Time Effects on Performance, Phasic Cardiac Responses, and Their Intercorrelation in Choice Reaction Time. *Psychophysiology*, *14*(3), 297–307. https://doi.org/10.1111/j.1469-8986.1977.tb01179.x

Kern, M., Aertsen, A., Schulze-Bonhage, A., & Ball, T. (2013). Heart Cycle-Related Effects on Event-Related Potentials, Spectral Power Changes, and Connectivity Patterns in the Human Ecog. *NeuroImage*, *81*, 178–190. https://doi.org/10.1016/j.neuroimage.2013.05.042

Kleiner, M., Brainard, D., Pelli, D., Ingling, A., Murray, R., & Broussard, C. (2007). What's New in Psychtoolbox-3. *Perception*, *36*(14), 1–16.

Kloosterman, N. A., Meindertsma, T., Hillebrand, A., van Dijk, B. W., Lamme, V. A. F., & Donner, T. H. (2015). Top-down Modulation in Human Visual Cortex Predicts the Stability of a Perceptual Illusion. *Journal of Neurophysiology*, *113*(4), 1063–1076. https://doi.org/10.1152/jn.00338.2014

Komiyama, T., Takedomi, H., Aoyama, C., Goya, R., & Shimegi, S. (2023). Acute Exercise Has Specific Effects on the Formation Process and Pathway of Visual Perception in Healthy Young Men. *European Journal of Neuroscience*, *58*(5), 3239–3252. https://doi.org/10.1111/ejn.16082

Kuwamizu, R., Yamazaki, Y., Aoike, N., Ochi, G., Suwabe, K., & Soya, H. (2022). Pupil-Linked Arousal with Very Light Exercise: Pattern of Pupil Dilation During Graded Exercise. *The Journal of Physiological Sciences*, *72*(1), 23. https://doi.org/10.1186/s12576-022-00849-x

Lacey, B. C., & Lacey, J. I. (1974). Studies of Heart Rate and Other Bodily Processes in Sensorimotor Behavior. In *Cardiovascular psychophysiology: Current issues in response mechanisms, biofeedback and methodology* (pp. 538–564). AldineTransaction.

Lacey, B. C., & Lacey, J. I. (1980). Cognitive Modulation of Time-Dependent Primary Bradycardia. *Psychophysiology*, *17*(3), 209–221. https://doi.org/10.1111/j.1469-8986.1980.tb00137.x

Lacey, J. I. (1967). Somatic Response Patterning and Stress: Some Revisions of Activation Theory. In M. H. Appley & R. Trimbull (Eds.), *Pyschological Stress: Issues in Research*. Appleton Century-Crofts.

Lacey, J. I., & Lacey, B. C. (1958). The Relationship of Resting Autonomic Activity to Motor Impulsivity. *Research Publications of the Association for Research in Nervous & Mental Disease*, *36*, 144–209.

Lacey, J. I., & Lacey, B. C. (1970). Some Autonomic-Central Nervous System Interrelationships. In P. Black (Ed.), *Physiological Correlates of Emotion* (pp. 205–227). Academic Press. https://doi.org/10.1016/B978-0-12-102850-3.50016-5

Leutheuser, H., Gradl, S., Anneken, L., Arnold, M., Lang, N., Achenbach, S., & Eskofier, B. M. (2016, July 21). *Instantaneous P- and T-Wave Detection: Assessment of Three ECG Fiducial Points Detection Algorithms*. 2016 IEEE 13th International Conference on Wearable and Implantable Body Sensor Networks (BSN), San Francisco, CA, USA. https://doi.org/10.1109/BSN.2016.7516283

Maris, E., & Oostenveld, R. (2007). Nonparametric Statistical Testing of EEG- and MEG-Data. *Journal of Neuroscience Methods*, *164*(1), 177–190. https://doi.org/10.1016/j.jneumeth.2007.03.024

McEwen, C., Paton, B., Tsuchiya, N., & van Boxtel, J. J. A. (2020). Motion-Induced Blindness as a Tool to Measure Attentional Biases and the Link to Attention-Deficit/Hyperactivity Traits. *Journal of Experimental Psychology: General*, *149*(9), 1628–1643. https://doi.org/10.1037/xge0000742

Mehling, W. E., Price, C., Daubenmier, J. J., Acree, M., Bartmess, E., & Stewart, A. (2012). The Multidimensional Assessment of Interoceptive Awareness (MAIA). *PLOS ONE*, *7*(11), e48230. https://doi.org/10.1371/journal.pone.0048230

Molle, L., & Coste, A. (2022). The Respiratory Modulation of Interoception. *Journal of Neurophysiology*, *127*(4), 896–899. https://doi.org/10.1152/jn.00027.2022

Motyka, P., Grund, M., Forschack, N., Al, E., Villringer, A., & Gaebler, M. (2019). Interactions Between Cardiac Activity and Conscious Somatosensory Perception. *Psychophysiology*, *56*(10), e13424. https://doi.org/10.1111/psyp.13424

Nes, B. M., Janszky, I., Wisløff, U., Støylen, A., & Karlsen, T. (2013). Age-Predicted Maximal Heart Rate in Healthy Subjects: The HUNT Fitness Study. *Scandinavian Journal of Medicine & Science in Sports*, *23*(6), 697–704. https://doi.org/10.1111/j.1600-0838.2012.01445.x

Oostenveld, R., Fries, P., Maris, E., & Schoffelen, J.-M. (2011). FieldTrip: Open Source Software for Advanced Analysis of MEG, EEG, and Invasive Electrophysiological Data. *Computational Intelligence and Neuroscience*, *2011*, 1–9. https://doi.org/10.1155/2011/156869

Pan, J., & Tompkins, W. J. (1985). A Real-Time QRS Detection Algorithm. *IEEE Transactions on Bio-Medical Engineering*, *32*(3), 230–236. https://doi.org/10.1109/TBME.1985.325532

Park, H.-D., & Blanke, O. (2019a). Coupling Inner and Outer Body for Self-Consciousness. *Trends in Cognitive Sciences*, *23*(5), 377–388. https://doi.org/10.1016/j.tics.2019.02.002

Park, H.-D., & Blanke, O. (2019b). Heartbeat-Evoked Cortical Responses: Underlying Mechanisms, Functional Roles, and Methodological Considerations. *NeuroImage*, *197*, 502–511. https://doi.org/10.1016/j.neuroimage.2019.04.081

Park, H.-D., Correia, S., Ducorps, A., & Tallon-Baudry, C. (2014). Spontaneous Fluctuations in Neural Responses to Heartbeats Predict Visual Detection. *Nature Neuroscience*, *17*(4), Article 4. https://doi.org/10.1038/nn.3671

Parviainen, T., Lyyra, P., & Nokia, M. S. (2022). Cardiorespiratory Rhythms, Brain Oscillatory Activity and Cognition: Review of Evidence and Proposal for Significance. *Neuroscience and Biobehavioral Reviews*, *142*, 104908. https://doi.org/10.1016/j.neubiorev.2022.104908

Petzschner, F. H., Weber, L. A., Wellstein, K. V., Paolini, G., Do, C. T., & Stephan, K. E. (2019). Focus of Attention Modulates the Heartbeat Evoked Potential. *NeuroImage*, *186*, 595–606. https://doi.org/10.1016/j.neuroimage.2018.11.037

Sandman, C. A., McCanne, T. R., Kaiser, D. N., & Diamond, B. (1977). Heart Rate and Cardiac Phase Influences on Visual Perception. *Journal of Comparative and Physiological Psychology*, *91*(1), 189–202. https://doi.org/10.1037/h0077302

Schandry, R., & Montoya, P. (1996). Event-Related Brain Potentials and the Processing of Cardiac Activity. *Biological Psychology*, *42*(1), 75–85. https://doi.org/10.1016/0301-0511(95)05147-3

Sedghamiz, H. (2014). *Matlab Implementation of Pan Tompkins ECG QRS detector.* [Computer software]. https://doi.org/10.13140/RG.2.2.14202.59841

Seth, A. K. (2013). Interoceptive Inference, Emotion, and the Embodied Self. *Trends in Cognitive Sciences*, *17*(11), 565–573. https://doi.org/10.1016/j.tics.2013.09.007

Skora, L. I., Livermore, J. J. A., & Roelofs, K. (2022). The Functional Role of Cardiac Activity in Perception and Action. *Neuroscience & Biobehavioral Reviews*, *137*, 104655. https://doi.org/10.1016/j.neubiorev.2022.104655

Somsen, R. J. M., Jennings, J. R., & Van der Molen, M. W. (2004). The Cardiac Cycle Time Effect Revisited: Temporal Dynamics of the Central-Vagal Modulation of Heart Rate in Human Reaction Time Tasks. *Psychophysiology*, *41*(6), 941–953. https://doi.org/10.1111/j.1469-8986.2004.00241.x

Stein, B. E., & Stanford, T. R. (2008). Multisensory Integration: Current Issues from the Perspective of the Single Neuron. *Nature Reviews Neuroscience*, *9*(4), 255–266. https://doi.org/10.1038/nrn2331

Tallon-Baudry, C. (2023). Interoception: Probing Internal State Is Inherent to Perception and Cognition. *Neuron*, *111*(12), 1854–1857. https://doi.org/10.1016/j.neuron.2023.04.019

Tallon-Baudry, C., Campana, F., Park, H.-D., & Babo-Rebelo, M. (2018). The Neural Monitoring of Visceral Inputs, Rather Than Attention, Accounts for First-Person Perspective in Conscious Vision. *Cortex*, *102*, 139–149. https://doi.org/10.1016/j.cortex.2017.05.019

Vázquez-Seisdedos, C. R., Neto, J. E., Marañón Reyes, E. J., Klautau, A., & Limão de Oliveira, R. C. (2011). New Approach for T-Wave End Detection on Electrocardiogram: Performance in Noisy Conditions. *BioMedical Engineering OnLine*, *10*(1), 77. https://doi.org/10.1186/1475-925X-10-77

3.7 Supplementary Information

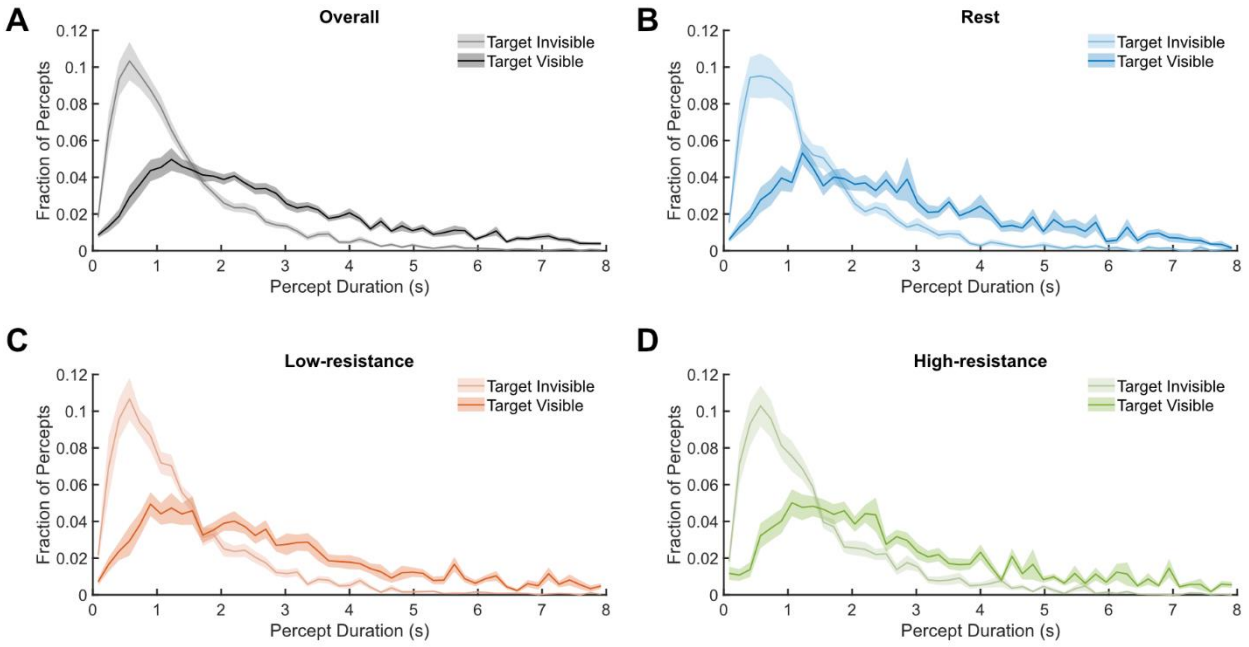

Figure S3-1 – Frequency distributions of target invisible and target visible durations

Group-averaged distributions of percept durations (*N* = 26) for MIB trials are shown for (**A**) all exercise intensity conditions combined, (**B**) the rest condition, (**C**) the low-resistance cycling condition, and (**D**) the high-resistance cycling condition. Shaded areas indicate the SEM.

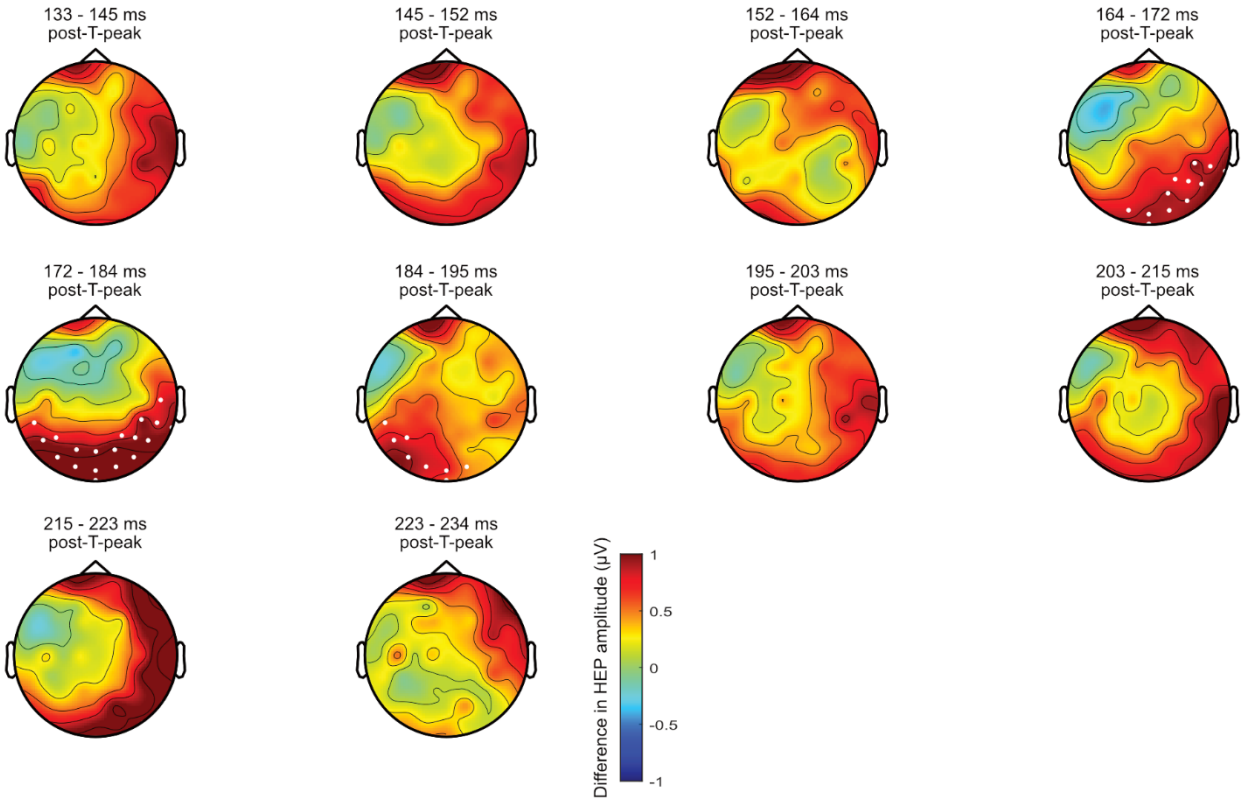

Figure S3-2 – Cluster based permutation analysis investigating differences in Heartbeat-Evoked Potentials (HEP) when target is present (visible) and when target is physically removed (invisible) in stimulus-locked analysis of Replay trials

Scalp topographies of the visible − invisible difference in HEP amplitude for 12-ms windows spanning the 100 ms to 400 ms post-T peak time window. Spatio-temporal clusters showing a significant difference between the two conditions are indicated by white dots ($p < 0.05$).

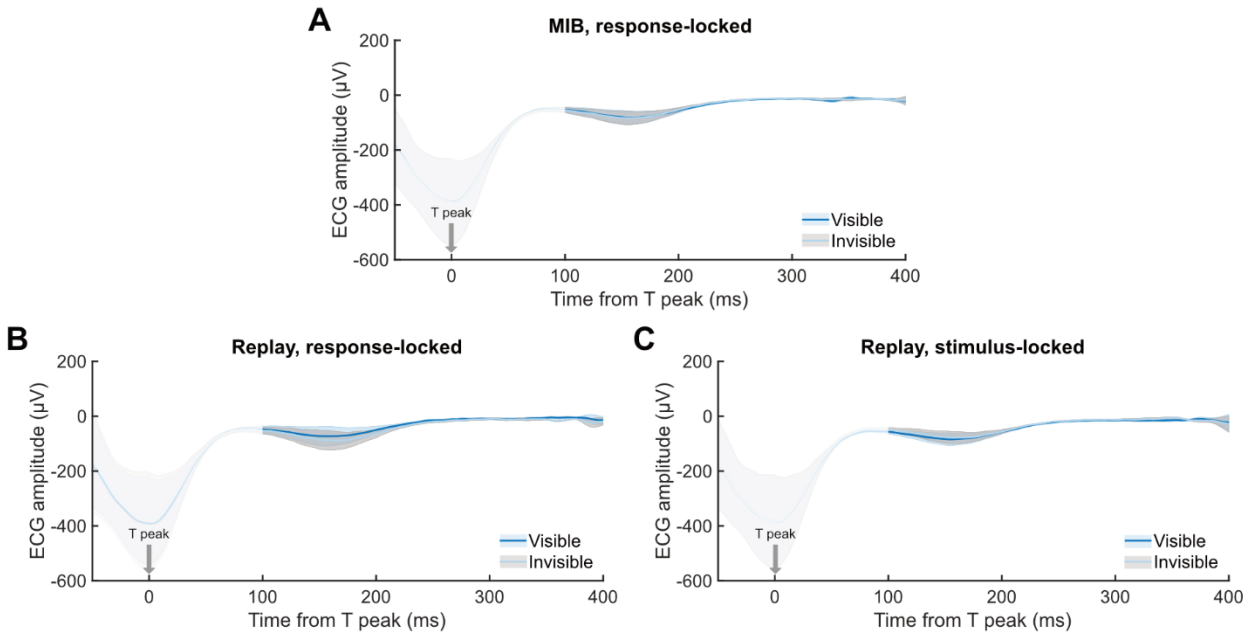

Figure S3-3 – Volume conduction control

Group-averaged T-peak locked ECG for the visible and invisible conditions for (**A**) response-locked analysis of MIB trials, (**B**) response-locked analysis of Replay trials and (**C**) stimulus-locked analysis of replay trials, in the same time window as the corresponding HEP analyses. The shaded areas denote the SEM for each time course. No significant differences were identified for all three analyses.

Chapter 4 General Discussion

The primary aim of this thesis was to investigate the interplay between interoceptive signals, specifically cardiac activity, and exteroceptive inputs, particularly in the context of conscious visual perception. The two studies presented sought to explore how heart rate, modulated by exercise, influences neural dynamics related to both interoception and exteroception, and how these dynamics shape perceptual outcomes in perceptual suppression paradigms. The following sections summarise the key findings of these studies, discuss their implications and limitations, and propose future directions and potential improvements throughout this chapter. Finally, the thesis concludes with overarching insights and an outlook on the broader implications of the work.

4.1 Summary and Implications of Findings

The influence of heart rate dynamics on conscious visual perception, particularly as manipulated by exercise, was a central focus of this thesis. In the Generalized Flash Suppression (GFS) study, we observed that exercise induced a lower likelihood of perceptual suppression, as well as an increased pre-stimulus heart rate. However, there was no significant correlation between these exercise-induced changes in heart rate and perceptual suppression. In the Motion-Induced Blindness (MIB) study, exercise did not induce changes in perceptual suppression rate or duration, nor were there any correlations between the exercise-induced changes in heart rate and changes in perceptual suppression rate or duration. These findings align with a previous study on somatosensory stimuli at threshold**,** which found no evidence that instantaneous heart rate before a stimulus affects its detection (Motyka et al., 2019). Our work extends this prior research by deliberately manipulating heart rate using an exercise intervention, providing further evidence that sustained heart rate increases during exercise are not directly linked to attentional or perceptual processes.

Instead, the sustained increase in heart rate observed during exercise likely reflects sympathetic dominance, which primes the system for action rather than perception (Skora et al., 2022). This heightened state of arousal may overshadow the more subtle

interoceptive effects that might contribute to perceptual suppression, masking their influence during exercise. In contrast, transient heart rate changes at rest, such as cardiac deceleration have consistently been observed in anticipation of a stimulus (Motyka et al., 2019; Skora et al., 2022; J. I. Lacey, 1967; B. C. Lacey & Lacey, 1974; Cobos et al., 2019; Park et al., 2014; Grund et al., 2022), reinforcing the robustness of this phenomenon. Although the magnitude of cardiac deceleration does not always predict subsequent perceptual outcomes (Grund et al., 2022; Park et al., 2014), this suggests that interoceptive influences may not align directly with perceptual outcomes but instead reflect attentional shifts that shape perceptual processing (Skora et al., 2022). The phenomenon of cardiac deceleration warrants further investigation to uncover the neural mechanisms that may link it to conscious perception and the potential attentional trade-offs between interoceptive and exteroceptive processing, particularly in naturalistic settings to assess its ecological validity. Additionally, future studies should account for parasympathetic/sympathetic tone and arousal levels when assessing the role of cardiac signals in neural and perceptual dynamics.

There is also some prior evidence from other multistable perception paradigms to suggest that cardiac influences on perceptual processing may be context-dependent. For example, a study using continuous flash suppression (CFS; a special case of binocular rivalry) demonstrated a suppressive effect of cardiac input on visual awareness, with higher thresholds for stimuli breaking through to awareness when masked stimuli were entrained to systole (Salomon et al., 2016). However, a separate binocular rivalry study observed increased awareness of stimuli presented during systole (Veillette et al., 2024). While these studies focused on cardiac phase effects rather than heart rate changes (as in our work), they offer valuable context for interpreting the role of cardiac signals in perception.

Our GFS results go beyond these previous studies by gauging cortical inhibition as indexed by alpha activity and finding exercise-induced increases in heart rate paralleled by decreased alpha activity/increased cortical excitability. However, there was no significant correlation between the changes in heart rate and alpha activity. Alpha activity,

as an index of cortical excitability, was not assessed in MIB study, limiting comparisons to the results of the GFS study. The GFS findings, however, challenge the notion that increased heart rate necessarily leads to increased cortical inhibition and suppressed sensory processing (B. C. Lacey & Lacey, 1974; J. I. Lacey, 1967), as posited by the baroreceptor hypothesis. Instead, the results emphasise the context-dependent nature of cardiac influences on neural dynamics and perception, which may vary based on the paradigm, other physiological factors, and specific neural mechanisms at play. Unravelling this context dependency, particularly in relation to the cardiac-related inhibition of cortical excitability implied by the baroreceptor hypothesis, is essential for understanding the proposed link between interoceptive-exteroceptive integration and conscious perception.

Beyond visual awareness paradigms, studies have indicated that visual skills such as discrimination (Pramme et al., 2014) and search (Pramme et al., 2016) are actually facilitated when stimuli are presented during systole, in contrast to the baroreceptor hypothesis. This has led to the proposal that cardiac inputs may exert a suppressive effect on the earliest stages of visual processing, as suggested by the baroreceptor hypothesis, but may also have more heterogeneous downstream effects (Veillette et al., 2024). These downstream effects could enable complex “cardiac gating” mechanisms that facilitate perception during tasks involving higher-level visual processing (Veillette et al., 2024). This highlights the importance of considering the level of processing when examining cardiac influences on perception, as the interaction between interoceptive signals and visual processing may vary depending on the cognitive and neural demands of the task. In the context of the mixed findings from our two studies, the role of interoceptive-exteroceptive dynamics in modulating perceptual suppression may depend not only on the specific neural mechanisms underlying perceptual suppression but also on how these mechanisms interact with cardiac influences at different stages of visual processing. Further research is needed to better understand how interoceptive signals interact with exteroceptive processing across different stages of visual processing.

The findings from the GFS study also provide tentative evidence that cardiac physiology, specifically heart rate, may influence HEPs, a neural marker of interoceptive processing. A decrease in HEP amplitudes was observed during cycling compared to rest, with statistical modelling suggesting that this effect was driven, at least in part, by the increase in heart rate, suggesting a reduction in interoceptive processing. This finding implies that, in our experimental context, attention may have shifted away from processing internal bodily signals to prioritising the external demands of simultaneously performing a perceptual and motor task. More importantly, this result supports the idea that heart-brain coupling may vary with cardiovascular changes and is unlikely to be an artifact of heart-related physiological noise affecting neural signals through volume conduction. In light of this, interpreting HEPs requires further careful consideration, particularly given the evolving methodologies used to measure and analyse these signals (Coll et al., 2021; Park & Blanke, 2019), and underscores the need for further research into HEP dynamics to refine their use as reliable markers of interoceptive processing and heart-brain coupling.

Additionally, HEPs have previously been found to predict the conscious perception of visual (Park et al., 2014) and somatosensory (Al et al., 2020, 2021) stimuli at threshold, though with opposing patterns: higher HEP amplitudes are associated with hits compared to misses for visual stimuli, whereas lower HEP amplitudes are associated with hits compared to misses for somatosensory stimuli. These differences highlight the potential modality-specific roles of interoceptive signals in shaping perception.

In contrast to these findings, our results from perceptual suppression paradigms (which differ fundamentally from threshold paradigms by focusing on the subjective disappearance of a salient stimulus rather than its detection) show that HEPs do not predict or correlate with perceptual suppression. In the GFS study, HEPs were not predictive of the likelihood of perceptual suppression, while in the MIB study, there was no difference in HEPs between the presence and perceptual suppression of the target.

This contrast suggests that interoceptive contributions, as indexed by HEPs, may engage distinct neural mechanisms underlying different types of perceptual processes. It further

emphasises that the role of cardiac-related interoceptive signals varies depending on the cognitive and neural demands, physiological context, and modality of the perceptual task, with our results indicating no clear role for HEPs in perceptual suppression.

The GFS results indicate that alpha activity is predictive of perceptual suppression, consistent with findings from previous GFS studies conducted at rest. However, HEPs do not show such an association. Taken together, these findings align with the notion that cardiac contributions to neural variability are likely smaller than the influence of neural sources of variability in visual processing. The concurrent observation of low alpha activity (indicating increased cortical excitability and sensory processing) and low HEP amplitudes (suggesting decreased interoceptive processing) hints at a potential attentional trade-off between exteroceptive and interoceptive processing, though further investigation is required to confirm this relationship.

4.2 Limitations of the Present Studies

While the results of this thesis provide some insight into the role of heart-brain interactions in conscious visual perception, several limitations must be acknowledged.

First, the GFS study yielded no significant differences in perceptual suppression or alpha activity between the two exercise conditions, and the MIB study yielded no significant difference in perceptual suppression rate and duration across the rest and exercise conditions. This may be due to the exercise intensity, although sufficient to induce significant changes in heart rate in both studies, being insufficient to elicit the necessary physiological range to observe distinct effects in perceptual processing. We had to limit exercise intensity to light intensity to allow participants to effectively perform the perceptual tasks simultaneously with the exercise. This constraint was informed by several practical considerations: preventing an increase in cognitive load by making the exercise more difficult, ensuring the fixation requirements of the perceptual paradigms were met (as higher exercise intensities would increase head movement), and minimising muscular and body movement artifacts in the EEG data.

Despite efforts to minimise both cognitive load and head movement, the dual-task nature of the experiment and residual head motion may still have influenced the results. The added complexity of performing both the perceptual and motor tasks simultaneously might have made it more difficult to disentangle the effects associated with the perceptual task from those related to the motor task (Zink et al., 2016). The simultaneous attentional demands of the two tasks may have masked the potential attentional shifts associated with interoceptive processing.

Exercise elicits a gamut of physiological responses across virtually all tissues and organs in the human body, beyond changes in cardiac activity (Heinonen et al., 2014), which may have overshadowed more subtle cardiac interoceptive effects. These widespread physiological changes could make it difficult to isolate specific heart-brain interactions. For example, the observed increase in cortical excitability, as indexed by decreases in alpha activity during exercise, concurrent with an increase in heart rate, contradicts predictions based on the baroreceptor hypothesis. This discrepancy may reflect the complexity of the physiological processes involved, since cortical excitability is likely influenced by a variety of neural and physiological factors, not solely cardiac signals. Furthermore, persistent changes in neural and physiological states have been observed after exercise. For instance, EEG microstates and heart rate variability do not return to baseline for up to an hour after submaximal exercise (Spring et al., 2018). This suggests that our rest condition may not have represented a true rest, even though heart rate was allowed to return to baseline levels between rest and exercise runs, and may instead reflect post-exercise changes in cardiac and neural processes, and subsequent perception. In future studies, it may be beneficial to perform rest and exercise conditions consecutively or even on separate days, rather than interleaving them, to better isolate the effects of exercise and ensure a true baseline for the rest condition.

Another limitation of the present study is that the measures used, such as heart rate and HEP amplitudes, are inherently indirect markers of heart-brain coupling. These measures serve as proxies for underlying physiological mechanisms, such as baroreceptor activity, which were not directly measured in these studies. Although these measures offer

meaningful insights into the relationship between interoception and exteroception, interpretations about their role in influencing perceptual suppression or interoceptive-exteroceptive integration are speculative. Future research utilising direct assessments of baroreceptor activity or pharmacological interventions will be crucial for understanding the connection between cardiac signals and sensory processing. It should also be noted that while the literature on cardiac influences on sensory processing and conscious perception focuses on baroreceptor activity, any of the pathways involved in cardiac interoception mentioned in the introduction to this thesis (**Section 1.1.1**) might be involved, which would have implications for the latencies of cardiac-neural interactions and therefore perception, and these are also worth investigating further.

4.3 Final Conclusions and Outlook

In conclusion, this thesis provides novel insights into the complex interplay between cardiac and neural activity in shaping conscious visual perception. The findings underscore the context-dependent nature of heart-brain interactions, highlighting the influence of factors such as autonomic state (parasympathetic vs. sympathetic tone), the specific cognitive demands of the perceptual paradigm, and the levels of neural processing involved. Although we do find subtle hints of attentional trade-offs between interoceptive and exteroceptive processing, the lack of a clear relationship between interoceptive signals and perceptual outcomes suggests that interoception may play an indirect, modulatory role rather than a deterministic one. Moreover, the findings support the notion that neural sources of variability in perceptual processing contribute more significantly than cardiac sources.

Establishing a causal role of cardiac signals in modulating conscious access to exteroceptive visual inputs is particularly challenging in the field as a whole. In humans, causality remains difficult to establish not only due to the reliance on largely non-invasive methods, which limit the ability to directly manipulate and probe underlying mechanisms, but also due to the complexity of interacting systems. The tight coupling between respiration and cardiac function (Parviainen et al., 2022) suggests that respiration should also be considered as a key factor in studies investigating heart-brain interactions and

their influence on conscious perception. Perhaps such future studies may benefit from the various mathematical modelling methods that infer causality and directionality of the parallel heart-brain interactions have been proposed for EEG-ECG studies in humans (Candia-Rivera et al., 2024), to gain a clearer understanding of heart-brain coupling and its role in conscious perception.

Going beyond non-invasive studies in humans to gain a mechanistic understanding of heart-body-perception interactions is critical but presents significant challenges. While intrinsic brain rhythms are relatively conserved across species (Buzsáki et al., 2013), bodily rhythms such as cardiac and respiratory cycles vary significantly (Engelen et al., 2023). For example, rodents' heart rates are approximately 8–12 times faster than those of humans, making it difficult to obtain neurophysiological evidence (Engelen et al., 2023), and rendering HEP analysis impossible. These between-species differences raise important questions about their functional consequences for heart-brain coupling and perception.

There is a possibility that cardiac-related fluctuations in perception may be epiphenomenal, arising from coincidental alignments of physiological and perceptual rhythms, rather than conferring a direct functional advantage. On the other hand, the unclear role of cardiac signals in influencing neural activity and conscious perception may reflect limitations in current methodological and technological approaches to studying these processes, rather than a lack of the importance of afferent interoceptive signals and their processing in the brain.

These challenges and our results highlight the need for comparative investigations across sensory modalities, experimental paradigms, measurement and analysis techniques, and species to determine whether interoceptive contributions to perception are mechanistic or simply reflective of underlying biological constraints. This is a rapidly evolving field, characterised by an abundance of theoretical frameworks but a relative lack of established, replicable findings, as the response space is still being mapped out. Overall, incorporating internal bodily signals into the study of how external information is

processed will deepen our understanding of both conscious perception and the brain's broader functions.

4.4 References

Al, E., Iliopoulos, F., Forschack, N., Nierhaus, T., Grund, M., Motyka, P., Gaebler, M., Nikulin, V. V., & Villringer, A. (2020). Heart–Brain Interactions Shape Somatosensory Perception and Evoked Potentials. *Proceedings of the National Academy of Sciences*, *117*(19), 10575–10584. https://doi.org/10.1073/pnas.1915629117

Al, E., Iliopoulos, F., Nikulin, V. V., & Villringer, A. (2021). Heartbeat and Somatosensory Perception. *NeuroImage*, *238*, 118247. https://doi.org/10.1016/j.neuroimage.2021.118247

Buzsáki, G., Logothetis, N., & Singer, W. (2013). Scaling Brain Size, Keeping Timing: Evolutionary Preservation of Brain Rhythms. *Neuron*, *80*(3), 751–764. https://doi.org/10.1016/j.neuron.2013.10.002

Candia-Rivera, D., Chavez, M., & Fallani, F. D. V. (2024). Measures of the Coupling Between Fluctuating Brain Network Organization and Heartbeat Dynamics. *Network Neuroscience*, *8*(2), 557. https://doi.org/10.1162/netn_a_00369

Cobos, M. I., Guerra, P. M., Vila, J., & Chica, A. B. (2019). Heart-Rate Modulations Reveal Attention and Consciousness Interactions. *Psychophysiology*, *56*(3), e13295. https://doi.org/10.1111/psyp.13295

Coll, M.-P., Hobson, H., Bird, G., & Murphy, J. (2021). Systematic Review and Meta-Analysis of the Relationship Between the Heartbeat-Evoked Potential and Interoception. *Neuroscience & Biobehavioral Reviews*, *122*, 190–200. https://doi.org/10.1016/j.neubiorev.2020.12.012

Engelen, T., Solcà, M., & Tallon-Baudry, C. (2023). Interoceptive Rhythms in the Brain. *Nature Neuroscience*, *26*(10), 1670–1684. https://doi.org/10.1038/s41593-023-01425-1

Grund, M., Al, E., Pabst, M., Dabbagh, A., Stephani, T., Nierhaus, T., Gaebler, M., & Villringer, A. (2022). Respiration, Heartbeat, and Conscious Tactile Perception. *Journal of Neuroscience*, *42*(4), 643–656. https://doi.org/10.1523/JNEUROSCI.0592-21.2021

Heinonen, I., Kalliokoski, K. K., Hannukainen, J. C., Duncker, D. J., Nuutila, P., & Knuuti, J. (2014). Organ-Specific Physiological Responses to Acute Physical Exercise and Long-Term Training in Humans. *Physiology*, *29*(6), 421–436. https://doi.org/10.1152/physiol.00067.2013

Lacey, B. C., & Lacey, J. I. (1974). Studies of Heart Rate and Other Bodily Processes in Sensorimotor Behavior. In *Cardiovascular psychophysiology: Current issues in response mechanisms, biofeedback and methodology* (pp. 538–564). AldineTransaction.

Lacey, J. I. (1967). Somatic Response Patterning and Stress: Some Revisions of Activation Theory. In M. H. Appley & R. Trimbull (Eds.), *Pyschological Stress: Issues in Research*. Appleton Century-Crofts.

Motyka, P., Grund, M., Forschack, N., Al, E., Villringer, A., & Gaebler, M. (2019). Interactions Between Cardiac Activity and Conscious Somatosensory Perception. *Psychophysiology*, *56*(10), e13424. https://doi.org/10.1111/psyp.13424

Park, H.-D., & Blanke, O. (2019). Heartbeat-Evoked Cortical Responses: Underlying Mechanisms, Functional Roles, and Methodological Considerations. *NeuroImage*, *197*, 502–511. https://doi.org/10.1016/j.neuroimage.2019.04.081

Park, H.-D., Correia, S., Ducorps, A., & Tallon-Baudry, C. (2014). Spontaneous Fluctuations in Neural Responses to Heartbeats Predict Visual Detection. *Nature Neuroscience*, *17*(4), Article 4. https://doi.org/10.1038/nn.3671

Parviainen, T., Lyyra, P., & Nokia, M. S. (2022). Cardiorespiratory Rhythms, Brain Oscillatory Activity and Cognition: Review of Evidence and Proposal for Significance. *Neuroscience and Biobehavioral Reviews*, *142*, 104908. https://doi.org/10.1016/j.neubiorev.2022.104908

Pramme, L., Larra, M. F., Schächinger, H., & Frings, C. (2014). Cardiac Cycle Time Effects on Mask Inhibition. *Biological Psychology*, *100*, 115–121. https://doi.org/10.1016/j.biopsycho.2014.05.008

Pramme, L., Larra, M. F., Schächinger, H., & Frings, C. (2016). Cardiac Cycle Time Effects on Selection Efficiency in Vision. *Psychophysiology*, *53*(11), 1702–1711. https://doi.org/10.1111/psyp.12728

Salomon, R., Ronchi, R., Dönz, J., Bello-Ruiz, J., Herbelin, B., Martet, R., Faivre, N., Schaller, K., & Blanke, O. (2016). The Insula Mediates Access to Awareness of Visual Stimuli Presented Synchronously to the Heartbeat. *The Journal of Neuroscience: The Official Journal of the Society for Neuroscience*, *36*(18), 5115–5127. https://doi.org/10.1523/JNEUROSCI.4262-15.2016

Skora, L. I., Livermore, J. J. A., & Roelofs, K. (2022). The Functional Role of Cardiac Activity in Perception and Action. *Neuroscience & Biobehavioral Reviews*, *137*, 104655. https://doi.org/10.1016/j.neubiorev.2022.104655

Spring, J. N., Bourdillon, N., & Barral, J. (2018). Resting EEG Microstates and Autonomic Heart Rate Variability Do Not Return to Baseline One Hour After a Submaximal Exercise. *Frontiers in Neuroscience*, *12*. https://www.frontiersin.org/journals/neuroscience/articles/10.3389/fnins.2018.00460

Veillette, J. P., Gao, F., & Nusbaum, H. C. (2024). Cardiac Afferent Signals Can Facilitate Visual Dominance in Binocular Rivalry. *ELife*, *13*, RP95599. https://doi.org/10.7554/eLife.95599

Zink, R., Hunyadi, B., Huffel, S. V., & Vos, M. D. (2016). Mobile EEG on the Bike: Disentangling Attentional and Physical Contributions to Auditory Attention Tasks. *Journal of Neural Engineering*, *13*(4), 046017. https://doi.org/10.1088/1741-2560/13/4/046017

Acknowledgements

I would like to express my sincerest gratitude to everyone who has supported, guided, and inspired me throughout this journey.

I would like to thank Prof. Melanie Wilke for giving me this unique opportunity for learning and growth. I also extend my thanks to Dr. Roberto Goya-Maldonado and Prof. Ulrich Parlitz for participating in my TAC and providing insight and guidance over the years. I would also like to thank Dr. Dechent, Prof. Focke, Prof. Mani and Prof. Schwiederzik for serving on my exam board.

Many thanks to Dr. Eva Poland for introducing me to the fascinating world of EEG. To Sensei Dr. Iris Steinmann, thank you not only for teaching me about EEG and table tennis but also for being an all-round great friend – I'd be lost without you. Thanks also to my other inspiring EEG teachers, Profs. Mike X Cohen, Steven Luck, and Arnaud Delorme, whose emphasis on methodological rigour has profoundly shaped my approach to research. I also extend my thanks to Dr. Hyeong Dong Park and Prof. Catherine Tallon-Baudry for their invaluable guidance, particularly in navigating the field of heart-brain interactions. I am also grateful to Dr. Yuranny Cabral-Calderin, Dr. Jan-Mathijs Schoffelen, and the UMG Statistische Betreuung team for their statistical guidance. Finally, I am deeply grateful to Prof. Stephen Van Hooser for his mentorship over the past 12 years, and for exemplifying what it means to be both a good scientist and an upstanding human being.

My sincerest thanks to my lovely colleagues: it has been a pleasure to get to know you all, I will carry you with me always. Shirin, I cannot begin to express how much your constant support and companionship have meant to me, thanks for everything. My thanks to the best officemate, Severin, for being someone I can always count on. My heartfelt thanks to Hanna for being the first to break the ice, I cannot imagine what my life would be now if you hadn't. On to the best lunch companions ever. Peter, thank you for your warmth and kindness and for not letting me capsize our canoe. Carsten, thank you for your insightful conversations, gentleness, and patience.

Areej, Svenja, Sukanya – thank you, I hope you learnt as much from me as I did from you. Dany, thank you for cheering me on, feeding me and of course, IT support. Ege and Shamim, I am so grateful for our invaluable scientific discussions. Ilona, Britta, Kristin, Daniela – thanks for all the laughs, cookies, and chocolates. Many thanks to the HiWis and study nurses who have helped over the years – Peter N., Maria W., Alina, Anna-Lena, Maria M, and Sarah.

My sincerest thanks to the BeCog coordination team, Rebecca and Rowan, we are so lucky to have you! BeCog folks – your passion for science and your kindness always delight and inspire me. Sabine and Laura – there's no one else I'd rather organise a retreat with, thanks for all the suikas. My Famous People, Mareike and Pia, here's to many more Aperols. To the IMPRS gang – you made settling into a new country so fun and easy. Special thanks to all my flatmates – Elsa, Inés, Delane, Miguel, and Milena (honorary). Mathis, thanks for our wonderful chats on consciousness and for always pushing me to switch to Python (I still haven't). Marysol, Carlos, Jessica – thank you for

your support and for the countless board game nights that provided much-needed laughter, relaxation, and balance.

My thanks to Roberta for encouraging me to grow into the best version of myself.

My utmost thanks to the Science Gals, Abby, Emily, Jackie, Katie, Rachel. Words do not do justice to what you and your support mean to me.

Salonee – thank you, I don't know whom I'd be without you.

To my parents, Savita and Ranjit, thank you for absolutely everything. I soar higher knowing you're always there to catch me.

And to Jimmy – thank you for bringing joy and sustenance to my life these last few months.